



Gaugler
Ends at *Do*
AKA
LR 28573
Library

CONTRACT NAS1-14000

Advanced Manufacturing Development of a Composite Empennage Component for L-1011 Aircraft

DRL 003

QUARTERLY TECHNICAL REPORT - NO. 9

This report is for the period 1 January 1978 through 31 March 1978

Lockheed Corporation
Lockheed-California Company
Post Office Box 551
Burbank, California 91520



(NASA-CR-162862) ADVANCED MANUFACTURING
DEVELOPMENT OF A COMPOSITE EMPENNAGE
COMPONENT FOR L-1011 AIRCRAFT Quarterly
Technical Report, 1 Jan. 1978 - 31 Mar. 1978
(Lockheed-California Co., Burbank.) 130 p G3/24 33567
N80-18104
HC A07/MF A01
Unclas



14 April 1978

Prepared for Langley Research Center

CONTRACT NAS1-14000

Advanced Manufacturing Development of a Composite Empennage Component for L-1011 Aircraft

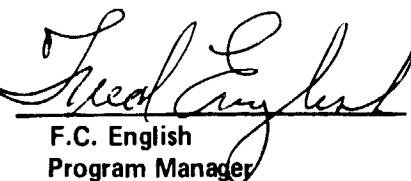
DRL 003

QUARTERLY TECHNICAL REPORT – NO. 9

This report is for the period 1 January 1978 through 31 March 1978

Lockheed Corporation
Lockheed-California Company
Post Office Box 551
Burbank, California 91520

Approved By:


F.C. English
Program Manager

14 April 1978

Prepared for Langley Research Center

FOREWORD

This report was prepared by the Lockheed-California Company, Lockheed Corporation, Burbank, California, under contract NAS1-14000. It is the ninth quarterly technical report covering work completed between 1 January 1978 and 31 March 1978. The program is sponsored by the National Aeronautics and Space Administration (NASA), Langley Research Center. The Program Manager for Lockheed is Mr. Fred C. English. Mr. Louis F. Vosteen is Project Manager for NASA, Langley. The Technical Representative for NASA, Langley is Mr. Herman L. Bohon.

"Page missing from available version"

SUMMARY

The technical activities performed in this reporting quarter and documented in this report are related to tasks associated with Phase II and Phase III of the Advanced Composite Vertical Fin (ACVF) Program. These tasks include: in Phase II, Component Definition, Material Verification, Process Verification, and Concept Verification; and in Phase III, Test Support. The discussion of technical activities related to these tasks is presented separately for each of the ACVF team members. The team member responsibilities are: prime contractor, Lockheed-California Company for the covers, ribs, and overall design; and subcontractor, Lockheed-Georgia Company for the spars and box assembly.

The primary activity during this reporting period was directed toward development of tooling concepts which would permit the cocuring of the hat stiffeners to the skin to form the cover assembly in a single autoclave cycle. These tooling concepts include the use of solid rubber mandrels, foam mandrels, and formed elastomeric bladders.

The design and analysis of the covers, ribs and spars are continuing as planned. A simplification of the root end design of the cover hat stiffeners was accomplished in order to facilitate fabrication. The conversion of the 3D NASTRAN model from level 15 to level 16 was completed and a successful check run accomplished.

The Production Readiness Verification Testing (Phase III) test support continued this reporting period with a detailed analysis of the thermal load requirement for the environmental chambers. Based on the thermal analysis, test function requirements, load inputs and ease of access, a system involving four chambers, two for the covers containing 6 and 4 specimens, respectively, and two for the spars containing 6 and 4 specimens, respectively, evolved.

The indicated weight saving for the ACVF is currently at 24.2 percent (207.8 pounds) including a 24-pound growth allowance. Without the growth allowance, a weight saving of 27.0 percent (231.8 pounds) is anticipated. Composite material utilization is currently predicted to be 77.4 percent of the redesigned fin box weight.

TABLE OF CONTENTS

Section	Page
FOREWORD	111
SUMMARY	v
LIST OF FIGURES	ix
LIST OF TABLES	xiii
1 INTRODUCTION	1-1
2 PHASE II - DESIGN AND ANALYSIS OF RIBS AND COVERS	2-1
2.1 COMPONENT DEFINITION	2-1
2.1.1 Detail Design	2-1
2.1.2 Structural Analysis	2-3
2.2 MATERIAL VERIFICATION	2-4
2.2.1 Design Data	2-7
2.3 PROCESS VERIFICATION	2-10
2.3.1 Materials and Producibility Studies	2-11
2.3.2 Process Development Studies	2-14
2.4 QUALITY ASSURANCE	2-32
2.4.1 Laboratory Tests	2-32
2.4.2 Nondestructive Inspection (NDI)	2-33
3 PHASE II - DESIGN AND ANALYSIS - SPARS	3-1
3.1 COMPONENT DEFINITION	3-1
3.1.1 Detail Design	3-1
3.1.2 Structural Analysis	3-1
3.2 PROCESS VERIFICATION	3-5
3.2.1 Tool Development and Process Verification Test Specimen - H14	3-5
3.2.2 Process Bulletin Refinements	3-28
3.3 CONCEPT VERIFICATION	3-32
3.3.1 Spar Test Fixture	3-32
3.3.2 Rear Spar Test Specimens - Test Item H20	3-33
3.3.3 Spar Web Test Specimens - Test Item H21	3-37

TABLE OF CONTENTS (Continued)

Section		Page
3.3.4	Front Spar Test Specimen - Test Item H23A	3-43
3.4	QUALITY ASSURANCE	3-43
3.4.1	Laboratory Tests	3-43
3.4.2	Nondestructive Inspection (NDI)	3-45
4	PHASE III - PRODUCTION READINESS VERIFICATION TESTS	4-1
4.1	TEST SUPPORT	4-2
4.1.1	Environmental Chamber Design	4-2
4.1.2	Durability Test Specimens	4-10

LIST OF FIGURES

Figure		Page
1-1	ACVF Program Master Schedule	1-3
2-1	Weight Time History	2-5
2-2	Preliminary Cover Strains (Ultimate)	2-6
2-3	Cracked Specimen Geometry	2-8
2-4	Hat Stiffener Root End Configuration	2-12
2-5	Composite Stiffener Skin Specimen Calibration Curve	2-15
2-6	Cured Hat/Skin Cover Specimens. Solid rubber mandrels are shown partially withdrawn. Caul in foreground is steel, caul in background is fiberglass.	2-16
2-7	Thinning of Hat Flange Attributed to Pressure Imbalance	2-18
2-8	Outside Skin Surface of Cured Specimens. "H" on specimen indicates 350°F cure. "L" indicates 250°F cure with 350°F postcure. Mark-off is more pronounced on "H" specimens.	2-19
2-9	Single-Stage Cure Root End Assembly	2-19
2-10	Three Hat Wide Cured Panel	2-23
2-11	Cured Hat/Skin Specimen. Bagged foam mandrel shown partially withdrawn. Unused foam mandrel is shown adjacent with caul plate in background.	2-23
2-12	Hat-to-Skin Assembly Using a Foam Mandrel	2-25
2-13	Original and Improved System for the Foam Mandrel System	2-26
2-14	Three Hat Wide Panel Cured Using the Foam Mandrel Concept	2-27
2-15	Interior of Hat Showing Clean Release of Foam Mandrel	2-27
2-16	Mark-off Due to Lifting of Hat Flanges	2-28
2-17	Rotational Casting Machine for Development of Cast Bladders	2-29
2-18	Formed Rubber Mandrels. Bladder on left is pressurized through a short length of tubing. Bladder on right has a full length perforated tube.	2-30

LIST OF FIGURES (Continued)

Figure		Page
2-19	Bandsaw Equipped with Spiral (Tyler) Blade	2-33
2-20	Areas of Initial Single Stage Cure Cover Assembly Specimens Ultrasonically Inspected	2-37
2-21	Photographs of Reflected Through Transmission of Ultrasonic C-Scans of Two-Stage Cured (250°F) Group B Specimens	2-38
2-22	Photographs of Reflected Through Transmission of Ultrasonic C-Scans of Two-Stage Cured (250°F) Group B Specimens	2-39
2-23	Photographs of Reflected Through Transmission Ultrasonic C-Scans of Two-Stage Cured (250°F) Group B Specimens	2-40
2-24	Rib Cap Areas Ultrasonically Inspected	2-42
2-25	Reflected Thru-Transmission Ultrasonic C-Scan of Actuator Rib Cap and Truss Rib Cap Specimens	2-42
2-26	NDI Standards for Evaluation of Inspection Methods	2-44
2-27	Layout of Trim and Testing to be Performed on Tool and Production Graphite Epoxy Panels	2-44
2-28	Data Code for Tool and Process Development Panels	2-49
2-29	Photograph of Reflected Through Transmission Ultrasonic C-Scan with Transducer Focused on Reflector Plat of Panel Section L-044S-R-N-2-1	2-50
2-30	Photograph of Ultrasonic Through Transmission Acoustic Image of Panel Section L-044S-R-N-2-1	2-51
3-1	Front Spar Web Thickness, Cap Area & Moduli	3-2
3-2	Rear Spar Web Thickness, Cap Area & Moduli	3-2
3-3	Diagram Showing Summary of Margins of Safety in Front Spar	3-3
3-4	Rear Spar Margins of Safety	3-4
3-5	Stiffener Trim Templates	3-6
3-6	Placing Stiffeners in Tool	3-7
3-7	Stiffeners in Place & Ready for Web	3-8
3-8	Layup of Web	3-9
3-9	Web in Place with Armalon Bleed Cloth and Turning +45° Web Plies Into Cap	3-10

LIST OF FIGURES (Continued)

Figure		Page
3-10	Final Lay-up of Spar in Bond Tool	3-11
3-11	Details of Lower End of H14 Showing Removal of Armalon and Some Fiber Wash	3-12
3-12	Aft Side of Front Stub Spar (H14) As Removed From Tool Prior to Removing Armalon	3-13
3-13	Details of Upper End of H14, Aft Side, Prior to Removal of Armalon	3-14
3-14	Forward Side (Smooth Side) of H14 Prior to Removal of Armalon	3-15
3-15	Close-up Showing Removal of Armalon From Forward Side of H14	3-16
3-16	H14 Coupon Type Test Specimens	3-18
3-17	H14 Stub Spar and Locations of Test Coupons	3-19
3-18	H14 Laminate Tension Specimen A	3-20
3-19	H14 Rail Shear Specimen B	3-21
3-20	H14 Cap Compression Specimen C	3-22
3-21	H14 Cap Compression Strips D and Porosity Specimen E	3-23
3-22	H14 Fiber Volume, Resin Content and Sp. Gr. Specimen F	3-24
3-23	Summary of Test Results for H14 L. Hand & R. Hand Caps	3-26
3-24	Summary of Test Results for H14, Rib Angles and Stiffeners	3-27
3-25	Specimen A Interlaminar Tension Failure Mode	3-29
3-26	Specimens C and D Compression Failure Mode	3-30
3-27	Specimen B Rail Shear Failure Mode	3-31
3-28	Illustration of Time Scale Adjustment Required During Cure Cycle	3-32
3-29	Test Fixture for H20 and H23 Spar-to-Fuselage Specimens	3-34
3-30	Loading Bar for Applying Point Loads to H20 and H23	3-35
3-31	Diagram of Environmental Chamber for H20	
3-32	Calculated Moisture Pick-up for T300/5208 in Humidity Chamber	3-38
3-33	Test Set-up for H21A-1 RTD Shear Web Specimen	3-40
3-34	Failure Mode for H21A-1 RTD Specimen After Sustaining 170 Percent Limit Load	3-41

LIST OF FIGURES (Continued)

Figure		Page
3-35	Temperature Cycle for H21A-2	3-42
3-36	Illustration of H23 Front Spar-To-Fuselage Test Attachments	3-44
4-1	Cover Chamber and Loading Frame	4-3
4-2	Spar Chamber and Loading Frame	4-4
4-3	Thermal Cycle-PRVT	4-5
4-4	Chamber Schematic and Temperature Cycle	4-9
4-5	Spar PRVT Specimen	4-13
4-6	Twin Spar Beam	4-14
4-7	Cover PRVT Specimen	4-15

LIST OF TABLES

Table		Page
2-1	Current Weight Status	2-3
2-2	Summary of Weight Changes	2-4
2-3	H13AZ Tension 180°F Dry	2-10
2-4	Triple Notch Tests	2-11
2-5	Laboratory Test Results. Hat Flange-To-Skin Cocure	2-17
2-6	Laboratory Test Results Hat-to-Skin 250°F Cocure/ 350°F Postcure	2-20
2-7	Laboratory Test Results - Three Hat Wide Panel	2-22
2-8	Laboratory Test Results (Hat-to-Skin Cocure. Foam Mandrel.)	2-24
2-9	Laboratory Test Results Hat-to-Skin Cocure Foam Mandrel	2-25
2-10	T300/5208 Batch Acceptance Test Results	2-34
2-11	Inspection Results	2-41
2-12	Flat Laminates Inspected	2-43
2-13	NDI Evaluation Program Plan for Tool and Product Development	2-46
2-14	Process Development Summary	2-48
3-1	H14 Fiber Volume, Resin Content, Specific Gravity and Void Content	3-25
3-2	Receiving Inspection Tests - Batch 1015 (Per C-22-1379/111)	3-45
3-3	Results of H21A1 & H21A2 Process Control Tests	3-46
4-1	Chamber Load Summary - 6 Spars	4-8
4-2	Environmental Chamber Performance Prediction (h = 2.5)	4-11
4-3	Environmental Chamber Performance Prediction (h = 5.0)	4-12

SECTION 1

INTRODUCTION

The broad objective of the Aircraft Energy Efficiency (ACEE) Composite Structures Program is to accelerate the use of composite structures in new aircraft by developing technology and processes for early progressive introduction of composite structures into production commercial transport aircraft. This program, as one of several which are collectively aimed toward accomplishing that objective, has a specific objective: to develop and manufacture advanced composite vertical fins for L-1011 transport aircraft. Laboratory tests and analyses will be made to substantiate that the composite fin can be safely and economically operated under service loads and environments and will meet FAA requirements for installation on commercial aircraft. A limited quantity of units will be fabricated to establish manufacturing methods and costs. The Advanced Composite Vertical Fin (ACVF) will make use of advanced composite materials to the maximum extent practical and weigh at least 20 percent less than the metal fin it replaces. A method will be developed to establish cost/weight relationships for the elements of the composite and metal fins to establish cost effective limits for composite applications.

The ACVF to be developed under this program will consist of the entire main box structure of the vertical stabilizer for the L-1011 transport aircraft. The box structure extends from the fuselage production joint to the tip rib and includes the front and rear spars; it is 25 feet tall with a root box chord of 9 feet and represents an area of 150 square feet.

The primary emphasis of this program is to gain a high level of confidence in the structural integrity and durability of advanced composite primary structures. An important secondary objective is to gain sufficient knowledge and experience in manufacturing aircraft structures of advanced composite materials to properly assess its cost-effectiveness.

The duration of this program is 76 months, with completion scheduled for May 1983. The master schedule for this program is shown in Figure 1-1. The program is organized in four overlapping phases: Phase II - Design and Analysis; Phase III - Production Readiness Verification Tests (PRVT); Phase IV - Manufacturing Development; and Phase V - Ground Tests and Flight Checkout. Phase I was completed during 1976.

The Lockheed-California Company has teamed with the Lockheed-Georgia Company in the development of the ACVF. Lockheed-California Company, as prime contractor, has overall program responsibility and will design and fabricate the covers and the ribs, conduct the PRVT program, and conduct the full-scale ground tests; Lockheed-Georgia Company will design and fabricate the front, rear, and auxiliary spars, and assembly the composite fin at their plant in Meridian, Mississippi, where the present L-1011 vertical fins are assembled.

Phase I, Engineering Development, has been completed; and Phase II, Design and Analysis, is in progress.

Phase II consists of completing the detail design and analysis, characterization of the T300/5208 material system, initiating producibility studies, and conducting material, process, and concept verification tests. Phase III - Production Readiness Verification Testing (PRVT) is designed to provide information to answer the following questions:

- What is the range of production qualities that can be expected for components manufactured under conditions similar to those expected in production, and how realistic and effective are proposed quality levels and quality control procedures?
- What variability in static strength can be expected for production quality components, and are the margins sufficient to account for this variability?
- Will production quality components survive extended time laboratory fatigue tests involving both load and environment simulation of sufficient duration and severity to provide confidence in in-service durability?

Ten static strength tests and ten durability tests will be conducted on each of two key structural elements of the ACVF. One element will represent the front spar/fuselage attachment area, and the other element will represent the cover/fuselage joint area.



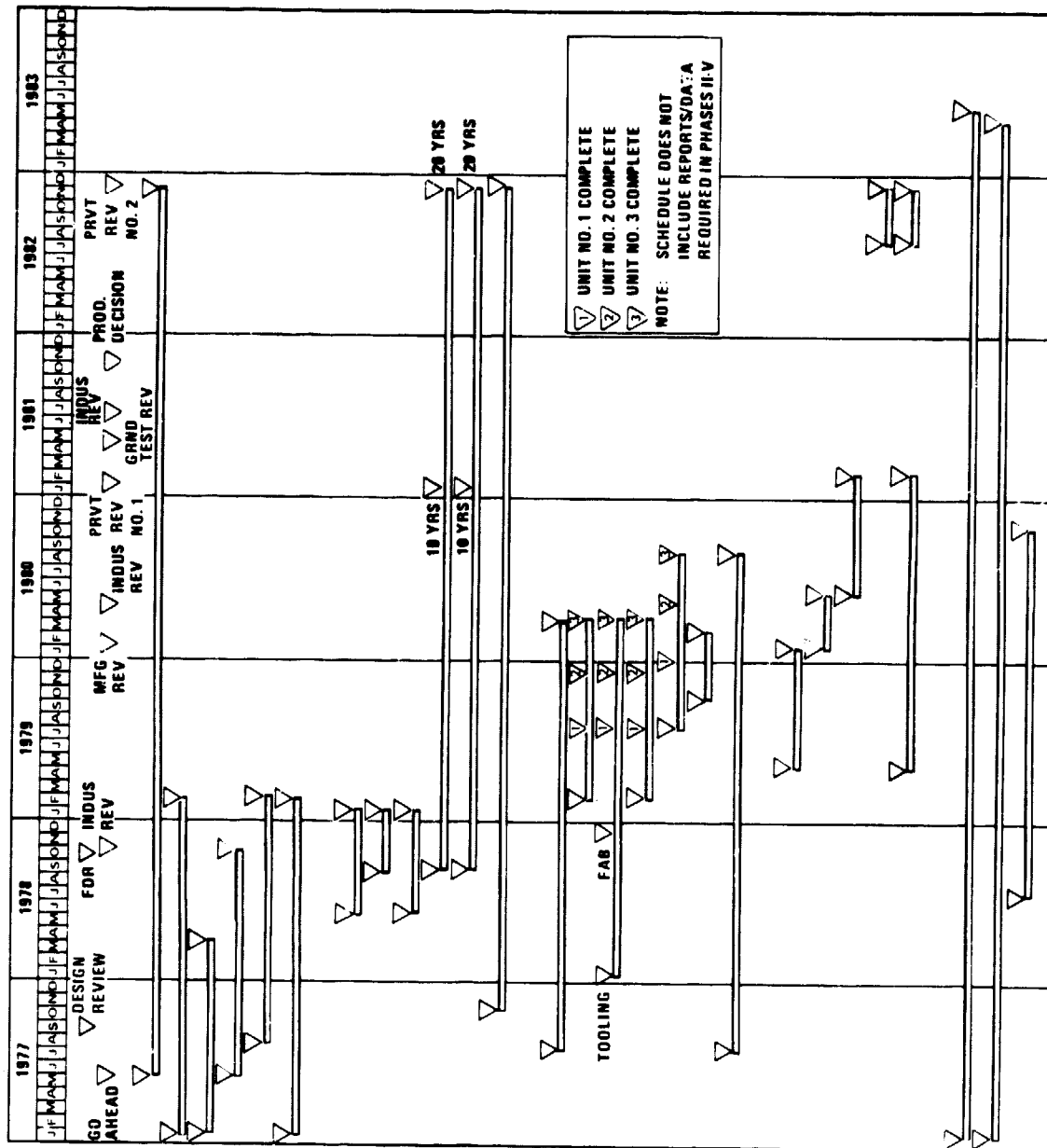


Figure 1-1. ACVF Program Master Schedule



Manufacturing Development, Phase IV, will be initiated early, concurrent with Producibility Studies, Process Verification, and Material Verification, to accommodate changes in tooling which might be caused by the change to 5208 resin material and to take advantage of development of low-cost manufacturing methods. Following NASA's approval of the design, three fins will be fabricated and assembled to prove the design, methods of manufacture, and quality. Actual costs will be documented during fabrication and components will be weighed to update cost and weight estimates.

The manufacturing cost history obtained through the fabrication of the PRVT specimens in a production environment will provide cost data for a starting point for this application of composite structure. Together, they will form the basis for reasonably confident estimates of future production costs.

Ground tests will be conducted on two full-scale fin box beam structures mounted on simulated fuselage support structures during Phase V. The test plan will include static tests, ultimate load and failure load tests on one GTA. Damage growth tests to two lifetimes, and fail-safe and residual strength tests will be done on the second GTA. Repair techniques for in-service maintenance and inspection will be employed throughout tests. Test results will be used to verify the analytical, design, and fabrication procedures; and are essential inputs to the FAA for certification of the aircraft with the ACVF installed. Certification will be based on satisfying both static strength and fail-safe requirements. FAA certification flight tests will also be conducted during this phase in order to obtain full FAA certification.

Throughout this program, technical information gathered during performance of the contract will be disseminated throughout the aircraft industry and Government. The methods used to distribute this information will be through Quarterly Reports, which will coincide with calendar quarters; and Final Reports of each phase to be distributed at the completion of each phase. All test data and fabrication data will be recorded on Air Force Data Sheets for incorporation in the Air Force Design Guide and Fabrication Guide for Advanced Composites. Oral Reviews will also be conducted at NASA, Langley to acquaint the aircraft industry and the Government with progress of the program.



SECTION 2

PHASE II - DESIGN AND ANALYSIS OF RIBS AND COVERS

Phase II, design and analysis of the ribs and covers, comprises the main engineering effort of Lockheed-California Company in the design, development, and fabrication of the eleven ribs and two cover assemblies for the L-1011 composite vertical fin. The engineering effort during this reporting period covered four tasks: component definition, material verification, process verification, and quality assurance.

2.1 COMPONENT DEFINITION

Component definition covers the detail design and structural analysis of the selected rib and cover configurations.

2.1.1 Detail Design2.1.1.1 Cover Design

During this reporting period, detail design activities relating to the covers consisted of completing the design and releasing the drawings.

A simplification of the root end design of the hat section stiffener has been completed and incorporated in the released drawings. Fabrication will be considerably simplified by this revision. The basic hat section and the root end doublers can now be laid up together, prebled and trimmed prior to rather than after curing. See Section 2.3.1.1.

2.1.1.2 Rib Design

All of the eleven rib designs have been revised as discussed in the last quarterly report and drawings released.

The shape of the longitudinal stiffeners on all rib webs have been modified to simplify tooling and fabrication. This was accomplished by changing the top portion of the stiffener from a flat surface to a full radius as shown below.



In addition, the lateral stiffeners on the three solid rib webs have been redesigned to replace the hollowbeaded sections with integrally bonded tee sections.

2.1.1.3 Fin/Rudder Interface Study

The thermal expansion joint design has been completed and drawings released. The selected design is Design "B" shown in the last quarterly report.

2.1.1.4 Weight Status

The current weight status is shown in Table 2-1. A weight savings of 24.2 percent (207.8 pounds) is currently being predicted including a 24-lb growth allowance. Without the growth allowance, a weight savings of 27.0 percent (231.8 pounds) is anticipated. Composite material use is currently predicted to be 77.4 percent of the redesigned fin box weight. A summary of weight changes since Quarterly Report No. 8 is presented in Table 2-2 and a weight-time history for the composite fin is provided in Figure 2-1.

Redesign of the upper four fin mounted rudder hinge fittings is required to accommodate the thermal expansion differential between the composite structure assembly and the metallic rudder. The addition of a gate assembly at each location results in a weight increase of 8.5 pounds per aircraft.

TABLE 2-1. CURRENT WEIGHT STATUS

Item	Metal Design Total Weight (lb)	Composite Design			Weight Change
		Target Weight (lb)	Total Weight (lb)	Composite Mat'l Wt (lb)	
Covers	460.4	368.4	353.7	341.3	
Spars	199.0	132.0	117.5	87.9	-4.2
Ribs	153.3	131.8	108.0	49.6	+0.6
Assembly Hardware	35.4	16.7	14.4	-	
Protective Finish	9.6	9.6	9.6	-	
Lightning Protection	-	15.5	14.2	-	
Installation Penalty	-	-	8.5	-	+8.5
Design Growth Allowance	-	-	24.0	24.0	
Total Fin Predicted					
Delivery Weight - lb	857.7		649.9	502.8	+4.9
Weight Saving - lb			207.8		
Percent Weight Saved			24.2%	77.4%	
Percent Composite Material					
Total Fin Current Indicated Weight - lb		674.0	625.9	478.8	
(Predicted Less Growth)			27.0%	76.5%	
Current Indicated Weight of Redesigned Component	825.4 Δ		618.4	(25.1% Weight Saved) Δ	
Weight Basis: 6% EST, 94% CALC, 0% ACT					
Δ Total metal design weight less weight of components not redesigned					
Δ Based on redesigned metal components					

Since the redesign is the resultant of the installation of the composite box assembly with the metallic rudder assembly, the weight increment is noted on the weight status as an installation penalty.

2.1.2 Structural Analysis

The preliminary cover analysis has been completed. The final analysis will be accomplished when the final allowables and loads are available. Analysis of the rudder support structure incorporating the modifications to handle the thermal expansion difference between the fin and the rudder was also completed in this reporting period

TABLE 2-2. SUMMARY OF WEIGHT CHANGES

Item	Weight Change (lb)		Remarks
	Total	Composite	
Ribs	+0.6	+0.6	Incorporate integrally bonded tee section stiffeners in lieu of a beaded web for the upper three (solid web) ribs, per revised stress analysis.
Spars	-4.2	-0.7	Revised weight estimate based on calculation of drawings and weight of the front spar stub molded assembly.
Install. Penalty	+8.5	0	Weight increase for redesign of upper four fin mounted rudder hinge fittings to accommodate thermal expansion differential between the composite structure assembly and the metallic rudder.
TOTAL	+4.9	-0.1	

2.1.2.1 Cover Analysis

The 3D NASTRANS model was updated from level 15 to level 16 and a verification run completed. The deflected rudder conditions were run with the model rudder deflected. None of the deflected rudder conditions exceeded the existing maximum design conditions. The cover is currently designed by a dynamic lateral gust condition. The strains associated with this condition are shown on Figure 2-2.

2.2 MATERIAL VERIFICATION

This task is structured to develop basic material properties for the T300/5208 unidirectional tape material system to derive design allowables for the ACVF.

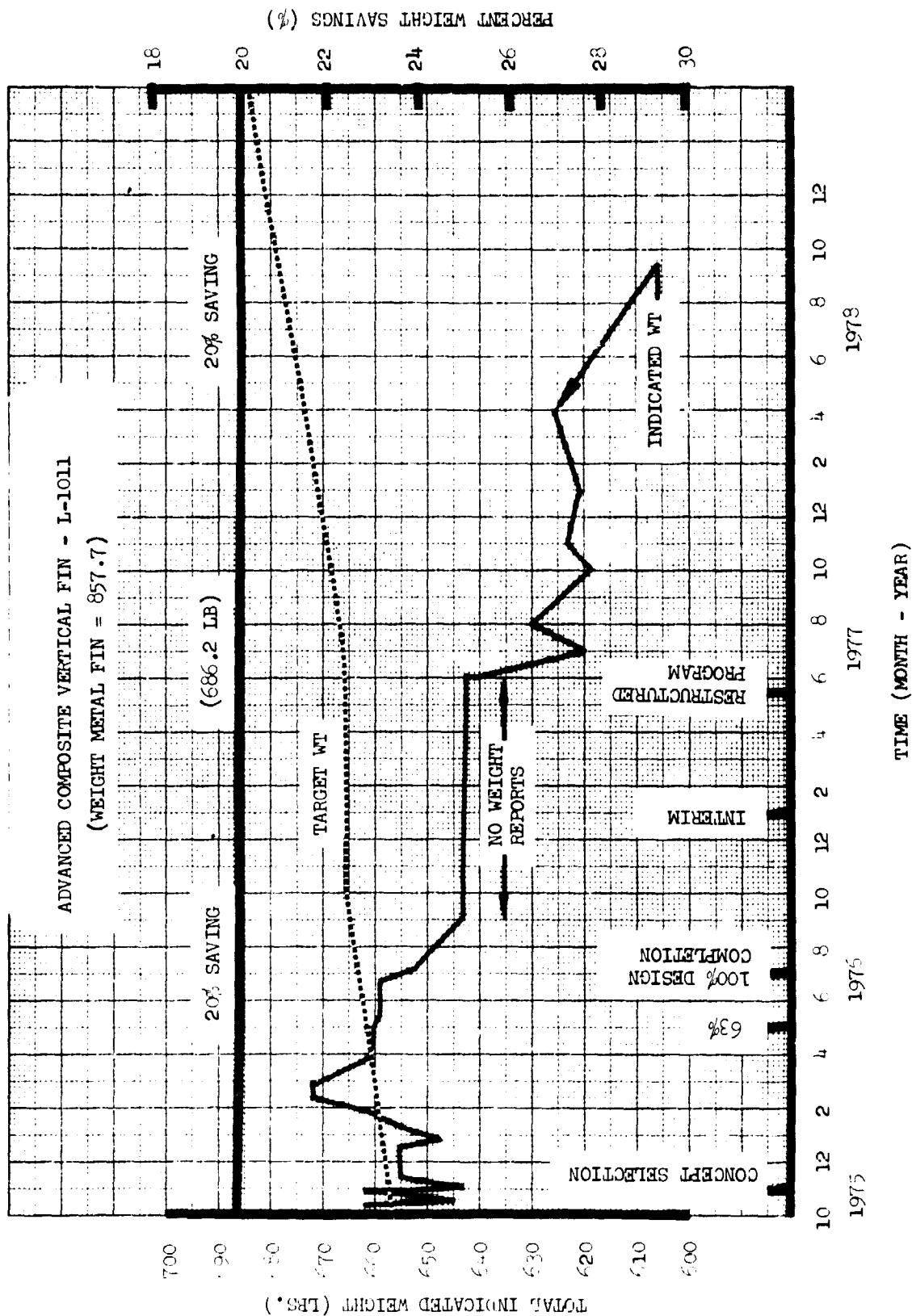


Figure 2-1. Weight Time History

COVER STRAINS (ϵ_x in μ in/in)
 CONDITION 59 - Dynamic Lateral Gust)

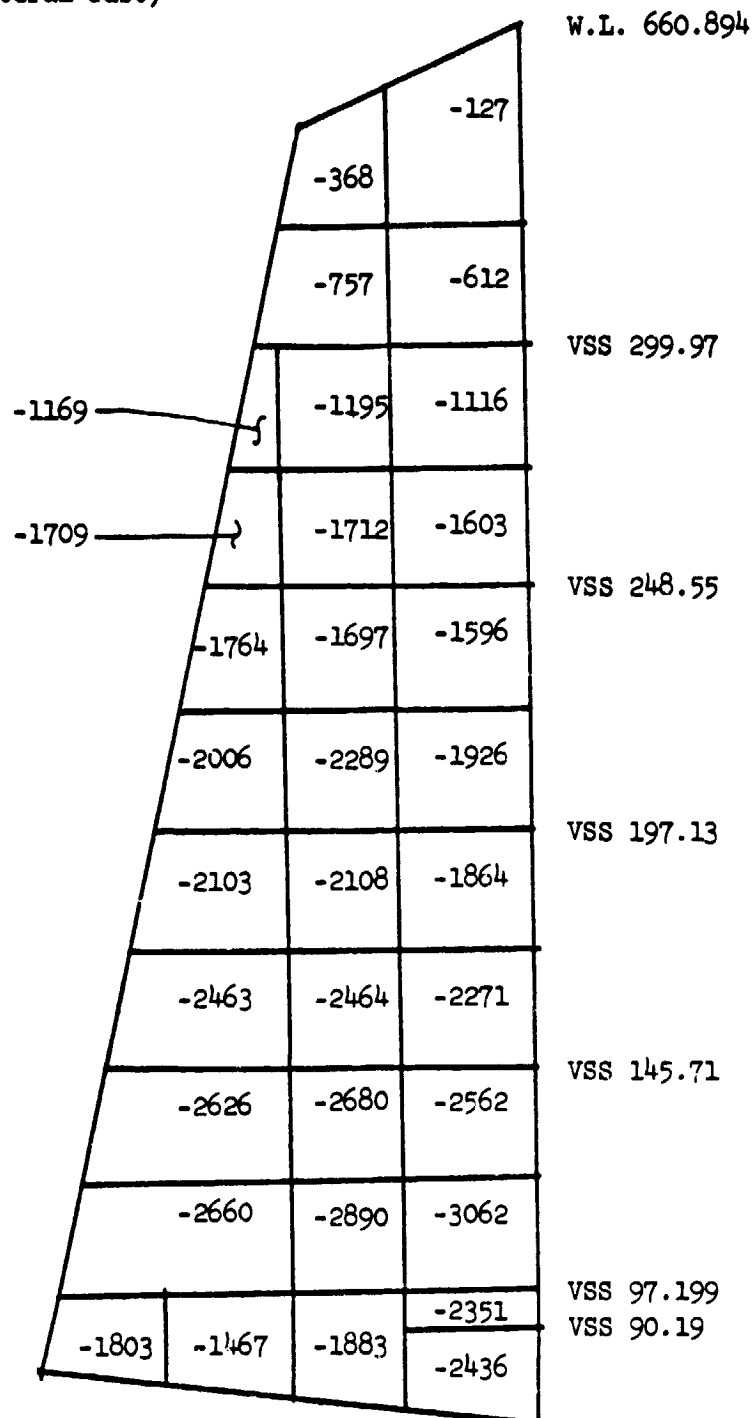


Figure 2-2. Preliminary Cover Strains (Ultimate)

2.2.1 Design Data

2.2.1.1 Damage Tolerance - Item H12A

Evaluation of Damage Tolerance in Composites, Item H12A, is a two part program. Part I consists of evaluating 16 ply 5208/T300 flat panels of $[\pm 45/0/\mp 45/\pm 45/0]_s$ layup. The testing is to be performed on center cracked tension specimens (CCT) in both static and spectrum fatigue modes. Static tests will be performed at -65°F , wet and dry, R.T. dry and 180°F wet. Fatigue coupons would be tested at R.T. dry and wet at conditions and spectrum specified. Wet refers to being conditioned at 150°F in 95 percent relative humidity to 1 percent moisture content.

Part II consists of testing hat stiffened panels that had been damaged by impact. This phase of Item H12A has not been initiated as yet.

The panels for Part I were machined into 18 coupons. Of these, 9 coupons were placed into conditioning at 150°F , 95% - 100% relative humidity until a measured moisture level in the panel had reached 1%. Static testing was initiated and completed using unconditioned specimens at -65°F and R.T. The results of these tests were very tight, with essentially no scatter in evidence.

The specimen configuration is shown in Figure 2-3. An analysis of this specimen was performed using the methods of Nuismer, R.J. and Whitney, J.M., "Uniaxial Failure of Composite Laminates Containing Stress Concentration, Fracture Mechanics of Composite AST17 STP 593 1975 pages 117-142. The analysis prediction was 16900 psi or 16270 psi gross area stress depending on which of the two methods was used. The prediction was based on an infinitely wide plate with a correction factor to account for the finite width.

The R. T. Dry tests failed at a mean gross area stress of 18,800 psi with a coefficient of variation of 2.5%. The -65°F dry tests failed at a mean gross area stress of 18,130 psi with a CV of 3.04%.

2.2.1.2 Defect Tolerance - Item H12B

Evaluation of defect tolerance in composites, Item H12B has the objective of assessing the tolerance to defects in the 5208/T300 composite Laminate.

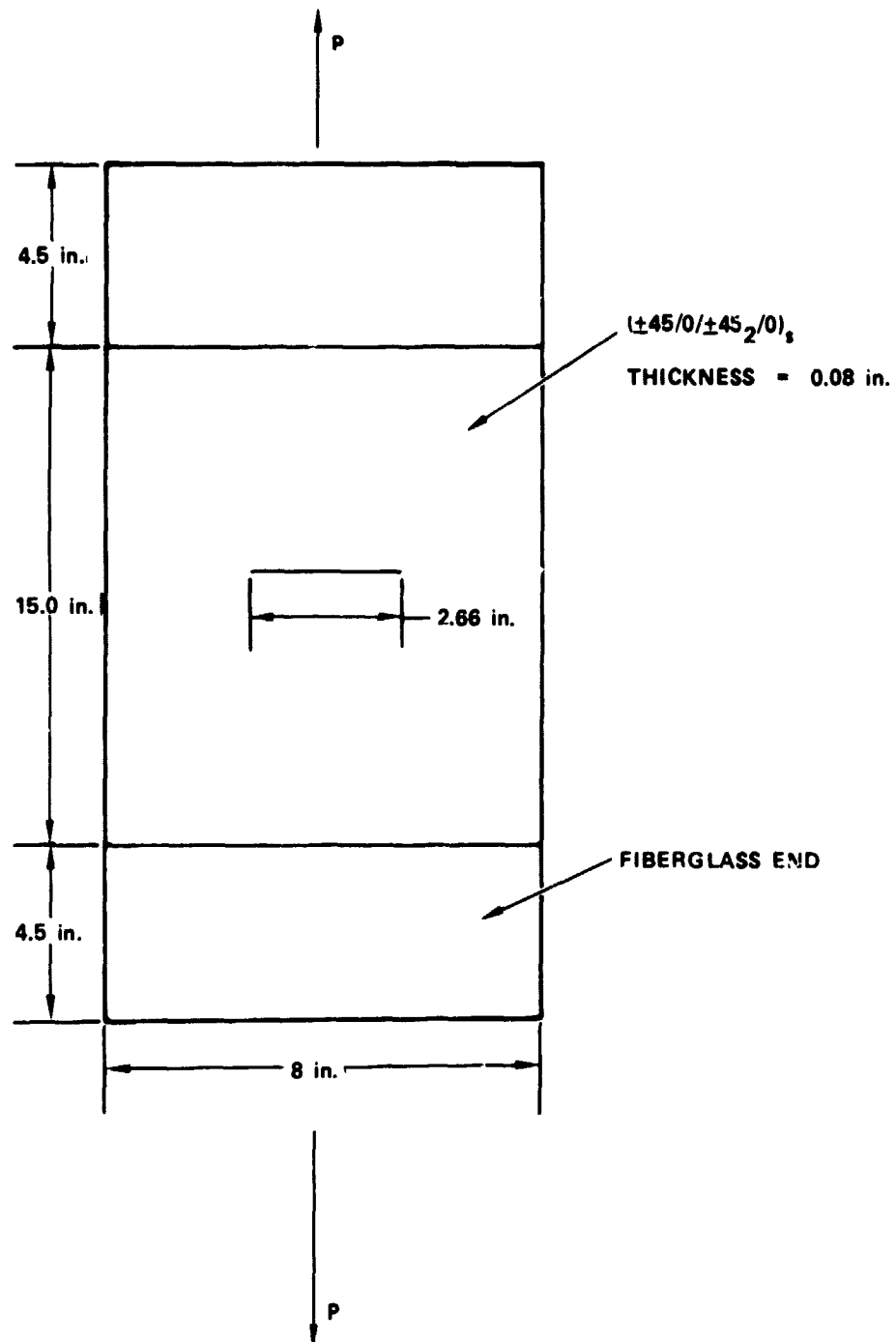


Figure 2-3. Cracked Specimen Geometry

The test program involves fabrication of a laminate containing known size and position defects. The laminate is then machined into coupons for spectrum fatigue testing and identifying the largest defect that can survive four life-times of test. Testing of coupons having 1-inch diameter defects located at two locations within the laminate layers will commence during the next reporting period.

2.2.1.3 Ply Level Data - Item H13AZ

The 180°F dry tension tests conducted on different material batches have been completed and the data summarized in Table 2-3.

2.2.1.4 Laminate Data - Item H13C

This ancillary test program has the objective of developing and verifying design allowable data in tension, compression and shear for cross plied laminates.

The test program consists of performing tests at -65°F, RT and 180°F on both dry and conditioned specimens that include notched and unnotched configurations. The specimens were machined from both 14 and 16 ply panel which had been fabricated at three different sources. Lockheed-California-Test Lab, Lockheed-California-Manufacturing, and Lockheed-Georgia Company.

A total of 365 tests have been performed. This includes 145 tension, 135 compression, 55 interlaminar shear, and 30 in-plane shear tests. Strain readouts were by both extensometer and strain gage methods. Where strain gages are used, tension tests have 1 "T" gage per coupon and compression tests have two axial gages, back-to-back, per specimen. Results obtained showed only small effect, if any, due to different panel fabrication source, but a usual degree of scatter was experienced.

Some poor results were experienced in several of the in-plane shear tests where failure was initiated and/or propagated through the fixture bolt hole

TABLE 2-3. H13AZ TENSION 180°F DRY

Batch	1	2
	196,700	182,300
	208,000	205,700
	233,600	196,400
	200,100	180,900
	175,800	204,400
Mean	202,840	193,940
Coefficient of Variation, C.V.%	10.31	6.09
Standard Deviation	20,911	11,825
Combined Batches		
Mean	198,390	
Coefficient of variation, C.V.%	8.41	
Standard Deviation	16,688	

pattern. This appeared to be a random occurrence and was the first tab failure problem experienced since the use of FM 300 adhesive was initiated.

The testing of the 3-inch wide triple notch tension and compression specimens have been completed. The results are given in Table 2-4. Single notch tests results are included for comparison purposes.

The results for the $[0/\pm 45]_3$ laminates show that there was no effect due to width. The $[0_2/\pm 45]_c$ laminate results were within about $\pm 10\%$ and because of the small number of test specimens this can be considered normal test scatter.

2.3 PROCESS VERIFICATION

This task is designed to develop and prove the manufacturing processes which will be used to produce ACVF components. This development is directed to component configurations and manufacturing processes derived from

TABLE 2-4. TRIPLE NOTCH TESTS

Laminate Type	Condition Notch	Tension R. T. Dry		Compression R. T. Dry	
		Triple	Single	Triple	Single
$[0_2/\pm 45]_c$	Mean	68,566	61,747	73,046	79,825
	C.V. %	8.01	2.92	3.14	6.31
	Std. Dev.	5,495	1,803	2,290	5,038
	No. of tests	3	4	4	5
$[0/\pm 45_3]_c$	Mean	33,894	32,408	42,266	42,151
	C.V. %	1.90	1.61	3.37	2.06
	Std. Dev	645	523	1,425	868
	No. of tests	5	5	4	5

producibility analyses. The principle work accomplished this quarter covered cure cycle and tooling development for cover and rib components.

2.3.1 Materials and Producibility Studies

2.3.1.1 Hat Stiffener Root End

The present hat stiffener root-end design uses a constant section hat stiffener with an 8-ply doubler reinforcement. The close tolerance machining of the root end required to match interface tooling coupled with considerable hand work during layup resulted in a costly fabrication process. Producibility studies conducted on this design resulted in the revised configuration shown in Figure 2-4. The doubler will be made from stepped preplied material and then draped and prebled on a simple straight section matched surface tool. It is then draped on the hat section and heat tacked in place. The cap slope is then machined in the prebled condition - close tolerance machining is not required for this operation.

NOTE: HAT SECTION, WITH 8 PLY DOUBLER IN PLACE, IS PREBLED
AND TRIMMED PRIOR TO LAYING 2 PLY DOUBLER IN PLACE

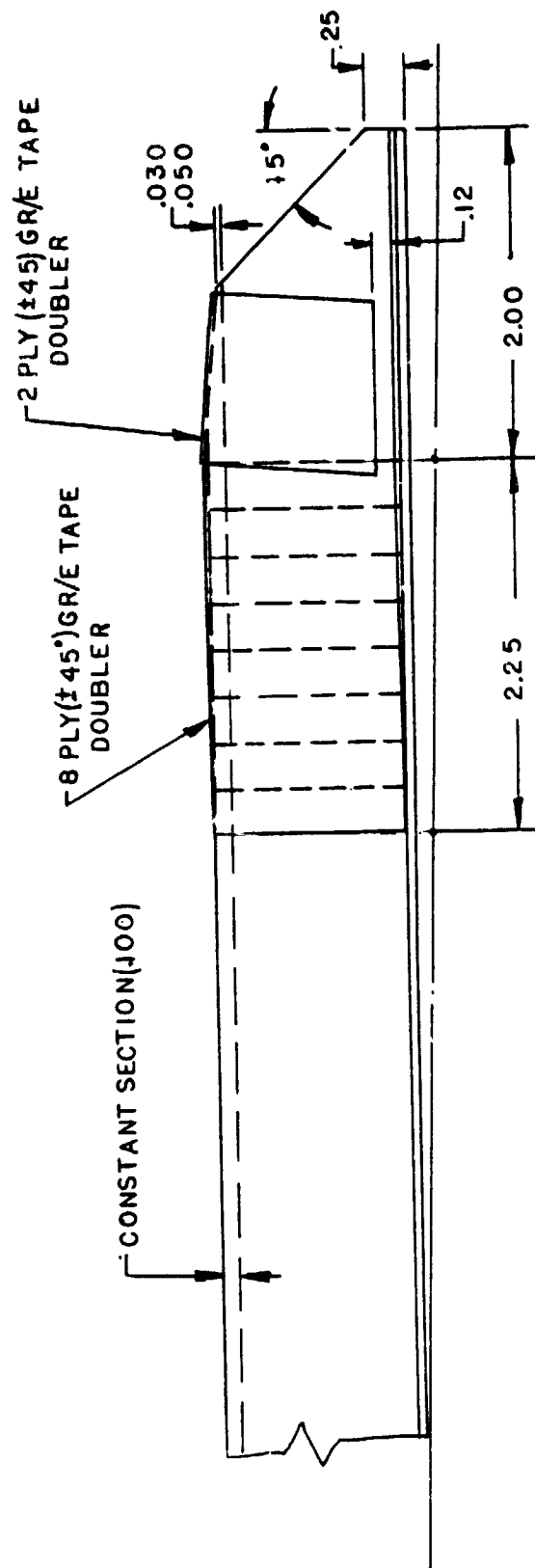


Figure 2-4. Hat Stiffener Root End Configuration

A (2-ply (± 45) doubler is applied as shown on Figure 2-4 to the root end (to protect the cutoff 0° cap plies) when the hat stiffeners are assembled to the skin cover for the single stage autoclave cure.

This revised design results in eliminating the close tolerance requirements and the meticulous hand layup of the doubler reinforcement.

2.3.1.2 Materials and Process Lab Evaluations

The following target values have been established for the various constructions to be used in evaluating the cover assembly and rib specimens made in the tooling and manufacturing development program.

<u>Category</u>	<u>Test</u>	<u>Value</u>	
<u>Visual</u>		PB80-577	
<u>Dimensional</u>	Thickness/ply configuration	0.0046 - 0.0053 inch Drawing req.	
<u>Physical</u>	Resin Content	26-30% by wt.	
	Specific Gravity	1.56 - 1.60	
	Void Content	Info. only	
	Moisture Pickup	0.33% by wt.	
<u>Mechanical</u>		R.T.	180°F Wet
	<u>Short Beam Shear (ksi)</u>		
	10 ply ($\pm 45, 0, \mp 45$) _s	--	--
	16 ply ($\pm 45, 0, \mp 45_2, 0$) _s	7.0	6.0
	16 ply ($0, \pm 45, 90$) _{s 2}	6.0	5.0
	20 ply ($\pm 45, 0, \mp 45, 0_5$) _s	11.0	10.0
	26 ply ($\pm 45, 0, \mp 45$) ₂ ($\pm 45, 0, \mp 45_2, 0$) _s	8.0	7.0
	34 ply (Root end of skin)	10.0	9.0

<u>Compression (ksi)</u>	<u>R.T.</u>	<u>180°F Wet</u>
10 ply	67	60
16 ply	75	70
16 ply (Quasi-isotropic)	90	75
20 ply	--	--
26 ply	78	73
34 ply	--	--

No SBS value is given for the ten-ply construction as it is too thin for this test. No compression values were set for the 20 and 34-ply constructions which have a 0° fiber content of 50 percent or greater because the simple compression test fixture that is used is not capable of transmitting sufficient load into the specimen.

Only limited hat-skin bond tests have been run on the single-stage cured specimens because of the nonuniform quality that exists in the first tooling and manufacturing development specimens. The preliminary results were lower than were obtained on a hat-skin bonded specimen using AF-55 adhesive. These results are shown in Figure 2-5.

2.3.2 Process Development Studies

2.3.2.1 Cover Development

Cover development has continued according to the Process Development Plan. This plan leads to the selection of a mandrel system and a caul material which, with appropriate processing methods, will consistently produce single-stage cured covers which will meet Engineering requirements at acceptable costs.

Solid Rubber Mandrel

During this reporting period, six cover specimens, each four feet long including a single hat stiffener were fabricated using the solid rubber mandrel concept. Three specimens, one with a steel caul, one with a fiber-glass caul, and one with a rubber sheet in lieu of a rigid caul, were cured

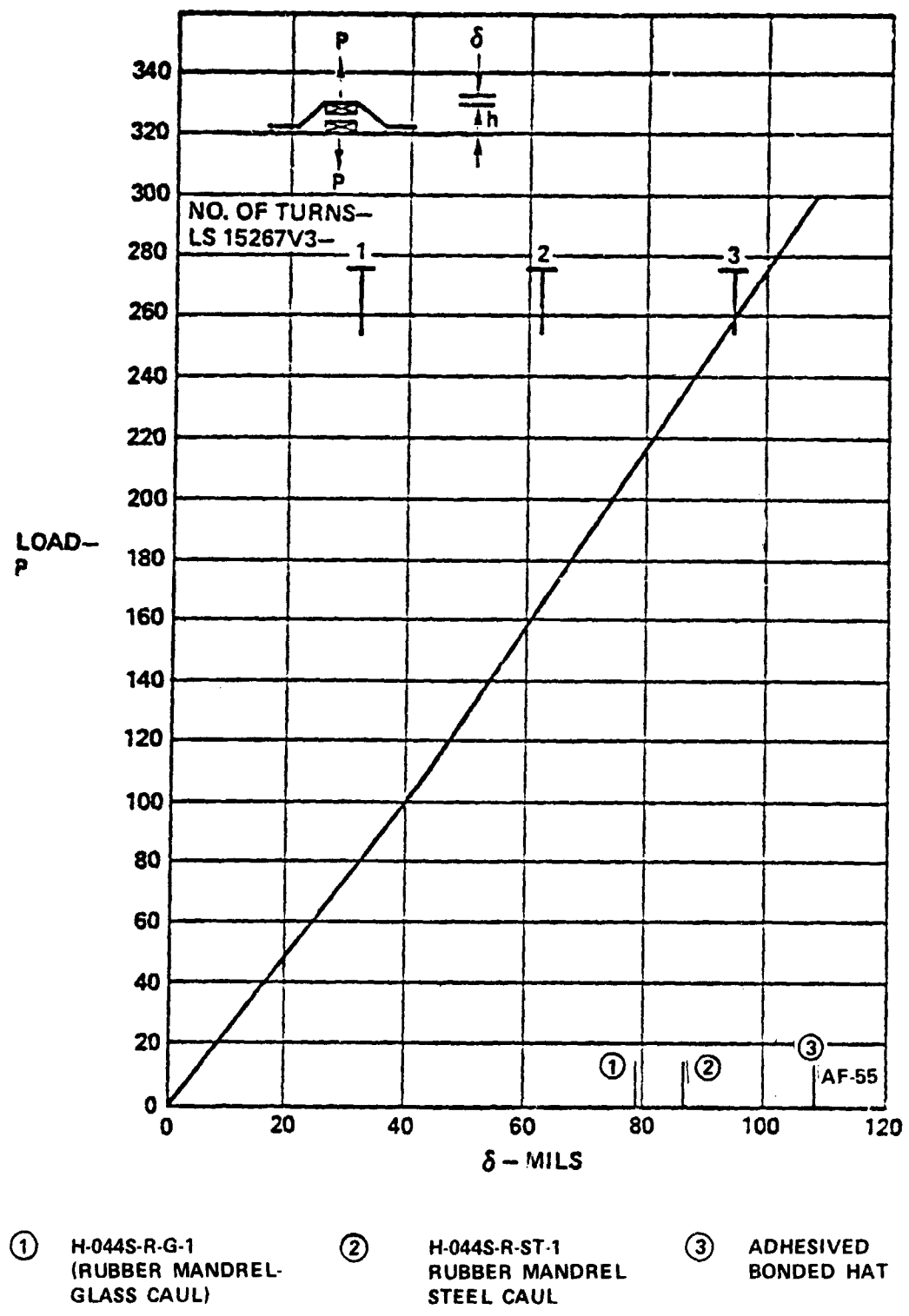


Figure 2-5. Composite Stiffener Skin Specimen Calibration Curve



using the 250°F/85 psi initial cure 350°F postcure regime. A second set of three was cured using the 350°F/85 psi regime with each of three caul systems. Figure 2-6 shows mandrel and caul arrangement. All solid rubber mandrels have been cast with Silastic J.

Examination of the hat flange-to-skin by C-Scan techniques showed that those specimens cured at 250°F/350°F postcure and those cured at 350°F contained discrepant areas. These C-scan NDI findings are reported more fully in Section 2.4.

Test results for the six cover specimens obtained from coupons cut from the hat flange-to-skin are shown in Table 2-5.

Analysis of the three specimens cured at 250°F indicates that a poor bond was obtained in the hat flange-to-skin area near the ends of the hat. These areas of poor bond directly relate to the use of rubber seal around the steel end blocks used to restrain the rubber mandrel during cure.

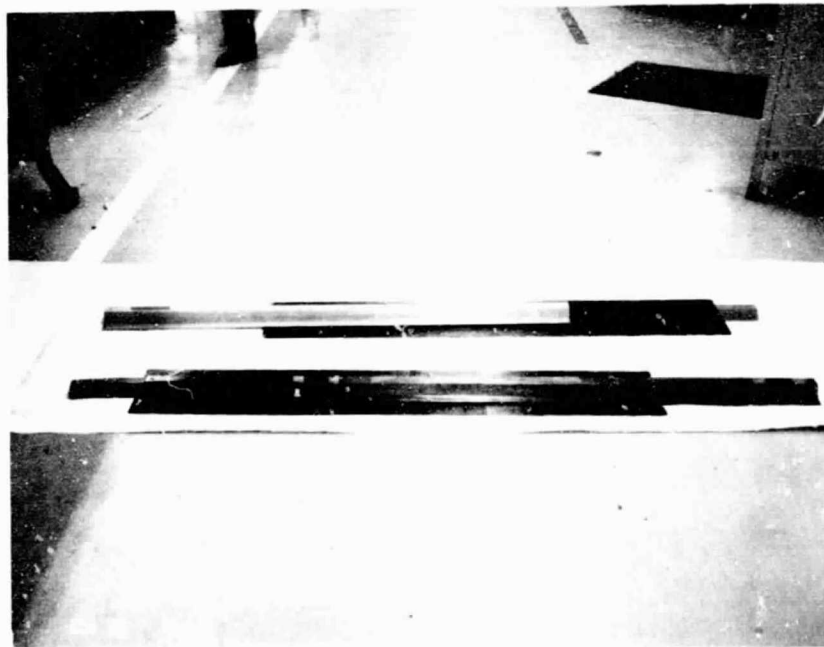


Figure 2-6. Cured Hat/Skin Cover Specimens. Solid rubber mandrels are shown partially withdrawn. Caul in foreground is steel, caul in background is fiberglass.

TABLE 2-5. LABORATORY TEST RESULTS. HAT FLANGE-TO-SKIN

Test Property	Spec. Req.	250°F Cure			350°F Cure		
		Glass Caul	Steel Caul	No Caul	Glass Caul	Steel Caul	No Caul
Specific Gravity	1.56-1.60	1.56	1.58	1.58	1.54	1.48	1.52
		1.59	1.56	1.58	1.55	1.47	1.51
Resin Content	26-30%	33.9	30.4	28.8	33.9	33.1	35.2
		28.2	33.4	29.4		32.4	34.8
Water Absorption	0.33%	0.19	0.16	0.19	0.59	2.77	1.55
		0.16	0.18	0.19		2.55	2.49
Short Beam Shear @ 75°F	8 ksi	8.4	8.0	7.5	5.9	4.6	4.8
		7.4	6.0	8.1		4.8	4.5

Rubber seals, used to prevent excessive outflow of the resin from under the hat during cure, expanded during the heat-up cycle, lifting the hat flange from the skin, thereby preventing a satisfactory bond.

Three specimens, with the caul materials described above were cured using the 350°F regime and with end blocks without the rubber seal. The high resin content, high water absorption, and low short beam shear values for these specimens are attributed to a vacuum bag seal leak which occurred during the autoclave cycle.

Both the 250°F and the 350°F cure of assemblies for all caul systems exhibited a decrease in the flange/skin thickness outward from the hat wall. (See Figure 2-7.) This taper effect indicates a pressure imbalance during cure. The pressure exerted by the rubber mandrel on the inner surface of the hat stiffener was greater than the counteracting autoclave pressure applied to the outer surface of the hat stiffener. This pressure imbalance results in inadequate pressure at the flange-to-skin interface and allows the hat to lift upward from the skin. To overcome this problem, autoclave pressure applied at 150-160°F will be increased from 10 psi to 20 psi to assure adequate pressure at the flange-to-skin interface and to introduce adequate resin flow prior to gelation. The additional pressure at this temperature is planned to counteract any lifting force exerted by the rubber mandrel.

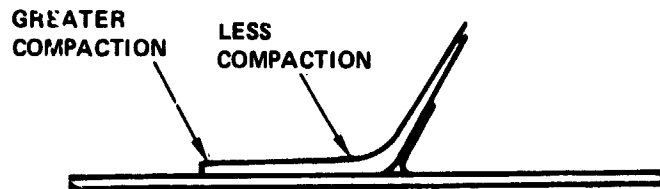


Figure 2-7. Thinning of Hat Flange Attributed to Pressure Imbalance

A recurring problem experienced with the solid rubber mandrel tooling approach has been mark-off on the outside skin surface along the inner hat radius and also along the flange edge. This condition may be observed in Figure 2-8. The mark-off lines indicate a lack of pressure during cure at these places. Investigation of methods of eliminating or minimizing this condition are continuing.

Development of tooling concepts for the cover configuration at the root end is also in process. Six hat/skin panels designated have been cured and processed through NDI and the QA laboratory. The root-end portion of one of these panels is shown in Figure 2-9. Tooling development is underway to improve the method of close-out at the end of the pretrimmed hat stiffener to provide better control of resin flow in this area.

These six panels were fabricated and cured in two separate batches. In the first batch, one fiber glass caul with pressure pads in the flange radii, one fiberglass caul without pressure pads, and one hat with no caul were used. Two glass cauls and a steel caul were used for the second batch. The physical and mechanical properties are given in Table 2-6.

Review of the dimensional data taken on these specimens confirms that the definition of the cured laminate is highly dependent on the accuracy of the caul system used. It was also concluded that laminates cured without the use of caul sheets were unsatisfactory. No particular problems were observed relative to the angular transition of the hat at the root end.

ORIGINAL PAGE IS
OF POOR QUALITY

LR 28573

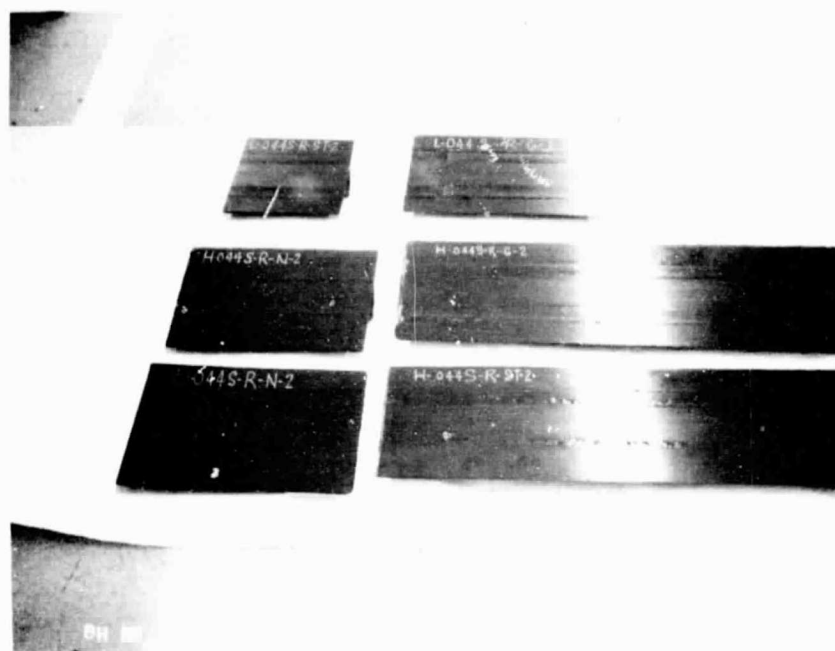


Figure 2-8. Outside Skin Surface of Cured Specimens. "H" on specimen indicates 350°F cure. "L" indicates 250°F cure with 350°F postcure. Mark-off is more pronounced on "H" specimens.

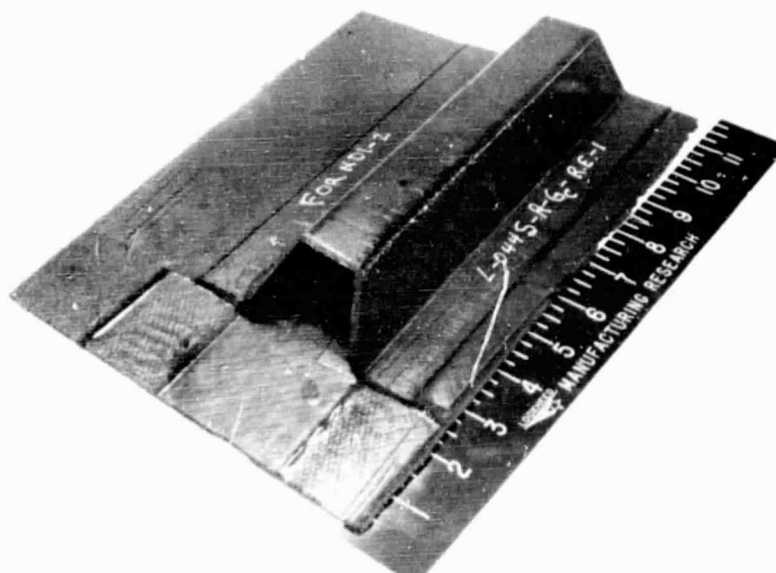


Figure 2-9. Single-Stage Cure Root End Assembly.

TABLE 2-6. LABORATORY TEST RESULTS HAT-TO-SKIN 250°F CURE/350°F POSTCURE
(Specimens Cut From Skin Under Hat)

Test Property	Target Values	Batch 1			Batch 2		
		Glass Caul W/ Press. Pads	Glass Caul	No Caul Press. Pads	Glass Caul	Steel Caul	No Caul
Resin Content	26-30%	27.4	27.4	35.3	27.5	24.7	
Specific Gravity	1.56-1.60	1.57	1.58	1.56	1.57	1.58	
Water Absorption							
2 hr	0.33%	0.33	0.09	0.16	0.12	0.12	
24 hr	0.75%	0.77	0.48	0.65	0.62	0.52	
Short Beam Shear	7 ksi	7.1	7.4	Not Avail	7.0	7.5	
Specimens Cut From Hat Flange/Skin Laminare							
Short Beam Shear	8 ksi	9.1	8.8	5.5	7.4	7.1	
		7.7	8.5	5.7	6.4	9.5	

An additional panel was fabricated using a convention 250°F cure cycle with 350°F postcure. This panel was 44 inches long and was three hat bays wide. Its purpose was to determine what effect, if any, a series of adjacent hats single-stage cured to a skin would have on the hat/skin assembly, particularly in the skin area between hats, and also to observe any variations due to the use of the solid rubber mandrel in combination with alternate caul materials. In the assembly, a fiberglass/phenolic caul was used on one outer hat, a fiberglass/epoxy caul on the other outer hat, and a steel caul on the center hat. This panel is seen in Figure 2-10. Examination of the panel indicated that no discrepancies were introduced by the multiple hat configuration. Again, the hat definition appeared to conform closely to caul variations. The fiberglass/phenolic caul, in particular, contained areas where the flange-to-skin radius was not sharply defined and the same condition was evident in the laminate in those areas.

Physical measurements of the sections cut from this panel also indicated an excess in mandrel pressure as evidenced by a thinner laminate at the outside edges of the hat flanges. As a result, a recheck of the mandrel sizing calculation was made and it was determined that the mandrels may have been oversized by the thickness of the internal two ply clip. New mandrels are being cast to the revised dimension.

The panel was inspected by ultrasonic C-scan (reported in the quality assurance section 2.4). Physical and mechanical properties of specimens cut from the panel are shown in Table 2-7.

Foam Mandrel

Development of the foam mandrel system, as an alternative to the solid rubber mandrel system, is continuing. As described in previous reports, a foam mandrel is used to support an internal hat bag until vacuum can be applied. Thus, with both an inner and outer bag, pressure is applied to the hat and skin during cure. In the cure process the foam shrivels and is easily removed with the inner bag. A four foot long section of hat was cured with a skin using a foam mandrel. Figure 2-11 shows this specimen after cure with the bagged mandrel partially removed. An unused foam mandrel is shown

TABLE 2-7. LABORATORY TEST RESULTS - THREE HAT WIDE PANEL
(Hat-To: n 250°F Cure/350°F Postcure)

Test Property	Target Value	Hat Cured W/F Glass Caul			Hat Cured W/Steel Caul		
		Hat Crown	Flange/ Skin Lam	Skin Ads To Hat	Hat Crown	Flange/ Skin Lam	Skin Ads To Hat
Resin Content	26-30%	24.8	28.4	24.3	24.1	27.3	26.0
Specific Gravity	1.56-1.60	1.59	1.58	1.59	1.59	1.54	1.57
Short Beam Shear Crown	11 ksi	9.0 9.0			10.7 12.3		
Flange/Skin	8 ksi		7.5 7.7			7.4 6.9	
Skin	7 ksi			6.5 6.5			8.2 7.5

ORIGINAL PAGE IS
OF POOR QUALITY



Figure 2-10. Three Hat Wide Cured Panel

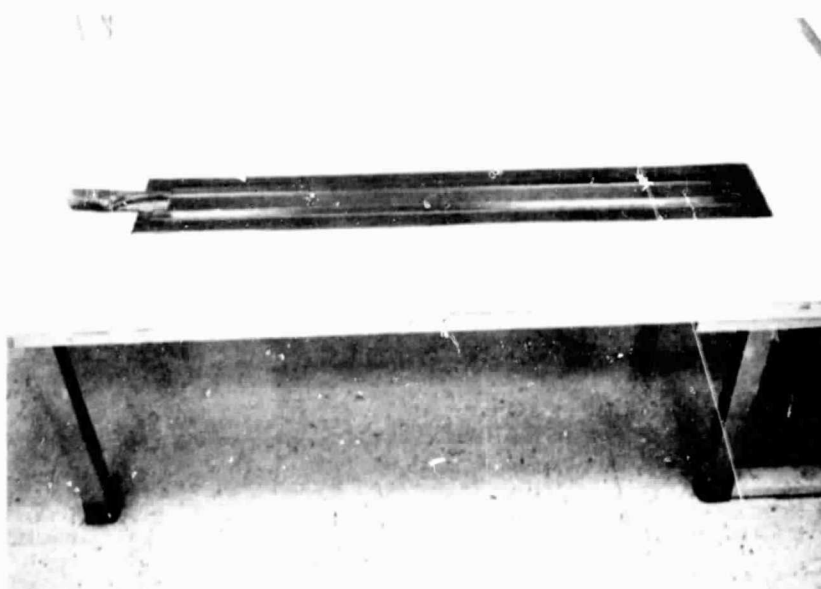
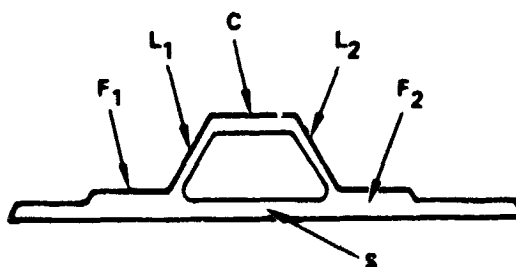


Figure 2-11. Cured Hat/Skin Specimen. Bagged foam mandrel shown partially withdrawn. Unused foam mandrel is shown adjacent with caulk plate in background.

TABLE 2-8. LABORATORY TEST RESULTS. (HAT-TO-SKIN COCURE. FOAM MANDREL.)

	Target	F ₁	F ₂	L ₁	L ₂	C	S
Resin Content %	26-30	28.6	29.0	29.2	30.6	29.2	30.3
Specific Gravity	1.56-1.60	1.58	1.57	1.56	1.56	1.58	1.56
Water Absorption %							
2 hr	0.33	0.12%	0.20%	0.47%	0.41%	0.16%	0.32%
24 hr		0.47%	0.50%	1.04%	1.00%	0.64%	0.74%
Short Beam Shear @ R.T. (in psi)	8,000 11,000	8,109	8,199	*	*	-- 10,285	*
Compressive Strength @ R.T. (in psi)	75,000	*	*	*	*	*	61,275

* - Not applicable



adjacent to it. The mark-off condition on the outer skin surface was also evident in this specimen. Test results are shown in Table 2-8.

A review of these results indicates that the foam mandrel concept is capable of producing satisfactory parts. NDI results verified external discrepancies noted by visual examination. Figure 2-12 shows a portion of this assembly. The wrinkled portion shown adjacent to near flange is due to the use of a rubber strip adjacent to the flange during cure. This was done in an attempt to assure application of pressure at the edge of the hat flange. This part was cured using a fiberglass caul. The prebled hat and skin layup was cured at 350°F.

A second hat/skin assembly using a foam mandrel was made. Test results are given in Table 2-9. This second assembly evaluated an improved method of

ORIGINAL PAGE IS
OF POOR QUALITY



Figure 2-12. Hat-to-Skin Assembly Using a Foam Mandrel

TABLE 2-9. LABORATORY TEST RESULTS HAT-TO-SKIN FOAM MANDREL

	Target Value	Actual
Resin Content %	26-30	29.1
Specific Gravity	1.56-1.58	1.59
Water Absorption %		
2 hr	0.33	0.12
12 hr	0.75	0.45
Short Beam Shear (ksi)		
Left flange/skin	8	7.3

wrapping the foam mandrel to provide a better release of the internal pressure bag after cure. On the first assembly a nylon film bag was used which did not release easily from the interior of the hat after cure. (See Figure 2-13). Also, a single ply of bleeder was added to the second assembly as shown to provide resin control in the skin area under the hat.

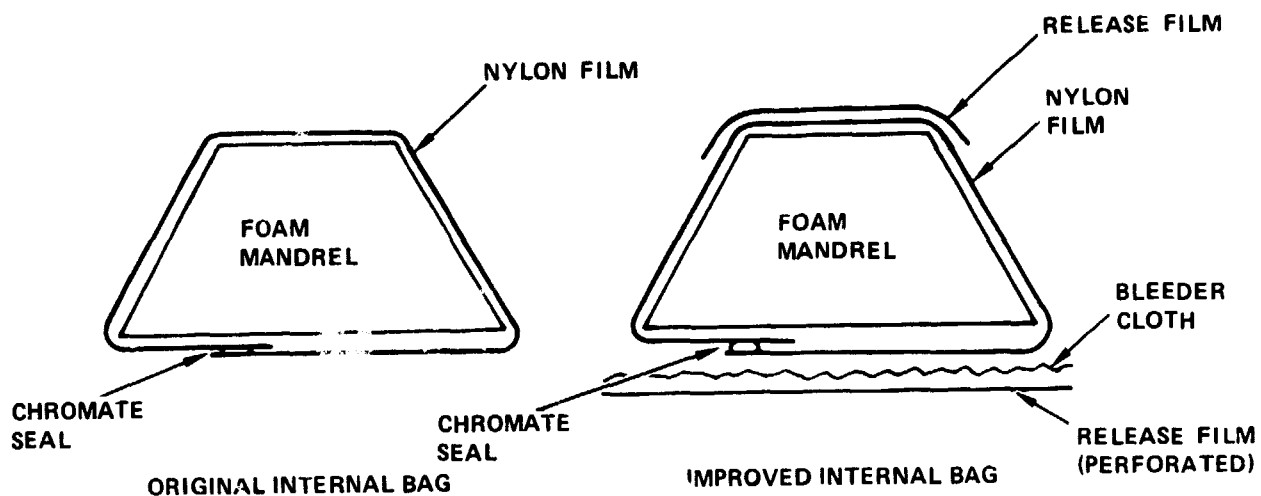


Figure 2-13. Original and Improved System for the Foam Mandrel System

The third panel made using the foam mandrel concept was 4 feet long and 3 hat bays wide. See Figure 2-14. Two phenolic/glass and one epoxy/glass hat caul sheets were used. To enhance corner definition at the hat/skin flange, metal close-out strips were used.

The part was cured in a continuous 350°F cure cycle. No problems were encountered with the removal of the mandrels after cure. In this hat/skin section, the mandrel was enveloped with a layer of tedlar release film. This measure was sufficient to promote easy removal. See Figure 2-15.

A visual inspection of the cured article indicated that some of the metal close-out strips were displaced during bagging or at some point prior to cure. This resulted in insufficient compaction in the affected areas, as reflected by excessive flange thicknesses and mark-off on the skin side. See Figure 2-16.

Another observation was, that the use of phenolic/glass hat caul sheets resulted in waviness and resin-rich corners, when compared to the hat section formed by the epoxy/glass caul sheet. This confirmed previous observations.

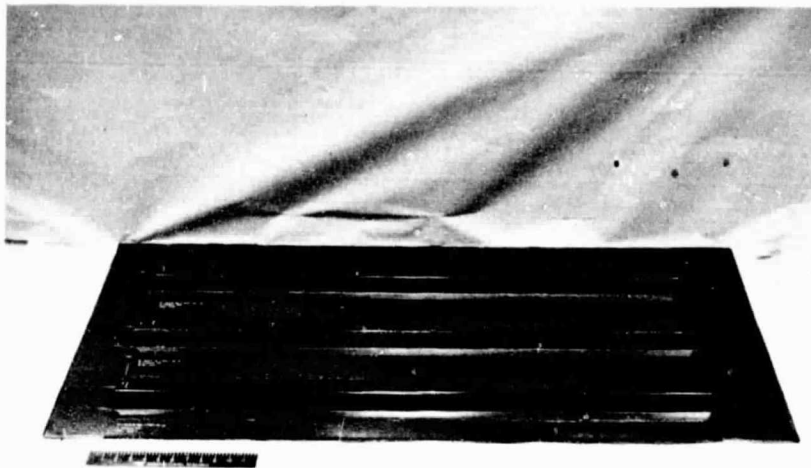


Figure 2-14. Three Hat Wide Panel Cured Using the Foam Mandrel Concept

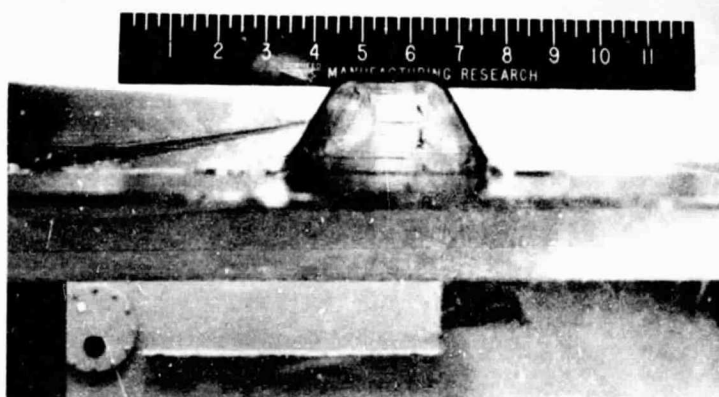


Figure 2-15. Interior of Hat Showing Clean Release of Foam Mandrel

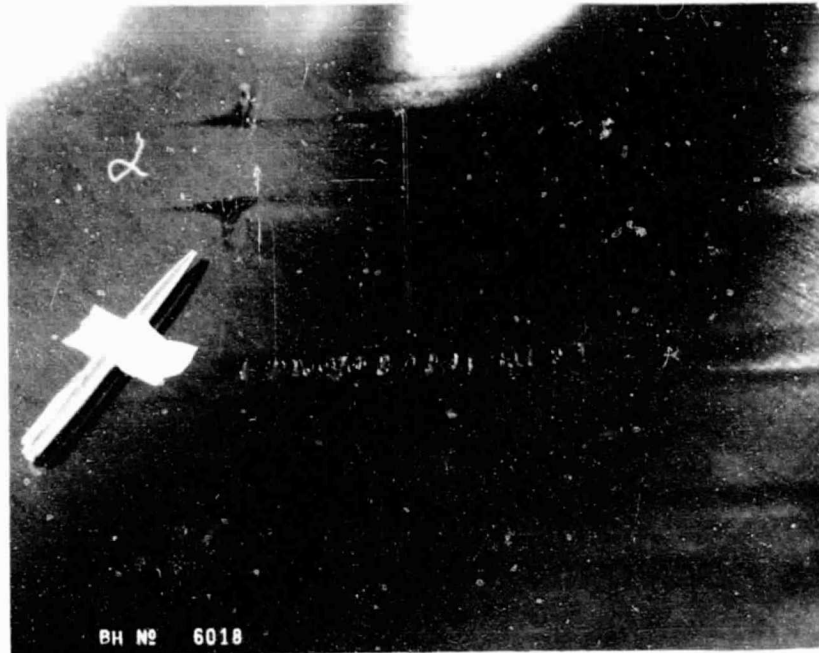


Figure 2-16. Mark-off Due to Lifting of Hat Flanges

The ultrasonic scan confirmed the existence of delamination in the areas where the dislodged metal close-out strips prevented the caul sheets from closing. Lab specimens of these areas will be compared to target values.

Cast Mandrels

The first eighteen inch long bladder has been rotationally cast to develop casting techniques. Silastic E rubber was used. The bladder had very uneven wall thickness. A single-stage cure hat/skin assembly was attempted with this bladder, but the bladder failed in the thin portions allowing loss of pressure on the part. The part was unacceptable and other than a C-scan no testing or evaluation was done.

Additional silastic E rubber has been received and casting development is continuing. Figure 2-17 shows the development set-up for casting mandrels.

ORIGINAL PAGE IS
OF POOR QUALITY

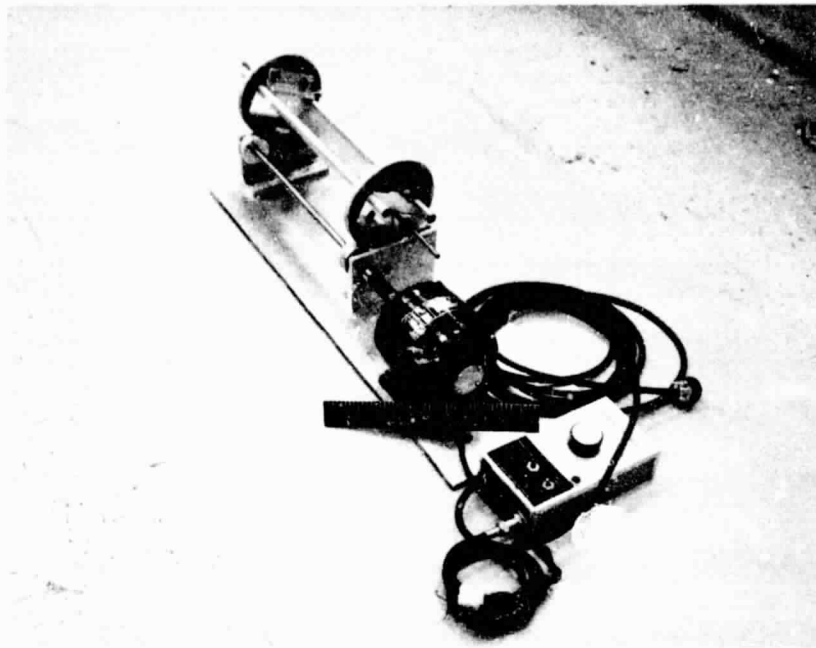


Figure 2-17. Rotational Casting Machine for Development of Cast Bladders

Formed Bladder

Another alternative to the solid rubber mandrel being investigated is the formed elastomeric bladder made by curing rubber sheet stock in a female mold configured to inside hat dimensions.

Two formed bladders have been made. The first was a bladder with fabricated end closures which each gripped a short length of copper tubing. This tubing allowed autoclave pressure to be applied to the inside of the bladder. A single-stage cure hat/skin assembly was fabricated with this bladder, but leakage occurred through the interface between the tubing and the end closures. Visual inspection of this part showed a good quality laminate with minimal evidence of porosity or low pressure areas on the skin surface. Ultrasonic inspection indicated some questionable areas in the hat-to-skin interface, but these could be attributed to the unevenness of the flanges on the steel caul which was used. The assembly was sectioned and two portions

were delivered to the QA laboratory for testing. Test results indicated the following:

	Target Value	Specimen Coupon
Resin Content %	26-30	32.7
Specific Gravity	1.56-1.58	1.56
Water Absorption %		
2 hr	0.33	0.15
24 hr	0.75	0.43
Short Beam Shear (ksi)	8.0	6.8-8.0

A second formed bladder was fabricated incorporating certain changes. One, a full length perforated tube, was used instead of the short tubes at each end which had been used on the first bladder. Additionally, the tube was sealed into the end closure of the bladder with silicone rubber R.T.V. sealant. (See Figure 2-18.) A hat/skin assembly was cocured with this bladder.

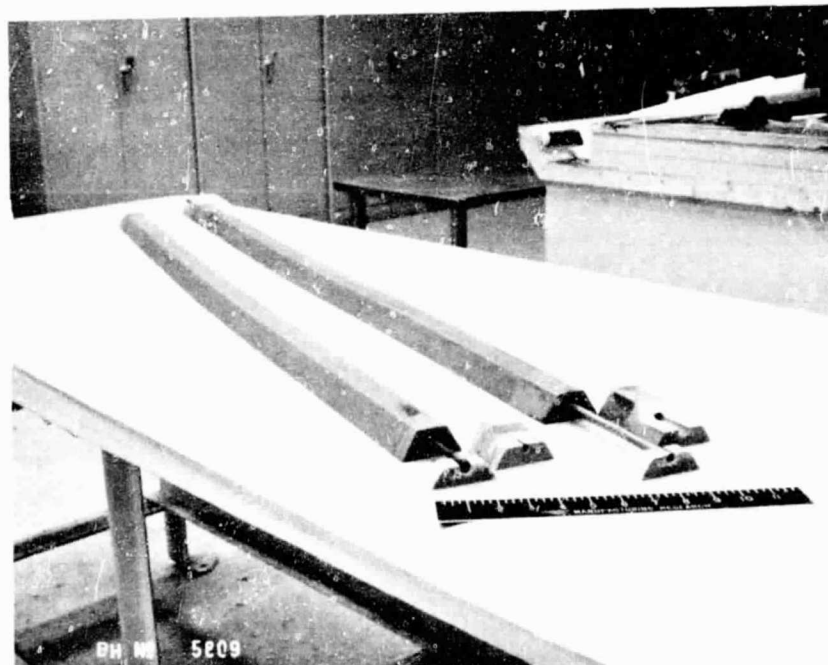


Figure 2-18. Formed Rubber Mandrels. Bladder on left is pressurized through a short length of tubing. Bladder on right has a full length perforated tube

Visual inspection of the cured part showed laminate quality to be similar to the first part. Ultrasonic inspection showed similar indications to the first part and in approximately the same locations. (The caul sheet has since been reworked to remove the waviness and angularly discrepant areas.) Upon removal, the bladder was torn at two locations because of adherence to the hat. Succeeding bladders will have mold release applied to prevent repetition of this condition.

Two portions of the part cured with the second bladder were tested. The results were as follows:

	Target Value	Specimen Coupon
Resin Content %	26-30	34
Specific Gravity	1.56-1.58	1.54
Water Absorption		
2 hr	0.33	0.27
24 hr	0.75	0.74
Short Beam Shear (ksi)	8.0	6.0-8.8

Modifications will be made in the construction of the bladder for the next part. These include closing one end completely and altering the configuration of the other end for better extraction clearance and improved tube to bladder bonding. These changes are being made on the tool design at present. After completion of the tool design changes, material will be ordered and tooling changes incorporated. After this third bladder is completed and checked, a hat/skin assembly which incorporates the root-end configuration will be single-stage cured and evaluated.

2.3.2.2 Rib Development

A series of tests are being conducted to corroborate the cure cycles prescribed in the process bulletin for the fabrication of the rib caps. Two sets of 20 inch long rib cap specimens were cured per the requirements of the process bulletin. Each set consists of a truss rib and an actuator rib specimen. Two additional sets of parts are being cured with a modified cure cycle whose intent is to shorten the elapsed cure time without detriment to the part. The first of these has been cured and the ends have been submitted to the Q.A. laboratory for testing. After the last of these four specimens has been cured and evaluated,

the data will be analyzed and used to establish a cure cycle for the ancillary test specimens.

The layup tool for the truss rib ancillary test specimens (H24AT, H20A) has been completed. Tool proving is scheduled during the next reporting period.

2.3.2.3 Cutting Machining, and Trimming

A bandsaw has been equipped with a spiral (Tyler) blade and associated guide roller. Preliminary tests indicate that this type of blade will be satisfactory for cutting through rib cap webs for hat clearance cut-outs. See Figure 2-19. Testing will continue.

Tooling for making the hat section cut-outs in the rib cap is being developed.

Tests to evaluate methods of cutting the root end of the prebled hat are continuing. Such techniques as abrasive saw, fine tooth jeweler's circular saw, and a knife edge circular saw have been tried without completely satisfactory results. Trial cuts of the hat clearance cutouts in the rib caps have been made using an abrasive saw to cut through the cap flange followed by spiral saw blade to cut the pattern of the hat cutout. Good results were obtained.

2.4 QUALITY ASSURANCE

2.4.1 Laboratory Tests

The Quality Assurance Laboratory performed the following basic functions during the reporting period: (1) Batch testing to assure that the graphite/epoxy material is acceptable prior to its use, and (2) Testing of parts fabricated for either the process development studies or the Engineering Ancillary Test Program.

2.4.1.1 Acceptance Tests

No new graphite material was received during the reporting period. However, batch numbers 798, 1015 and 1026 of T300/5208 graphite/epoxy material were retested to satisfy Engineering and Quality Assurance requirements. Excessive out time and poor packaging by the supplier were cited as reasons for retest. All three batches were accepted and test results are shown in Table 2-10.

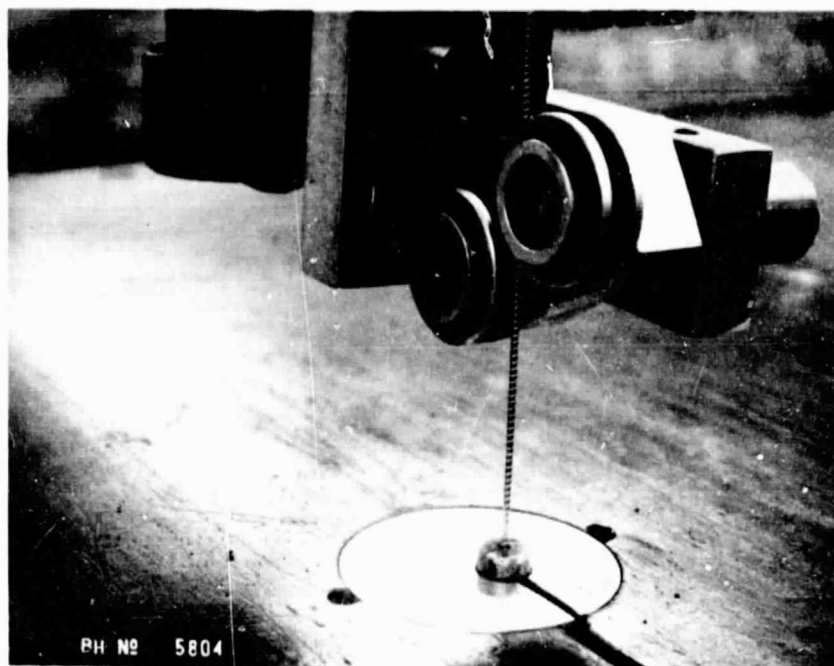


Figure 2-19. Bandsaw Equipped with Spiral (Tyler) Blade

2.4.1.2 Process Development Tests

The Quality Assurance Laboratory continued to support the single-stage process development program. Thirty hat/skin assemblies, twenty one flat panels and sixteen rib caps were tested per requests from Manufacturing Research and Engineering. Specific tests include: Compressive strength, short beam shear, hardness, resin content and specific gravity. Test results are shown in Tables 2-5 through 2-9.

2.4.2 Nondestructive Inspection (NDI)

During this reporting period activity has centered on the following areas:

- Support of Tool and Process Development Program.
- Support of Ancillary Tests.
- Implementation of the NDI Evaluation Program.

2.4.2.1 Process Development Specimens

Hat Stiffened Cover Specimens

As part of the tool and process development manufacturing effort the following hat stiffened panels were submitted for ultrasonic inspection:

TABLE 2-10. T300/5208 BATCH ACCEPTANCE TEST RESULTS

C22/1379/111 SPECIFICATION REQUIREMENTS	1	2	3	4	5	AVG
Flow (2) at 350°F at 85 psi	18.5	19.1				18.8
Gel Time (2) at 350°F	20.5	20.8				20.7
Cured Fiber Volume (3) 0.080 in. Panel	63.2	63.3	63.2			63.2
Specific Gravity (3) 0.080 in Panel	1.57	1.57	1.57			1.57
Flexural Strength (3) at 75°F	248	268	253			256
Short Beam Shear (3) at 75°F	15.5	15.3	14.7			15.2

LR 28573

NOTES: Batch 798 Retest
 Date 3-1-78
 Lab Report 345115



TABLE 2-10. T300/5208 BATCH ACCEPTANCE TEST RESULTS - CONT'D.

C22/1379/111 SPECIFICATION REQUIREMENTS		1	2	3	4	5	AVG
Flow (2) at 350°F at 85 psi	15-29%	20.9	20.5				20.7
Gel Time (2) at 350°F	Info only, minutes	19.5	20.1				19.8
Cured Fiber Volume (3) 0.080 in Panel	60-68%	62.4	61.8	62.1			62.1
Specific Gravity (3) 0.080 in Panel	1.55-1.62	1.57	1.57	1.57			1.57
Flexural Strength (3) at 75°F	210 ksi, min, ind	266	257	263			262
Short Beam Shear (3) at 180°F	12 ksi, min, ind	15.1	15.1	14.1			14.3

NOTES Batch 1015 Retest
 Date 3-1-78
 Lab Report 345500

LR 28573





TABLE 2-10. T300/5208 BATCH ACCEPTANCE TEST RESULTS - CONCLUDED

C22-1379/111 SPECIFICATION REQUIREMENTS		1	2	3	4	5	AVG
Flow (2) at 350°F at 85 psi	15-29%	20.9	20.7				20.8
Gel Time (2) at 350°F	Info only, minutes	21.5	21.4				21.5
Cured Fiber Volume (3) 0.080 in Panel	60-68%	64.8	64.5	65.1			64.8
Specific Gravity (3) 0.080 in Panel	1.55-1.62	1.58	1.57	1.58			1.58
Flexural Strength (3) at 75°F	210 ksi, min, ind	267	264	261			264
Short Beam Shear (3) at 75°F	13 ksi, min, ind	13.8	13.4	14.8			14.0

LR 28573

NOTES: Batch 1026 Retest
Date 3-1-78
Lab Report 345499

L-044S-R-N-2	H-044S-FO-G-2	L-044S-R-N-B-R/E-1
L-044S-R-G-2	H-018S-CB-ST-1	L-044S-R-G _c -R/E-1
L-044S-R-ST-2	H-046S-FB-ST-1	*L-048S-R-G ₁ -3
H-044S-R-S-2	L-048S-R-G-4	L-048S-R-ST-3
H-044S-R-N-2	*L-044S-R-N-R/E-1	L-048S-R-G ₂ -3
H-044S-R-G-2	L-044S-R-G _B -R/E-1	*H-044-TR-FO-3-L
H-044S-I-ST-1	L-044S-R-G _a -R/E-1	H-044-TR-FO-3-M
H-044S-FO-G-1	*L-044S-R-ST _a -R/E-1	H-044-TR-FO-3-R

*Single skin with three hat stiffeners.

These specimens produced with various cauls and two different cure cycles were ultrasonically inspected to obtain beneficial NDI baseline data. The areas inspected are shown in Figure 2-20.

This inspection was performed at various gain settings including a standard gain for 16 ply (see Figure 2-21) and a standard gain for 26 ply (see Figure 2-22). These are typical of the panel skin thickness and hat to skin thickness areas respectively. A higher gain inspection was performed, as shown in Figure 2-23 to evaluate relative performance of various cauls and

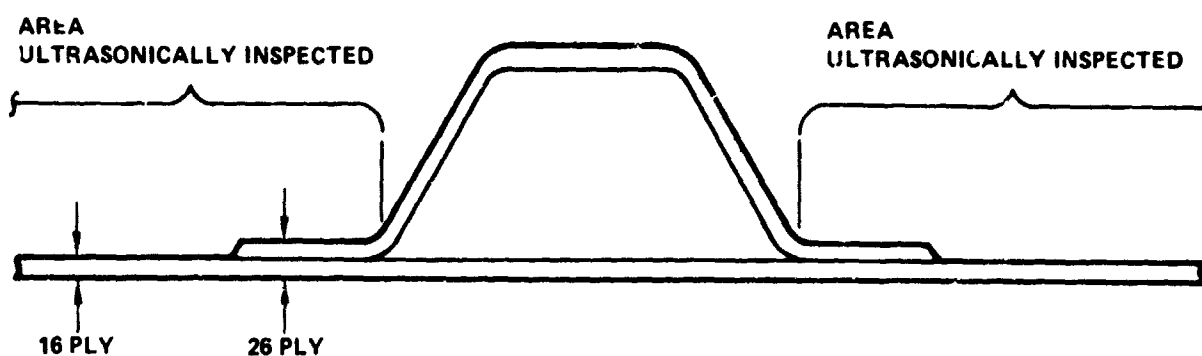
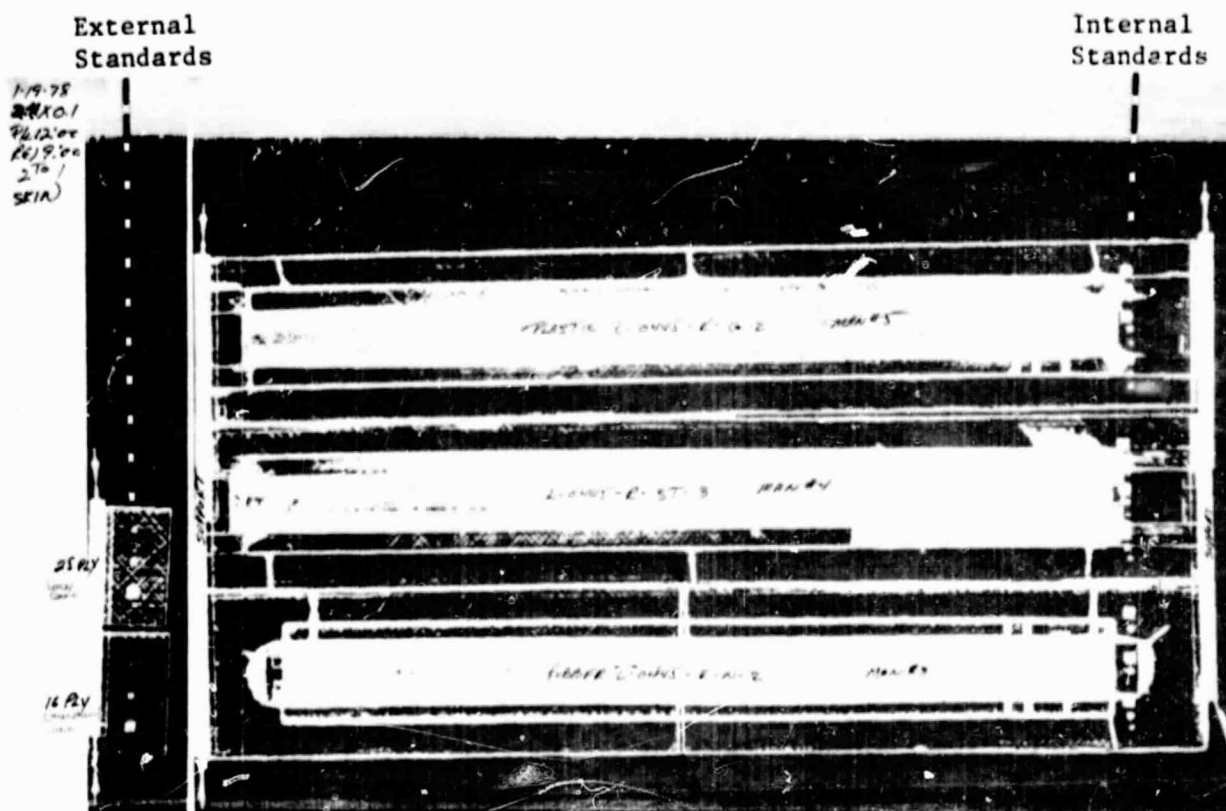
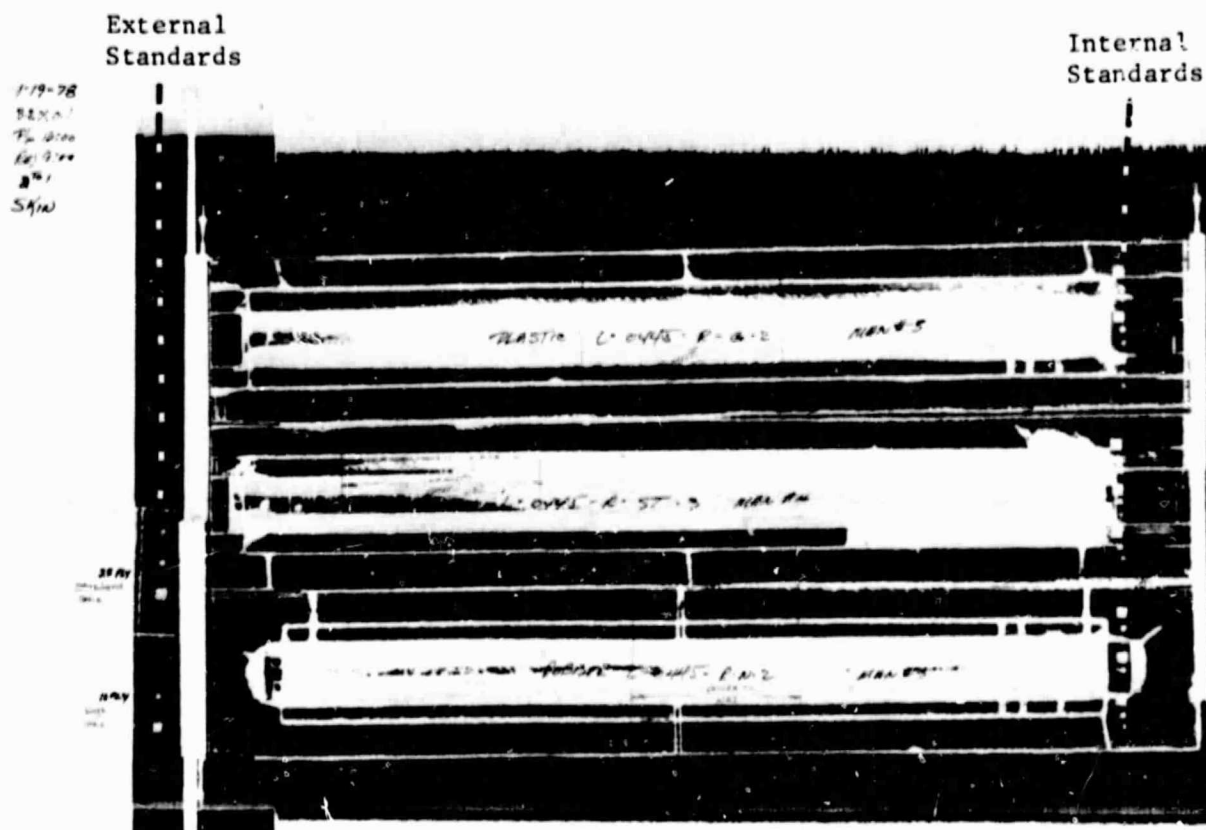


Figure 2-20. Areas of Initial Single Stage Cure Cover Assembly Specimens Ultrasonically Inspected



Standard gain for 16-ply skin areas.

Figure 2-21. Photographs of Reflected Through Transmission of Ultrasonic C-Scans of Two-Stage Cured (250°F) Group B Specimens



Intermediate gain standard for 26-ply hat flange to skin area. C-scans marked noting areas for sectioning and additional NDI evaluation.

Figure 2-22. Photographs of Reflected Through Transmission of Ultrasonic C-Scans of Two-Stage Cured (250°F) Group B Specimens

reveal areas of most concern for further NDI evaluation. These additional NDI evaluations are discussed in Section 2.4.2.2.

While there has been some improvement in quality during this period, specimens are not acceptable to current specification requirements.

To date six actuator and six truss rib specimens twenty inches long have been submitted for ultrasonic inspection. Specimen identification and the inspection results are shown in Table 2-11.

TABLE 2-11. INSPECTION RESULTS

Actuator Ribs		Truss Ribs	
Identification	Results	Identification	Results
RA-2	Unacceptable to Current Specification Criteria.	RA-1	Unacceptable to Current Specification Criteria.
RA-4		RA-3	
RA-6		RA-5	
RA-8-2		RA-7-2	
RA-10-2		RA-9-2	
RA-12-2		RA-11-2	

Figure 2-24 describes the areas which have been inspected on these specimens. The ultrasonic C-scan shown in Figure 2-25 are representative examples of both the truss and actuator rib caps.

2.4.2.2 Support of Ancillary Test Program

The flat laminate panels shown in Table 2-12 were inspected using reflected thru-transmission ultrasonic techniques.

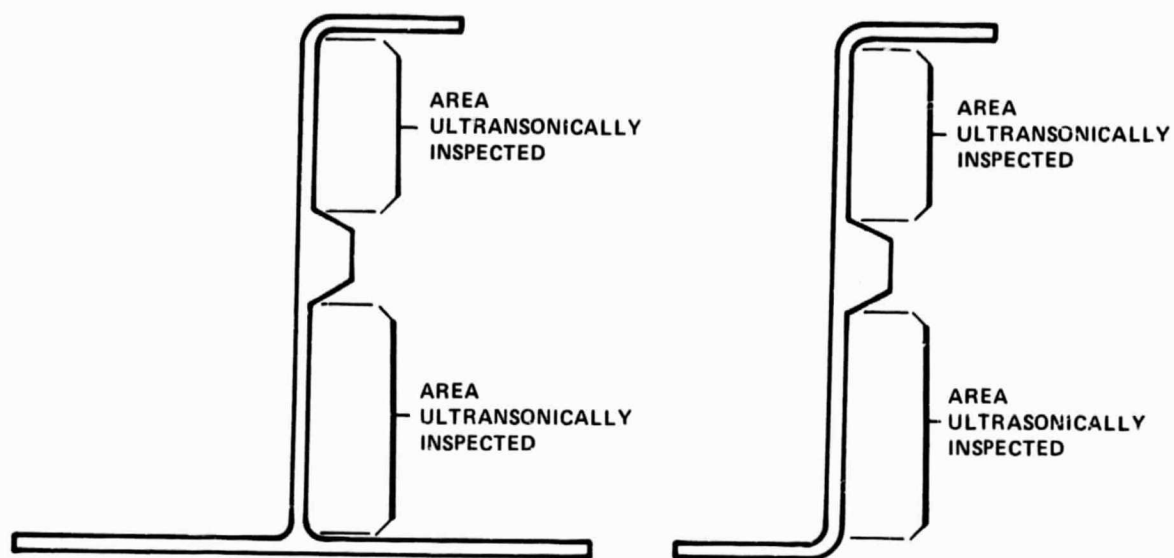


Figure 2-24. Rib Cap Areas Ultrasonically Inspected

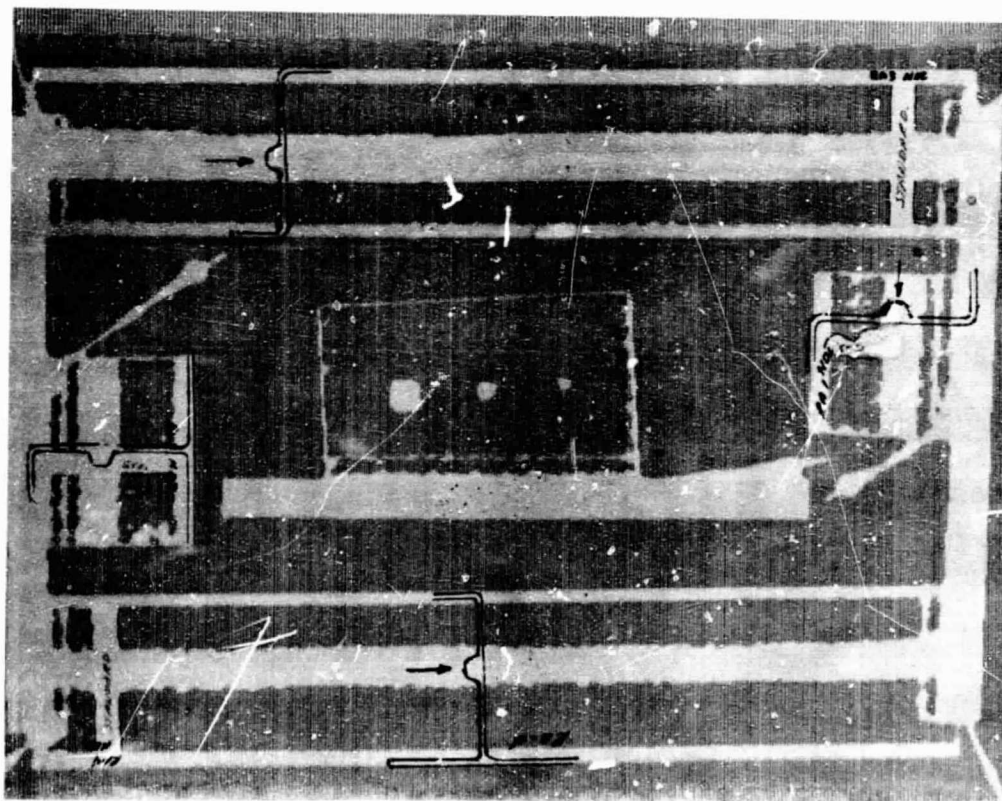


Figure 2-25. Reflected Thru-Transmission Ultrasonic C-Scan of Actuator Rib Cap and Truss Rib Cap Specimens

TABLE 2-12. FLAT LAMINATES INSPECTED

Size (in.)	No. of Ply	Ancillary Test Item	Results
44 x 52	16	H-12A	Accepted
44 x 52	16	H-12A	Accepted
36 x 46	16	H-12B	Accepted

The 36 inch by 46 inch 16 ply panel for ancillary test item H-12B submitted for ultrasonic inspection contained 1.0 inch diameter kapton-planned discontinuities. These planned areas were identified as being located at mid-ply and two ply from the surface. Two, eight ply laminates were prebled with the near surface kapton in place. These prebled laminates were then stacked with the mid-ply kapton in place and cured. An ultrasonic inspection was accomplished using the standard reflected thru-transmission technique. Only the planned areas located at mid-ply could be identified on the C-scan. The panel was reinspected from the opposite side with the same results. In an effort to identify the cause of this phenomenon without interrupting the test schedule an additional panel has been fabricated using the same techniques and procedures. The ultrasonic inspection of this panel, however, shows all the planned areas. The evaluation will be continued on one of the H-12B specimens.

2.4.2.3 NDI Evaluation Program

A plan was developed, to perform a comparative study of the various NDI methods available for the ACVF skin cover assembly. This plan is outlined in Table 2-13 and Figures 2-26 and 2-27, and is being performed concurrently with the tool and process development program. Teflon (TFE) pieces were placed in the critical area of the development panels to provide internal standards for NDI inspection. Subsequent to cure the panels were given the standard visual, dimensional and ultrasonic C-scan inspections. The results of these inspections were then reviewed and the panels marked for sectioning to include meaningful physical and mechanical testing as well as areas of interest for indepth comparative NDI method evaluations. These additional NDI methods include: pulse-echo and through transmission ultrasonic methods

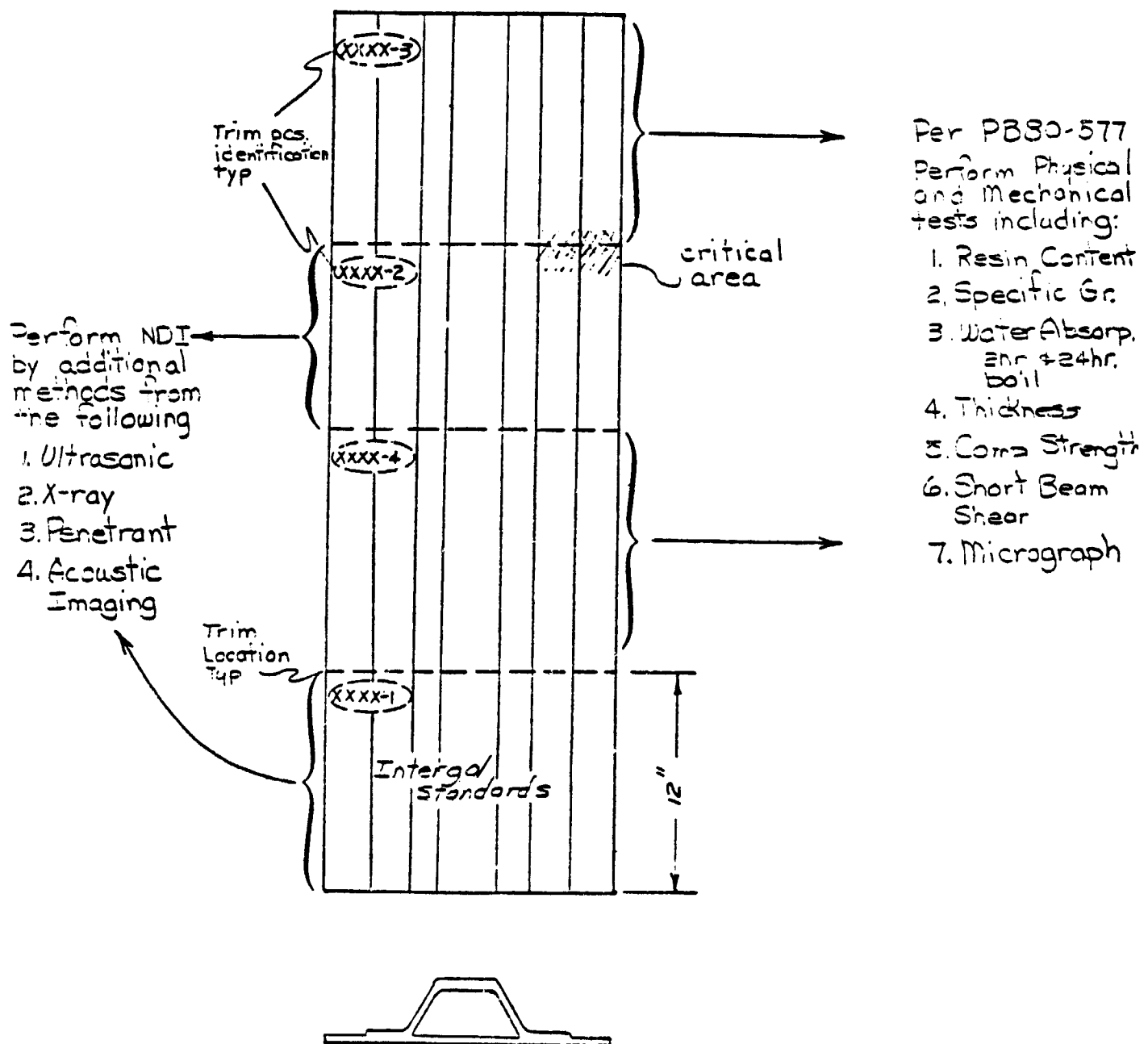


Figure 2-26. NDI Standards for Evaluation of Inspection Methods

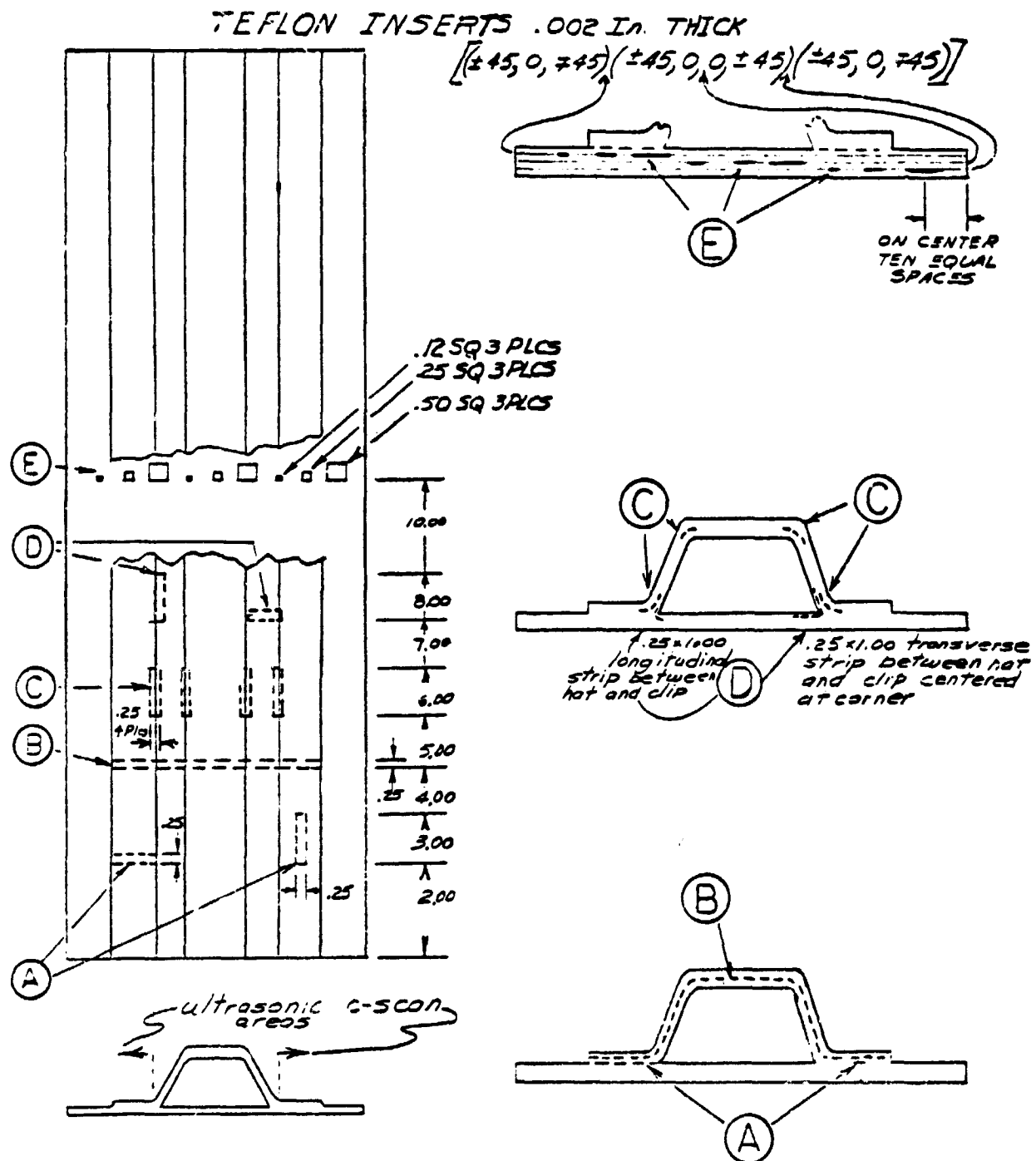


Figure 2-27. Layout of Trim and Testing to be Performed on Tool and Production Graphite/Epoxy Panels

TABLE 2-13. NDI EVALUATION PROGRAM PLAN FOR TOOL
AND PRODUCT DEVELOPMENT

1. Starting with Group B Development Panels build NDI standards, shown in Figure 2-26 into one end of each panel.
2. Perform ultrasonic C-scan inspection the full length of each panel with the external standards for each thickness of panel, where available. This inspection shall be at and outside of the hat flanges, see noted areas on Figure 2-27 and shall be at three gain settings to show most critical areas.
 - a. Nominal gain when compared to external standard.
 - b. Higher gain when compared to external standard.
 - c. Lower gain when compared to external standard.
3. Review C-scans with Materials & Processes (M&P) and Q.A. NDI. Referring to Figure 2-26 mark C-scan and panel with location of trimming and code number identification. Photograph C-scan making three copies.
4. Trim standards (XXXX-1) and approximately 10 inches of a selected critical area (XXXX-2) for NDI evaluation of methods.
5. Send XXXX-1 and XXXX-2 specimens to Q.A. NDI.
6. Send XXXX-3 and XXXX-4 specimens for physical and mechanical testing per PB80-577 to Q.A. Chemical Lab.
 - a. Resin content
 - b. Specific gravity
 - c. Water absorption with 2 and 24 hr boil
 - d. Thickness
 - e. Compressive strength
 - f. Short beam shear
 - g. Micrograph
7. XXXX-1 and XXXX-2 specimens will be used to evaluate ultrasonic techniques for entire specimen.

TABLE 2-13. NDI EVALUATION PROGRAM PLAN FOR TOOL
AND PRODUCT DEVELOPMENT (CONTINUED)

8. Subject XXXX-1 and XXXX-2 specimens to additional NDI methods including:

- a. Refine ultrasonic techniques
- b. X-ray
- c. Penetrant-black light photograph
- d. Acoustic imaging

The first three methods will be completed within three weeks (15 working days) of panel cure.

9. M & P collect results and perform comparative evaluation between M & P and Q.A. NDI.
10. Perform laboratory tests on XXXX-2 panels as determined by Step 9 above.

using various transducers, radiographic, liquid penetrant and acoustic image ultrasonic inspections.

Progress on the above efforts is summarized in Table 2-14 and its auxiliary Figure 2-28. Dimensional and mechanical data has been obtained on all 24 cured tool and product development panels. These panels were also evaluated by standard reflected through transmission ultrasonic C-scan and other various NDI methods where it was felt that beneficial baseline data could be obtained. The initial reflected through transmission ultrasonic C-scan were accomplished as outlined in Section 2.4.2.1.

The additional NDI evaluations involved reflected through transmission ultrasonic inspection with the transducer focused on the reflector plate and the panel between the transducer and the reflector plate. The objective of this effort is to develop higher quality or greater sensitivity C-scans. This was obtained as shown by Figure 2-29 which shows a clearer image of the internal defects in panel section L-044S-R-N-2-1

In addition, panel sections of interest were inspected by pulse echo ultrasonic C-scan inspection. This was done to differentiate between the types of defects that attenuate ultrasonic energy, such as, porosity, and

TABLE 2-14. PROCESS DEVELOPMENT SUMMARY

L-1011

ACVF Cover Assembly: Product Development Data Summary

Specimen Identification	Lab Report Number	NDI	Technique		Physical Properties				Mechanical Properties			Micrograph			
			Visual	Dimensional	Initial Ultrasonic	Resin Content	Specific Gravity	Void Content	Water Absorption 24 hrs	Short Beam Shear R.T.	Compression R.T.		180°F	180°F	
L-044S-R-G-1	343830	Unacc				▼	●	▲	—	—	—	—	—	—	—
L-017S-R-N-1	343888					▲	▼	▲	●	—	—	—	—	—	—
L-044S-R-S-2		Acc		Unacc	Unacc	▲	●	●	●	—	—	—	—	—	—
L-044S-R-N-2	344850	Unacc		Unacc	Unacc	●	●	▲	●	—	—	—	—	—	—
L-044S-R-G-2	344943	Unacc		Unacc	Unacc	▲	●	●	●	—	—	—	—	—	—
L-044S-R-ST-3	344114 & 15	Unacc				▲	●	▲	●	—	—	—	—	—	—
	344341					▲	●	▲	●	—	—	—	—	—	—
H-044S-R-ST-1	343898					▼	●	▲	●	—	—	—	—	—	—
H-044S-R-G-1	343901					▼	●	▲	▲	—	—	—	—	—	—
H-017S-R-N-1	343938					▲	▼	▲	▲	—	—	—	—	—	—
H-044S-R-S-2	344957	Unacc		Unacc	Unacc	▲	▼	▲	▲	—	—	—	—	—	—
H-044S-R-N-2	344957	Unacc		Unacc	Unacc	▲	▼	●	▲	—	—	—	—	—	—
H-044S-R-G-2	344957	Unacc		Unacc	Unacc	▲	▼	●	▲	—	—	—	—	—	—
L-044S-R-N-R-E.-1	345466					▲	▼	▲	▲	—	—	—	—	—	—
L-044S-R-ST _A -R-E.-1	345600					▲	▼	▲	●	—	—	—	—	—	—
	345599					▲	▼	▲	●	—	—	—	—	—	—
L-044S-R-G-R-E.-1	345468					▲	●	▲	●	—	—	—	—	—	—
L-044S-R-C-R-E.-1	345467					▼	●	▲	●	—	—	—	—	—	—
L-044S-R-C-R-E.-1	345601					▼	●	▲	●	—	—	—	—	—	—
	345602					▼	●	▲	●	—	—	—	—	—	—
H-044S-FO-G-1	345159	Unacc		Unacc	Unacc	●	●	▲	▲	—	—	—	—	—	—
H-044S-FO-G-2	345380	Unacc		Unacc	Unacc	●	●	▲	●	—	—	—	—	—	—
H-044TR-FO-G-3					Unacc										
H044TR-FO-G-3M-1					Unacc										
H-044TR-FO-G-3R-1					Unacc										
H-046S-FB-ST-1	345465	Acc			Unacc	▲	▼	▲	●	—	—	—	—	—	—
H-044S-I-ST-1	345059	Acc		Unacc	Unacc	▲	●	●	●	—	—	—	—	—	—
					Target Range	26-30%	1.56-1.60	1% Max	.33%	.75%	—	7 - 16	67 75 60	70 10 ply 16 ply	Mech. Prop.
● Values within target range											11	8 10 7	— 78 —	73 20 ply 26 ply	
▲ Values above target range															
▼ Values below target range															

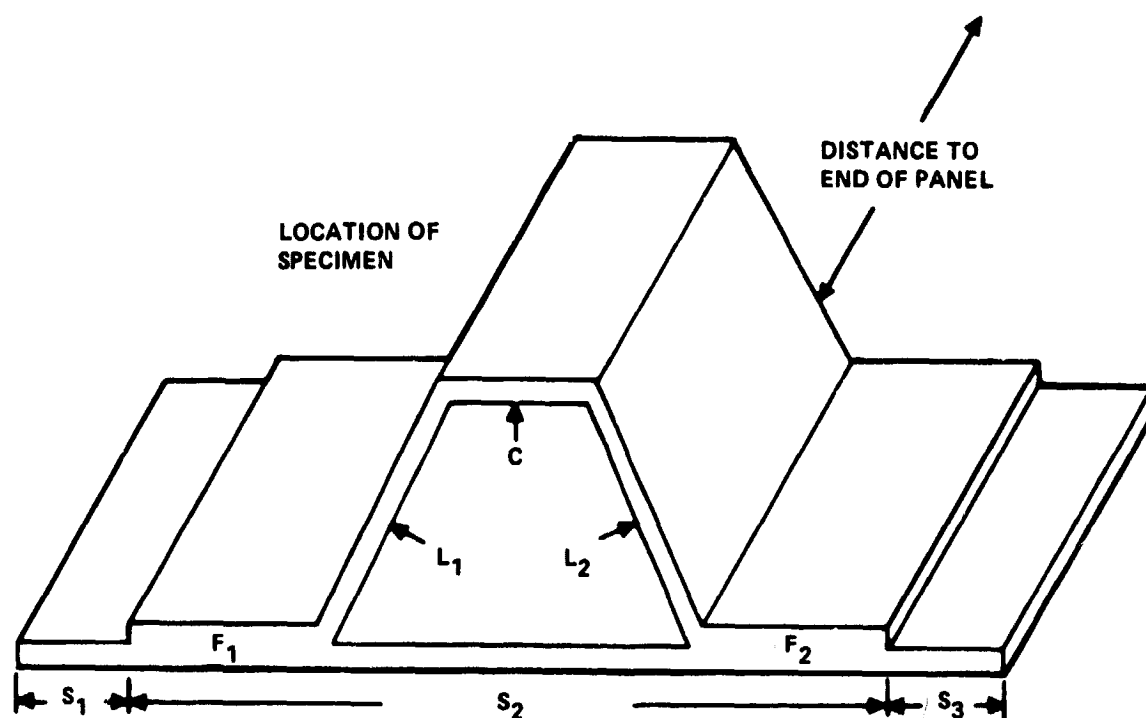


Figure 2-28. Data Code for Tool and Process Development Panels

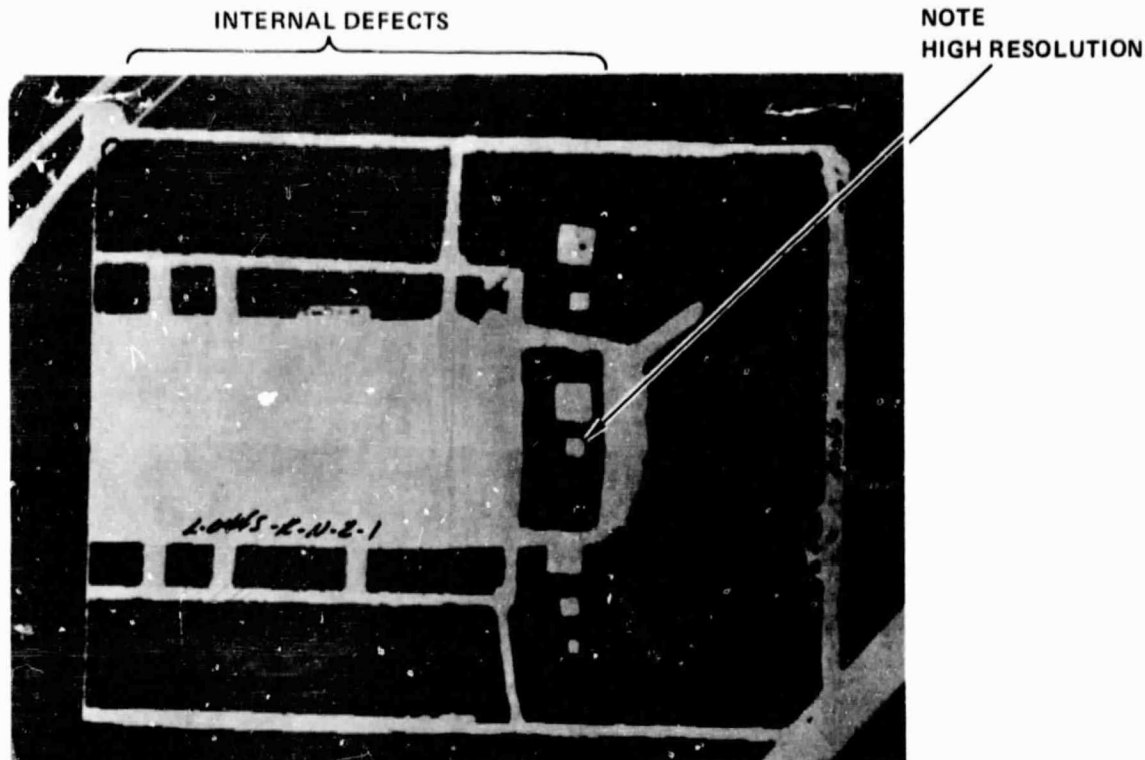


Figure 2-29. Photograph of Reflected Through Transmission Ultrasonic C-Scan with Transducer Focused on Reflector Plate of Panel Section L-044S-R-N-2-1

those which reflect energy, such as voids and delaminations. By comparing the through transmission and pulse echo C-scans it is felt the difference between porosity and voids or delaminations becomes apparent.

Pulse echo inspection of the hat stiffener cap or crown was also performed on selected panel sections in an attempt to develop capability to inspect this area. By getting between the front and back surface of the crown C-scans of the crown area were developed, however, thickness variations in this area made this procedure difficult.

Radiographs of the crown area of various panels were taken and this indicated longitudinal cracking through the plys. Micrographic evaluation of these indications is in progress.

In addition to these efforts conducted at the Lockheed-California Company two specimens have been inspected at the Lockheed Missile and Space Company Research Facility using their ultrasonic acoustic imaging capability.

This method of ultrasonic inspection converts the sound energy into light energy which is then collected and printed out as a photograph in an attempt to increase sensitivity and resolution. A comparison of the ultrasonic acoustic image data can be made by comparing Figure 2-30 with previous figures of C-scans of this panel section. The C-scan presents an area of sound attenuation as a white area while acoustic imagery shows this attenuation as a reduction in light transmission or a dark area. Similar in-depth NDI method comparisons are being conducted on panel sections as shown in Table 2-14.

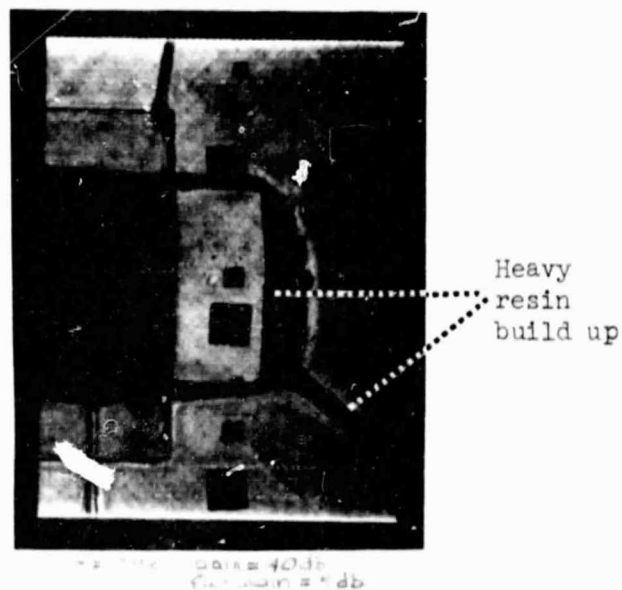


Figure 2-30. Photograph of Ultrasonic Through Transmission Acoustic Image of Panel Section L-044S-R-N-2-1

SECTION 3

PHASE II - DESIGN AND ANALYSIS - SPARS

Phase II design and analysis of the spars, comprises the main engineering effort of Lockheed-Georgia Company in the design, development, and fabrication of the front and rear spars for the L-1011 advanced composite vertical fin. The engineering effort during this reporting period covered three tasks: component definition, process verification and concept verification.

3.1 COMPONENT DEFINITION

Component definition covers the detail design and structural analysis of the selected front and rear spar configurations.

3.1.1 Detail Design

During this reporting period, detail design activities consisted of completing the design and releasing the drawings of the front and rear spars. The spar web and cap thicknesses and module for the front and rear spars are shown in Figures 3-1 and 3-2.

3.1.2 Structural Analysis

The preliminary structural analysis of the front and rear spars have been completed. Figures 3-3 and 3-4 shows the structural margins provides by the front and rear spar designs. Strength margins of safety are placed in three categories: low, medium, and high. Low margins are classed as less than +0.30, medium margins are classed as +0.30 to +0.99, and high margins are classed as +1.0 and higher. Margins on the spar caps reflect axial loads and are based on either net section tension, net section compression, or flange crippling. The margins at the edge of the access holes are based on transverse tensile strains, and have been found to be conservative in a multiple orientation

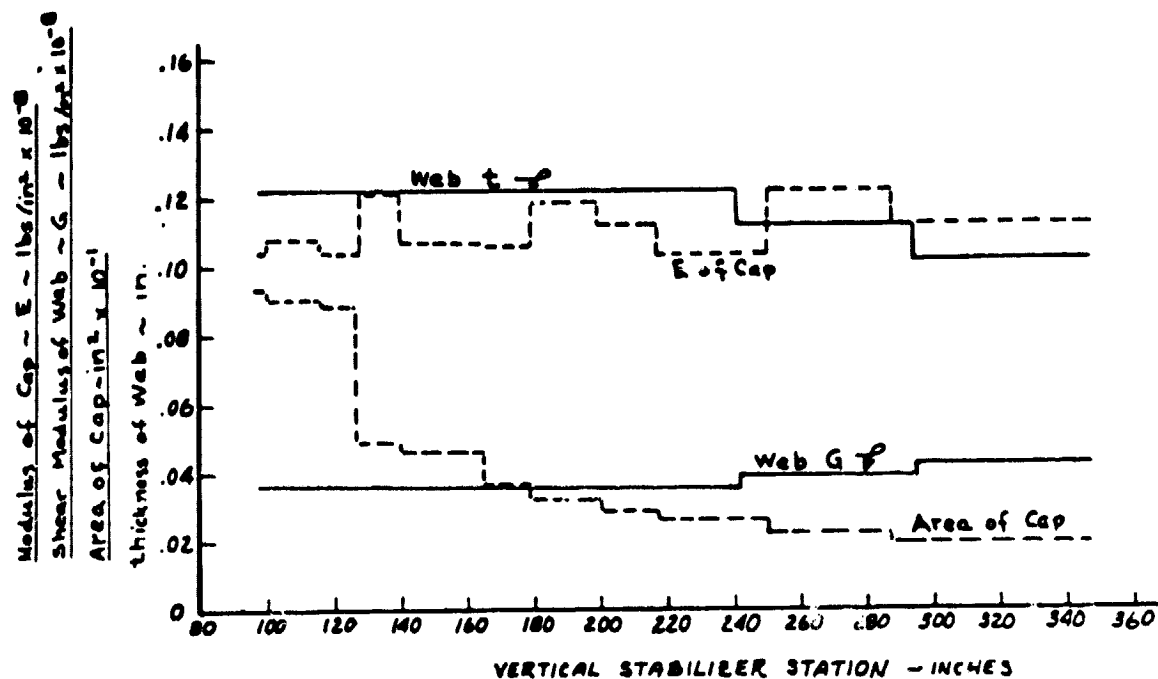


Figure 3-1. Front Spar Web Thickness, Cap Area & Moduli

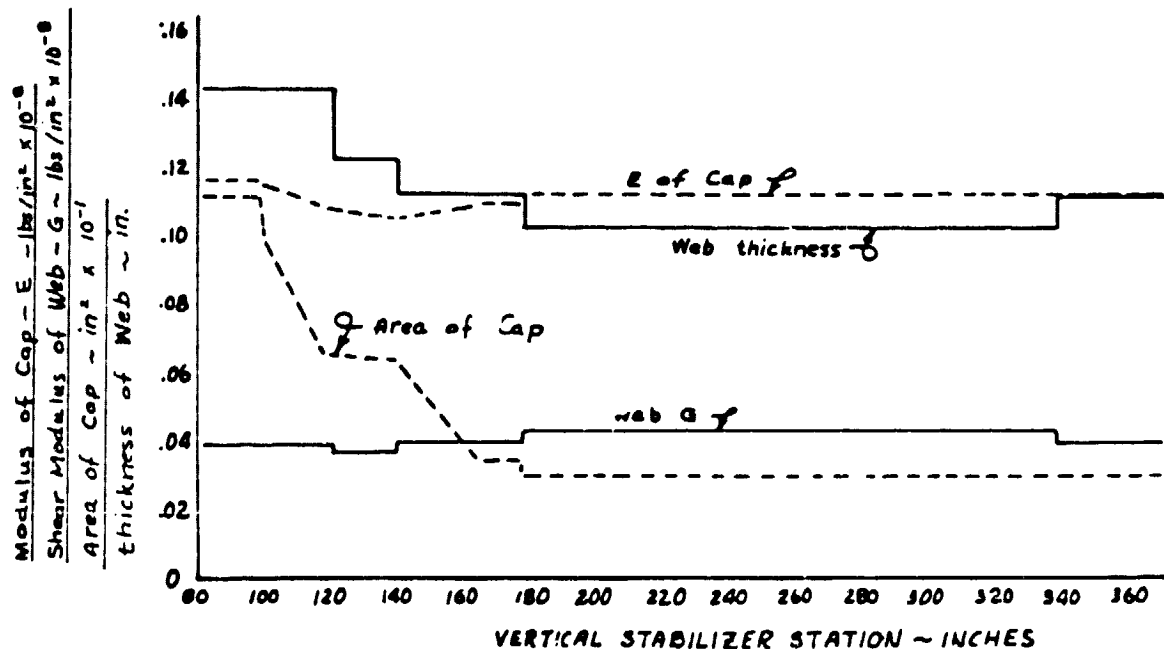


Figure 3-2. Rear Spar Web Thickness, Cap Area & Moduli

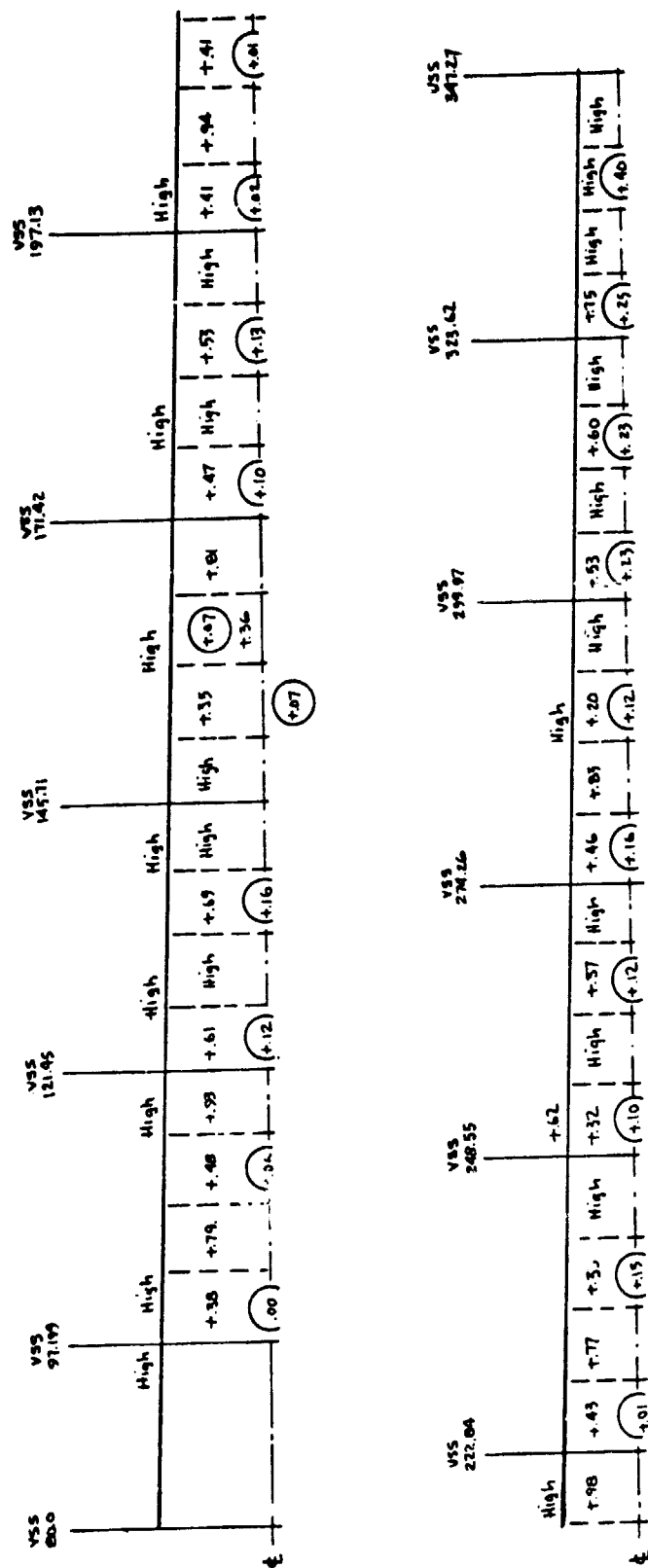


Figure 3-3. Diagram Showing Summary of Margins of Safety in Front Spar

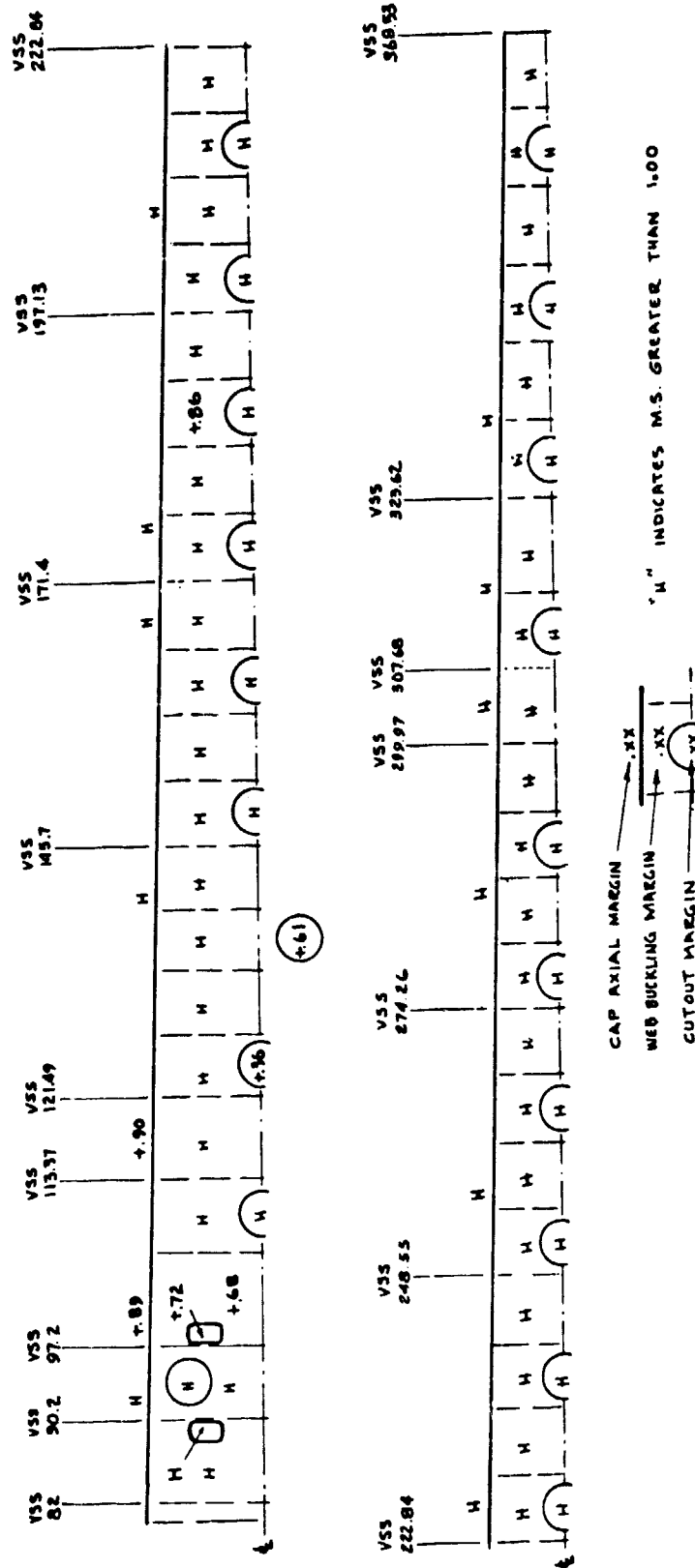


Figure 3-4. Rear Spar Margins of Safety

laminate typical of the spar webs. Tests of Ancillary Test Item H21 specimens have shown that the actual static failure loads at the edge of the access holes are more than 20 percent higher than the predicted static failure loads. Effects of strain concentrations due to fastener holes, etc. as well as the effects of temperature and moisture have been accounted for in the allowables data used in the margin calculations.

3.2 PROCESS VERIFICATION

The purpose of the process verification task is to develop and verify the elastomeric molded process (cure cycle) established for the fabrication of the front and rear spars.

3.2.1 Tool Development and Process Verification Test Specimen - H14

The process verification test specimen (Test Item H14) represents the lower 84-inches of the front spar. It was fabricated in an 8-foot, stub spar tool, and subjected to FAA and Company conformity inspection requirements. The layup of the stub spar is shown in Figures 3-5 through 3-10. Figures 3-11 through 3-15 shows the spar after removal from the bond tool prior to removal of the armalon and clean-up.

Although the H14 front stub spar was a process and tool development specimen, it was subjected to the same conformity inspection that would be performed on a flight article. In general, the inspection performed on this part was more thorough than would normally be performed on a production part. The objective of the thorough inspection was to locate all discrepancies prior to cutting the spar into the coupons. A discrepancy report was written as a result of the conformity inspections performed on the stub spar, see Section 3.4.2.

Disposition of the Discrepancy Report on H14 requires corrective action to be taken in the tool or in the manufacture of the part prior to fabrication of future parts; and approval of the disposition must be obtained by Lockheed Quality Assurance, Air Force Quality Assurance, and FAA Quality Assurance. Before accepting the H14 for planned coupon tests, discs taken from the five

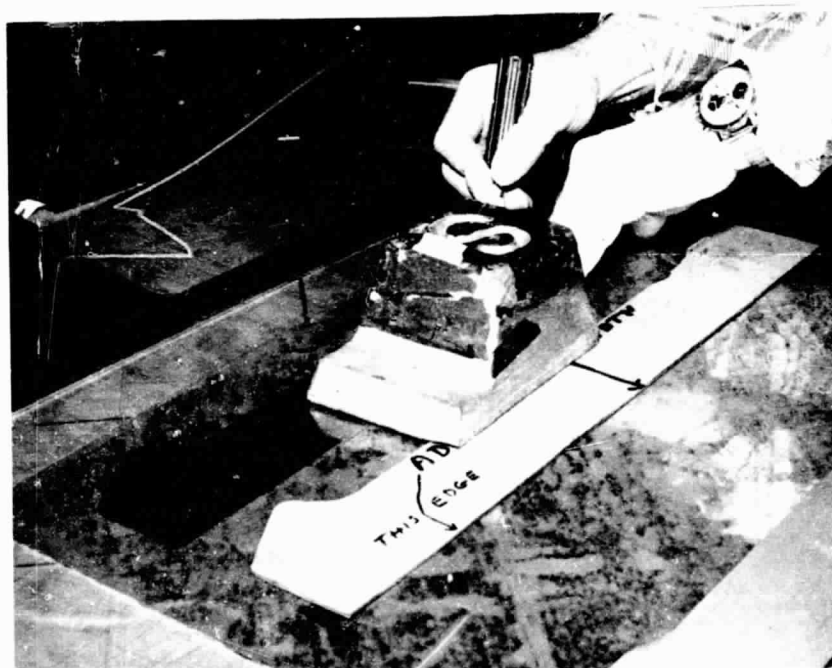


Figure 3-5. Stiffener Trim Templates

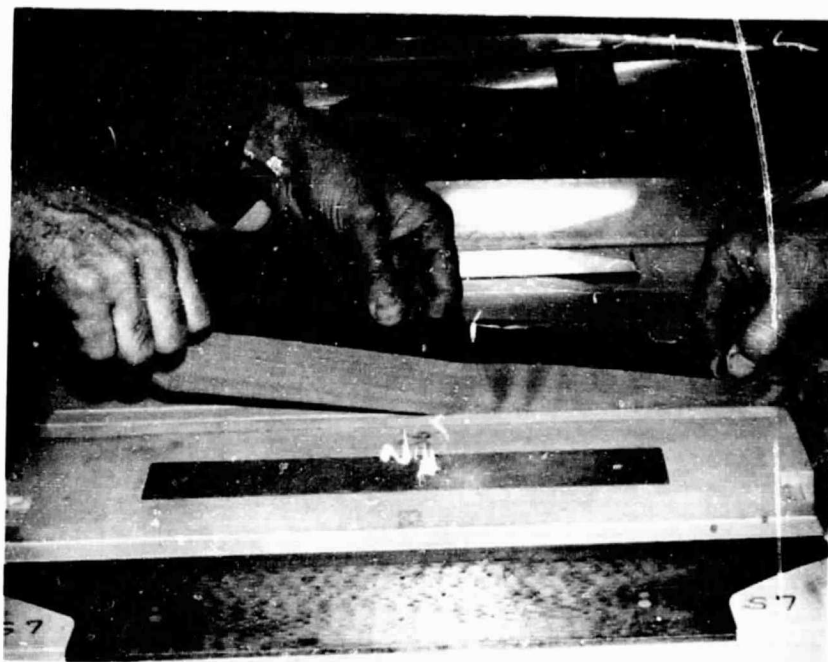


Figure 3-6. Placing Stiffeners in Tool

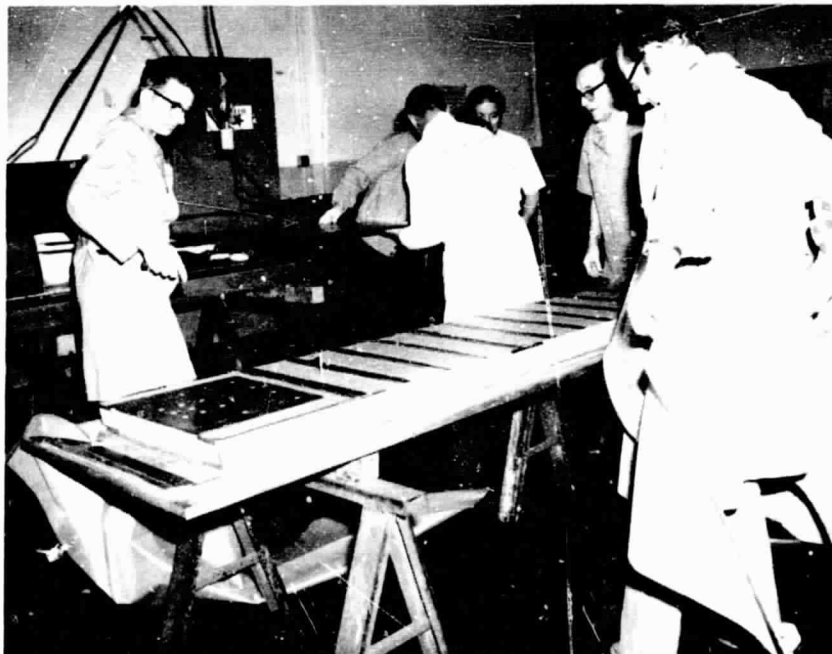
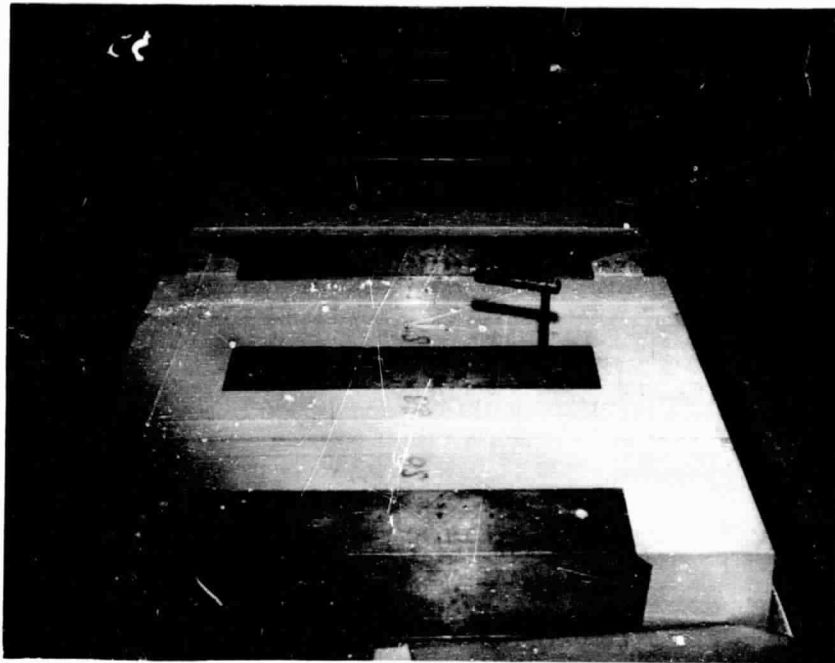


Figure 3-7. Stiffeners in Place & Ready for Web

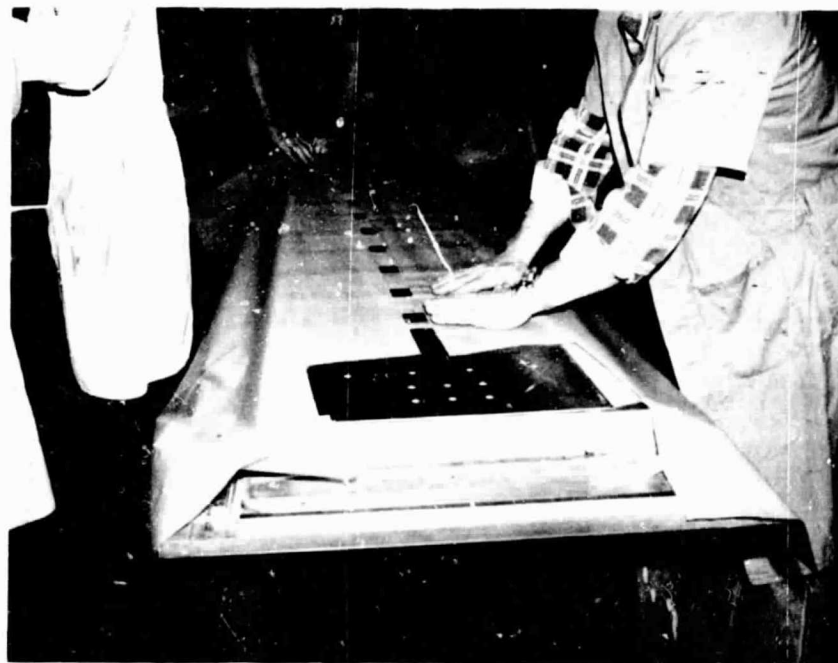
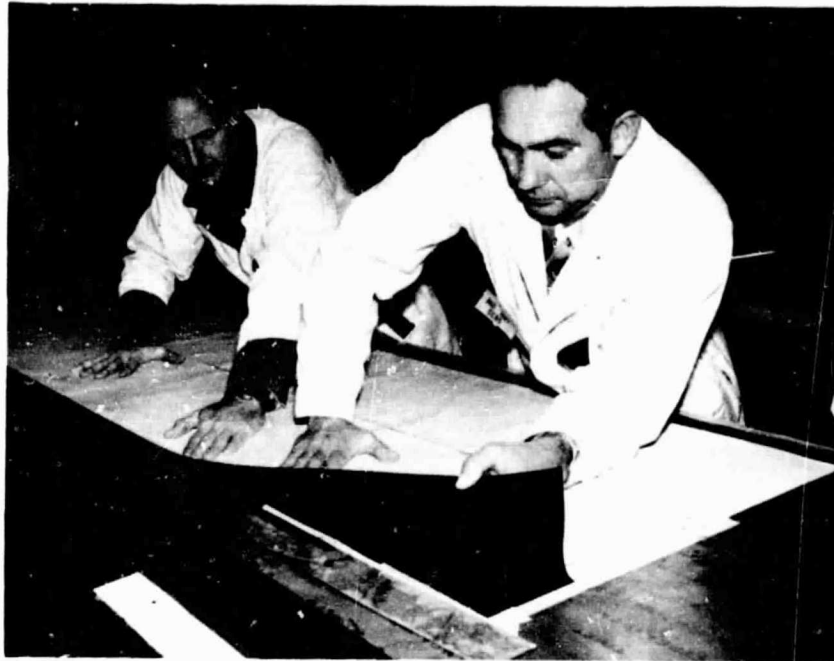


Figure 3-8. Layup of Web



Figure 3-9. Web in Place with Armalon Bleed Cloth and Turning $\pm 45^\circ$ Web Plies Into Cap



Figure 3-10. Final Lay-up of Spar in Bond Tool



Figure 3-11. Details of Lower End of H14 Showing
Removal of Armalon and Some Fiber Wash

3-12



ORIGINAL PAGE IS
OF POOR QUALITY

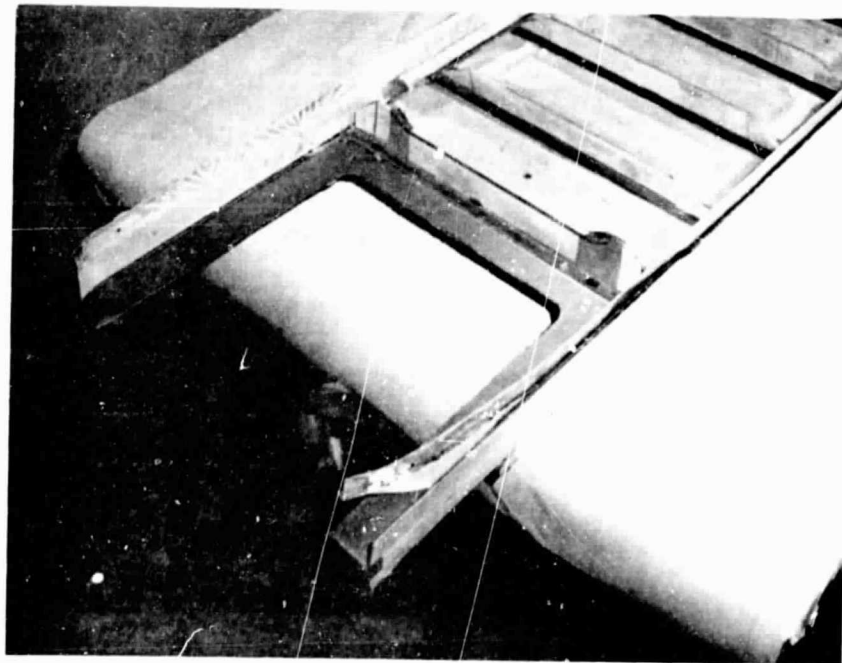


Figure 3-12. Aft Side of Front Stub Spar (H14) As Removed From Tool Prior to Removing Armalon

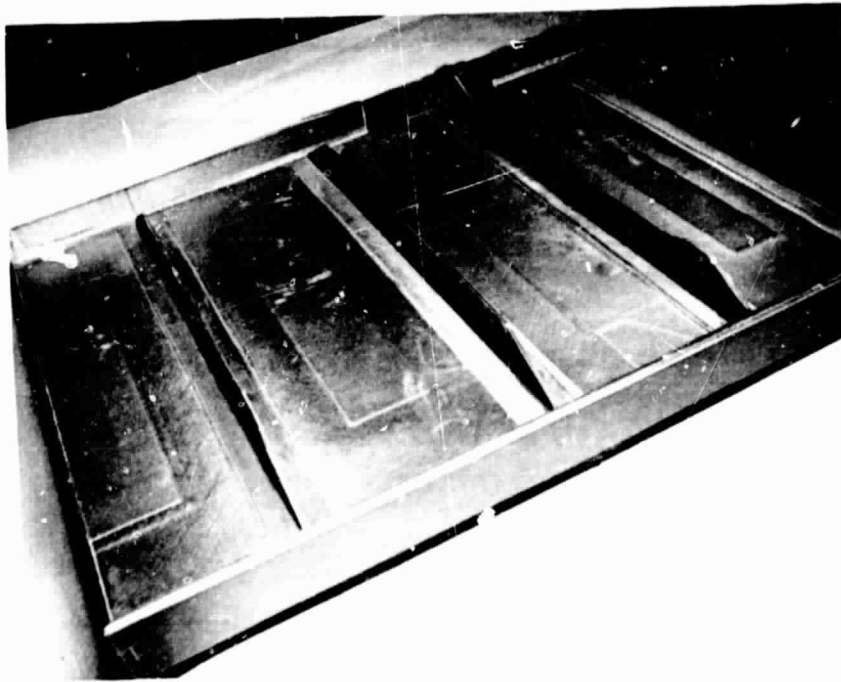


Figure 3-13. Details of Upper End of H14, Aft Side,
Prior to Removal of Armalon

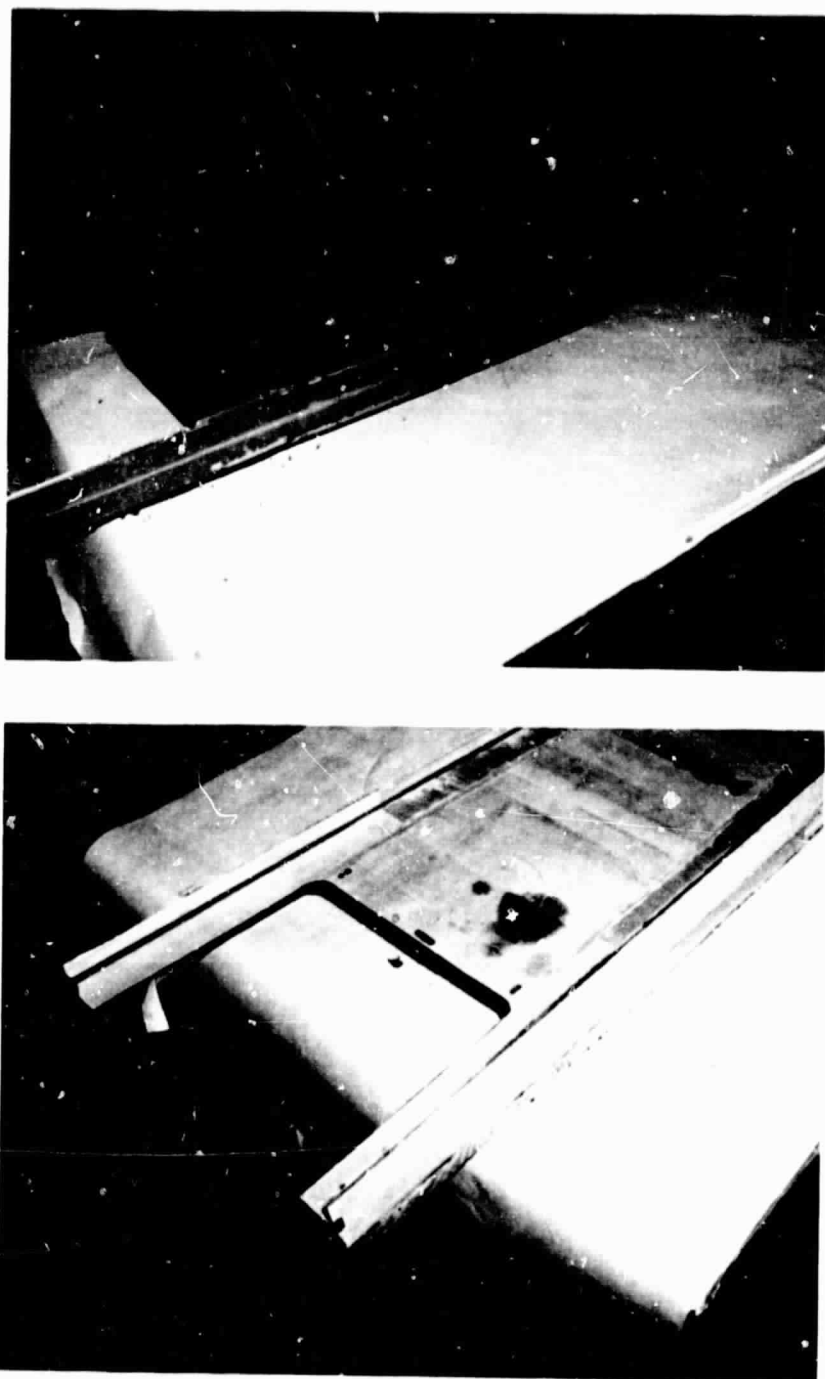


Figure 3-14. Forward Side (Smooth Side) of H14
Prior to Removal of Armalon

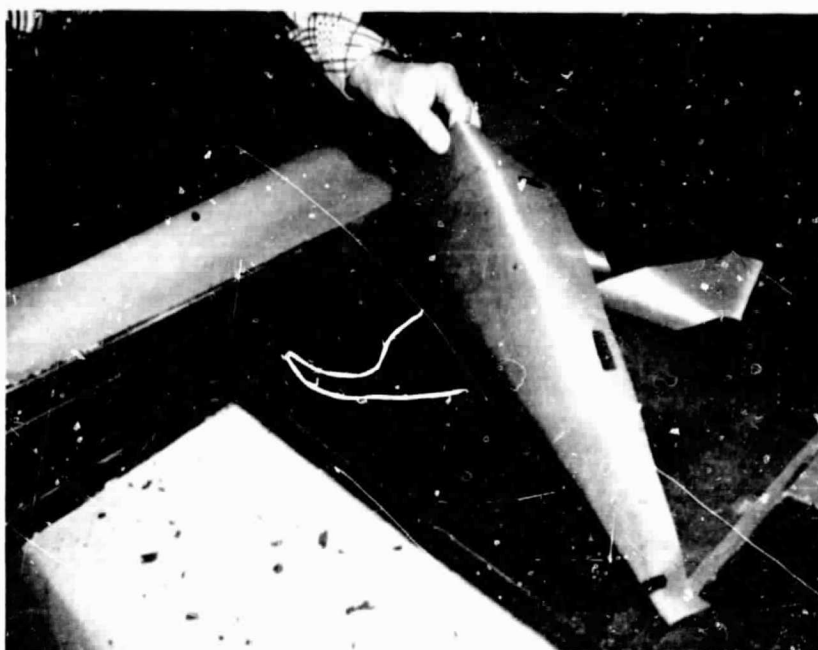
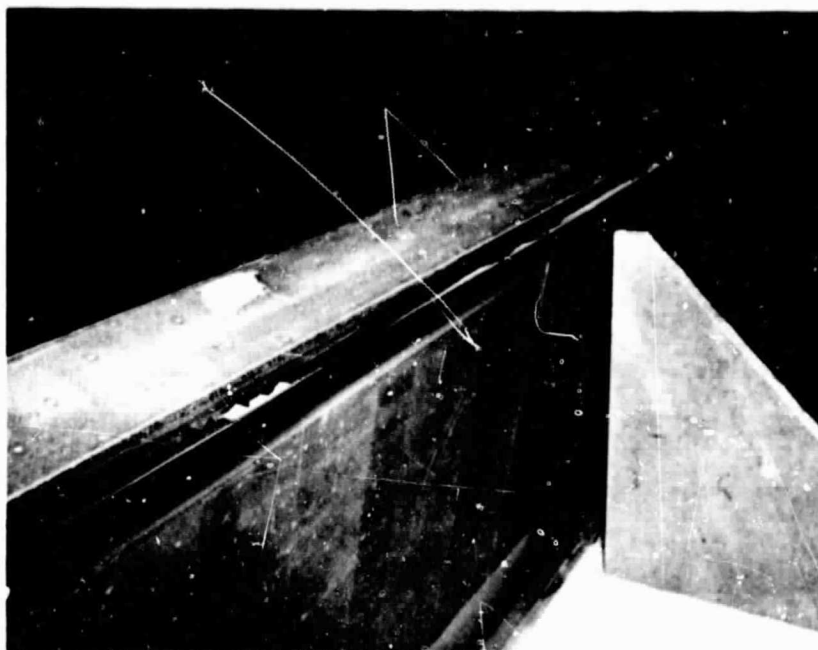


Figure 3-15. Close-up Showing Removal of Armalon
From Forward Side of H14

access holes were cut into process control type specimens and tested. Tests of the discs showed strengths well above predicted values, low porosity, and good fiber volume, resin content, and specific gravity. A specimen was cut out of the lower leg of the spar cap where NDI showed excessive porosity and sent to the laboratory for an analysis. The laboratory report verified the porosity found by NDI. Except for the local, porous area in the lower leg of the spar between VSS 80 and VSS 97, the overall quality of the spar was very good. Analysis of the thickness variation in the spar cap indicated a tool discrepancy which permitted excess thickness between VSS 80 and VSS 97. An analysis of the tool revealed that the steel rails used to mold the forward flanges of the spar cap were cut too deep, and that the fully expanded rubber would not compress these forward cap flanges. Corrective action has been taken to fill the excess depth prior to the fabrication of the Ancillary Test Item H23A spar.

Discrepancies above VSS 97 were considered as being correctable by "fine-tuning" the tool. These consisted of mark-off between the rubber and steel, some porosity which was later found to be acceptable and some local over tolerance thicknesses.

The H14 stub spar was cut into approximately 133 test specimens as shown in Figures 3-16 & 3-17. Specimen A was used to verify the interlaminar tensile strength at the intersections of the cap-to-web, rib angle-to-web and stiffener-to-web. Specimen B was a rail shear specimen used for comparison with previous T300/5209 rail shear specimens. Specimens C and D were compression specimens. Specimens E and F were used to observe porosity and to determine the composition of the laminate. These specimens are shown in Figures 3-18 through 3-22.

The F (fiber-volume, resin-content, specific-gravity and void-content) specimens have been evaluated, and the results of these specimens, tabulated in Table 3-1, verified the NDI results and demonstrated that, except for specimens F-1, F-2, F-15 and F-16 cut out of the lower leg of the spar, the overall quality of the spar was very good. Percent void contents in F-1, F-2, F-15 and F-16 were 1.29, 1.74, 2.37 and 3.30, respectively. Related

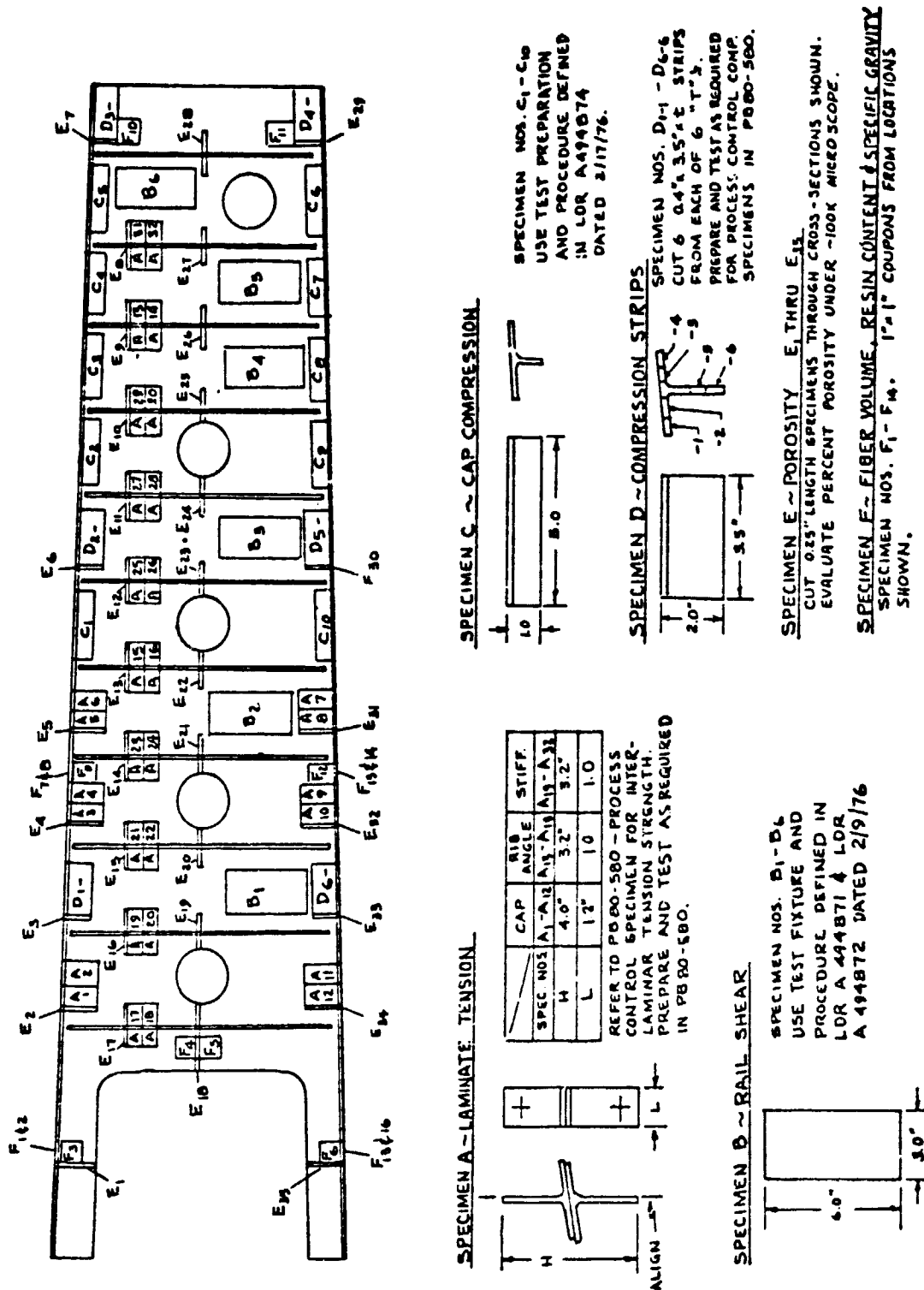


Figure 3-16. H14 Coupon Type Test Specimens

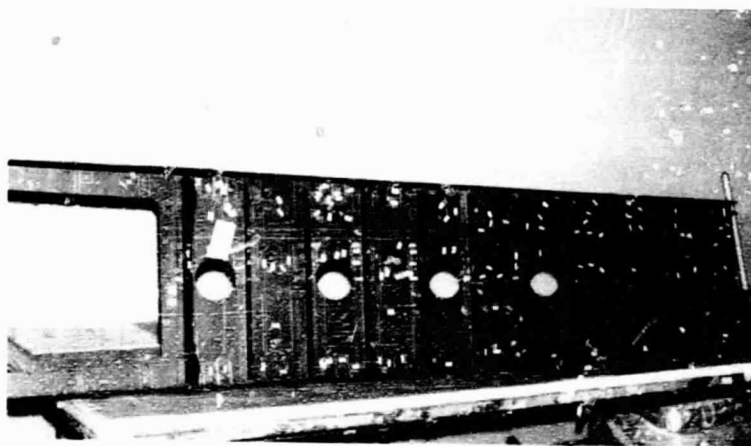
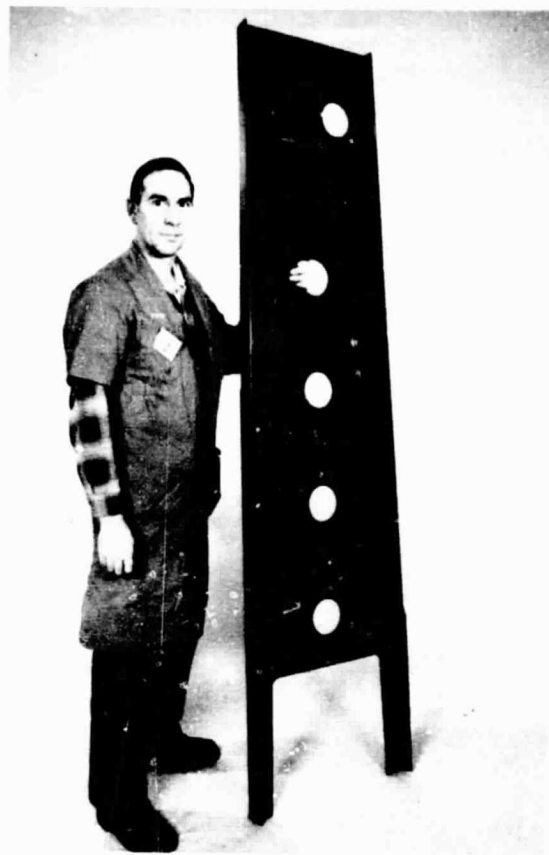
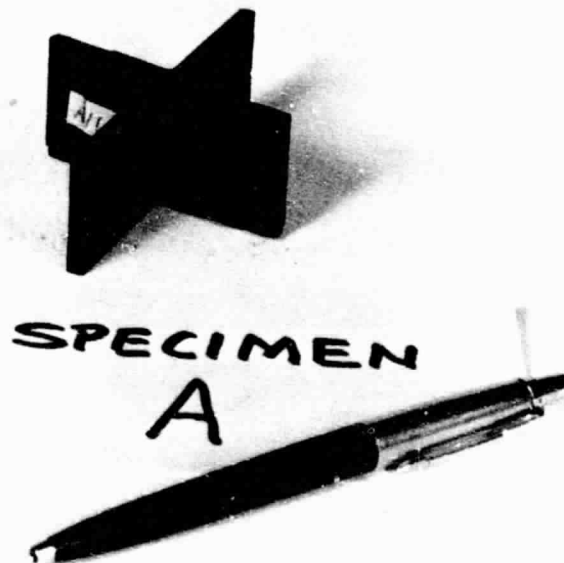
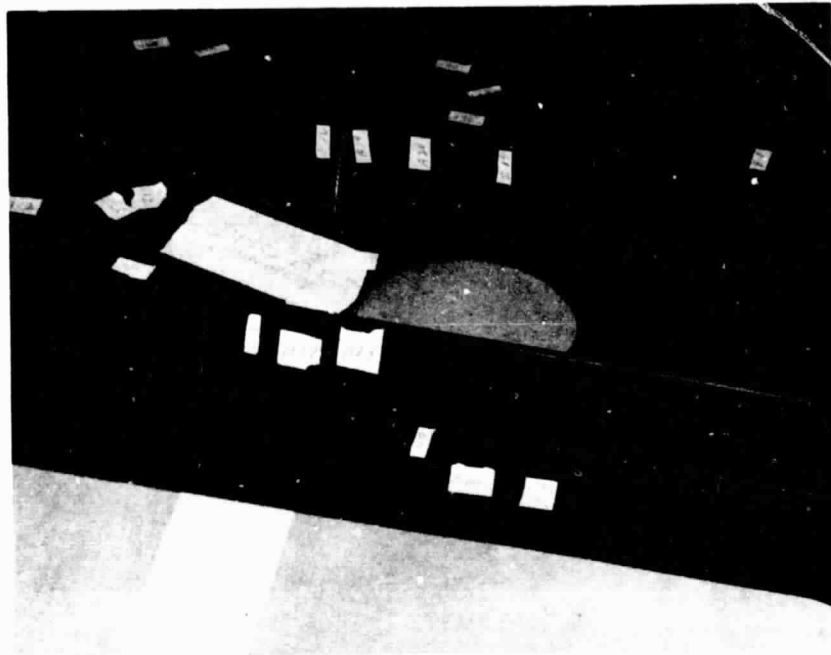
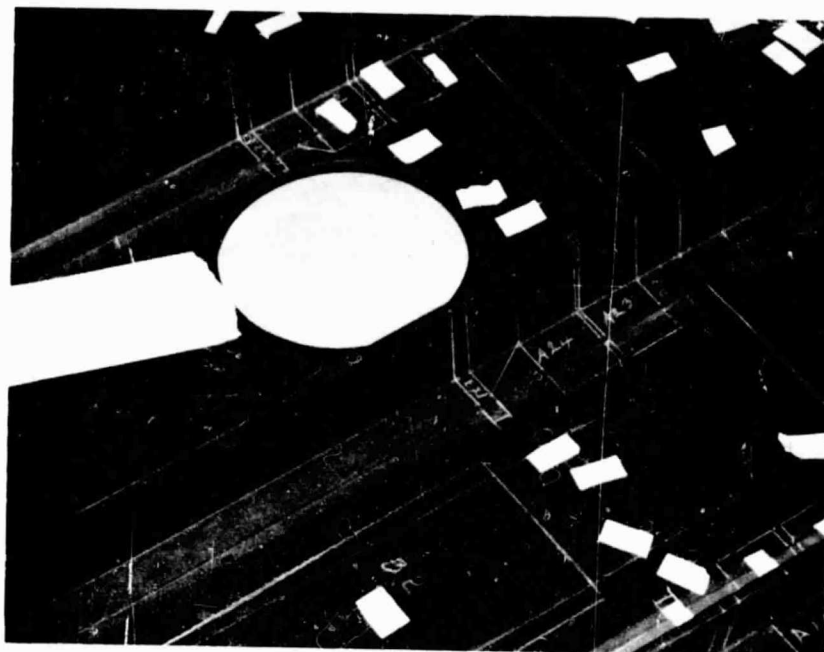


Figure 3-17. H14 Stub Spar and Locations of Test Coupons



ORIGINAL PAGE IS
OF POOR QUALITY

Figure 3-18. H14 Laminate Tension Specimen A



SPECIMEN

B



Figure 3-19. H14 Rail Shear Specimen B

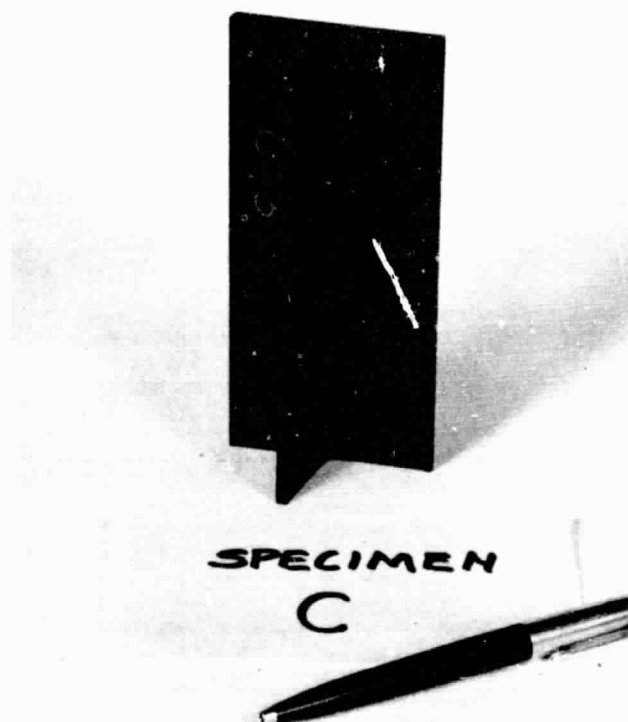
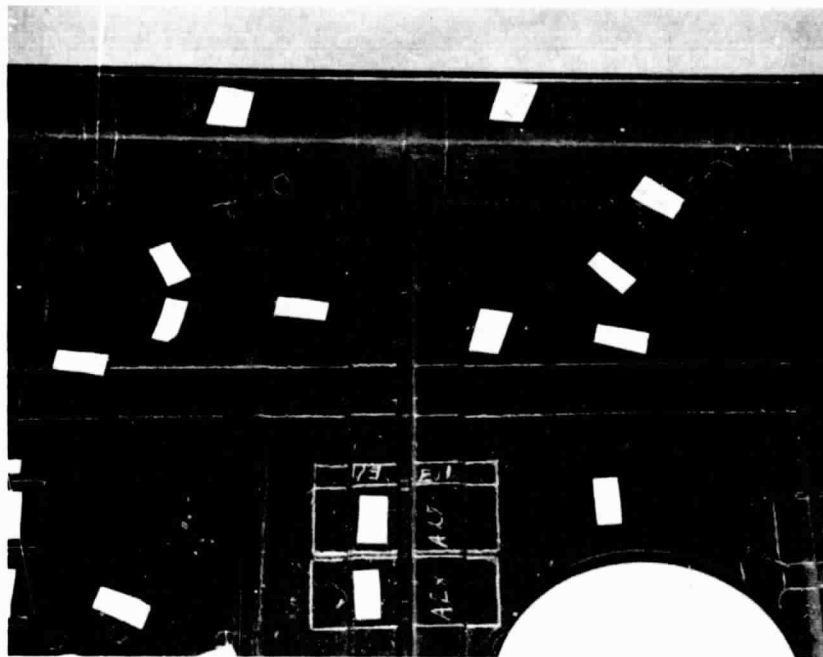
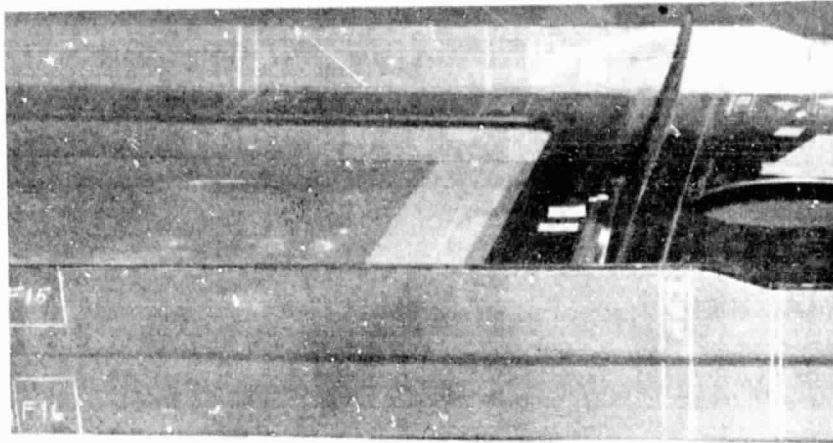


Figure 3-20. H14 Cap Compression Specimen C



Figure 3-21. H14 Cap Compression Strips D and Porosity Specimen E



SPECIMEN
F



**ORIGINAL PAGE IS
OF POOR QUALITY**

Figure 3-22. H14 Fiber Volume, Resin Content and Sp. Gr. Specimen F

TABLE 3-1. H14 FIBER VOLUME, RESIN CONTENT, SPECIFIC GRAVITY AND VOID CONTENT

Specimen Number	Percent Resin Weight	Percent Fiber Volume	Specific Gravity	Percent Void Content
F1	29.16	62.62	1.547	1.29
F2	36.20	54.76	1.502	1.74
F3	29.66	62.54	1.556	0.54
F4	30.01	62.31	1.558	0.29
F5	30.49	61.76	1.555	0.30
F6	29.05	62.96	1.553	0.95
F7	29.26	63.26	1.565	0.10
F8	25.70	67.12	1.581	0.37
F9	33.68	58.40	1.541	0.08
F10	22.88	70.28	1.595	0.52
F11	26.22	66.66	1.581	0.18
F12	31.90	60.40	1.552	-
F13	26.95	65.45	1.568	0.74
F14	26.29	66.17	1.571	0.79
F15	34.17	56.54	1.503	2.37
F16	32.41	57.86	1.498	3.30
PB80-580 REQ'M'T.	26-32	(Resin Content Req'd.)	1.54-1.60	< 2.00

resin content, fiber volume and specific gravity was also unacceptable in the specimens cut out of the lower legs below VSS 97 of the spar. These data and thickness surveys were all compatible with the condition of the tool for molding these lower legs of the spar. Above VSS 97, which is about 95% of the bonded spar, all test values obtained to date have shown good results. The F specimens in Table 3-1 all show good properties above VSS 97, and indicate very good quality.

Analysis of the test data obtained from the H14 specimens was completed and is summarized in Figures 3-23 and 3-24. Figure 3-23 shows the test

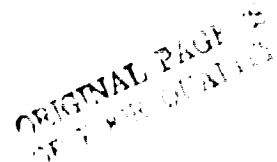


Figure 3-23. Summary of Test Results for H14 L. Hand & R. Hand Caps

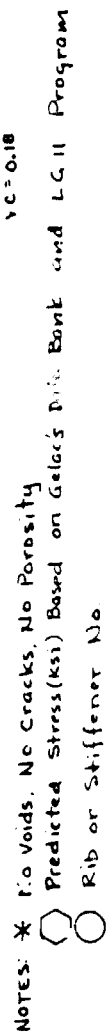


Figure 3-24. Summary of Test Results for H14 Web, Rib Angles and Stiffeners

results for the left hand and right hand caps. Porosity located by NDI in the forward flange of the LH and RH caps between VSS 80 and the first stiffener was verified by chemical analysis of the F_2 and F_{16} specimens and by the microscopic E2, E35, E36 and E37 specimens. The porous condition appeared to have been caused by cutting the steel rail used to mold the forward flange too deep, and the expanded rubber at 250°F barely contacted the forward flange in this area. This condition was believed to have been corrected prior to fabricating the H23A spar. As shown in Figure 3-23, all areas of the spar caps above the first stiffener had good physical properties.

Predicted compression loads and compression stresses are shown by the numbers in hexagons below the RH cap in Figure 3-23. These predicted values also apply to the opposite specimens in the LH caps. As shown, the test values were all above those predicted. Figures 3-25, 3-26 and 3-27 show typical failed specimens.

An experiment was conducted in the LH hand cap of H14 to determine the effect of adding a 90° cross ply between the stack of 0° plies. No resin micro-cracks were found in the E specimens from the LH cap; other properties were not affected. If microcracking is demonstrated to be a problem at a later date, a 90° cross ply can be added to the spar caps with a minimal impact on design and tooling.

3.2.2 Process Bulletin Refinements

The main objective of the process verification task is to produce a process bulletin which specifies the controls necessary to assure structural integrity in the full-length spars and in future production of parts using the same process. This bulletin is a living document, subject to modification as ancillary test specimens are fabricated to provide additional data, and as needed alterations to PB80-580 are discovered.

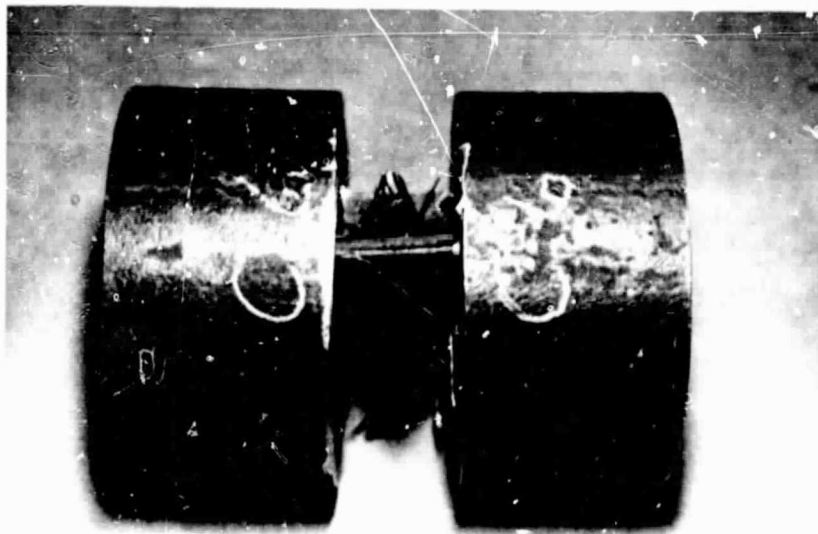
Amendment No. 1 to Process Bulletin 80-580 was issued this reporting period to incorporate needed revisions discovered during the processing and testing of H13, H14, H16 and H21 specimens. As additional parts are fabricated, other desirable changes will be recommended. For example, in processing the



ORIGINAL PAGE IS
OF POOR QUALITY



Figure 3-25. Specimen A Interlaminar Tension Failure Mode



e-2

Figure 3-26. Specimens C and D Compression Failure Mode



Figure 3-27. Specimen B Rail Shear Failure Mode

H23A stub spar it was noted that the process bulletin needs to include more definitive specifications for starting the cure cycle, for identification of control thermocouples, and for cool down rates. The procedure used for the specimens (H13, H14, H16, H21 and H23A) processed to date has been to plot the temperatures and pressures against time, continually review and analyze these data and make adjustments to the cure cycle time scale based on engineering judgement. Figure 3-28 illustrates the type of adjustment required.

After processing the stub spar for Ancillary Test Item H23A, additional process development work was indicated for the tool. The deeper than required cut in the rail used to form the cap flange for H14 was reworked, but it only partially solved the problem of cap flange over tolerance thickness. After processing the stub spar for H23A, it was noted that the steel channel appears to be locked inside the tool and not sliding, as would be needed to compress the cap flange. A solution to this condition will be pursued during the next reporting period.

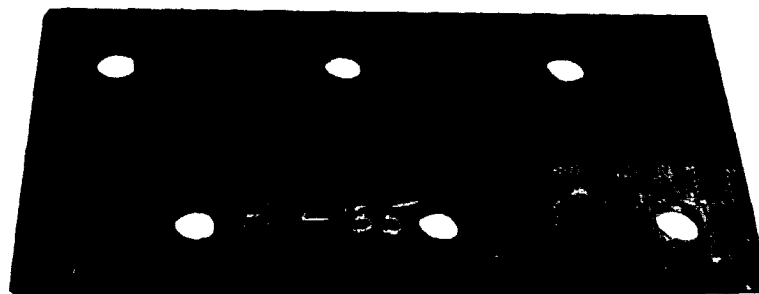


Figure 3-27. Specimen B Rail Shear Failure Mode

H23A stub spar it was noted that the process bulletin needs to include more definitive specifications for starting the cure cycle, for identification of control thermocouples, and for cool down rates. The procedure used for the specimens (H13, H14, H16, H21 and H23A) processed to date has been to plot the temperatures and pressures against time, continually review and analyze these data and make adjustments to the cure cycle time scale based on engineering judgement. Figure 3-28 illustrates the type of adjustment required.

After processing the stub spar for Ancillary Test Item H23A, additional process development work was indicated for the tool. The deeper than required cut in the rail used to form the cap flange for H14 was reworked, but it only partially solved the problem of cap flange over tolerance thickness. After processing the stub spar for H23A, it was noted that the steel channel appears to be locked inside the tool and not sliding, as would be needed to compress the cap flange. A solution to this condition will be pursued during the next reporting period.

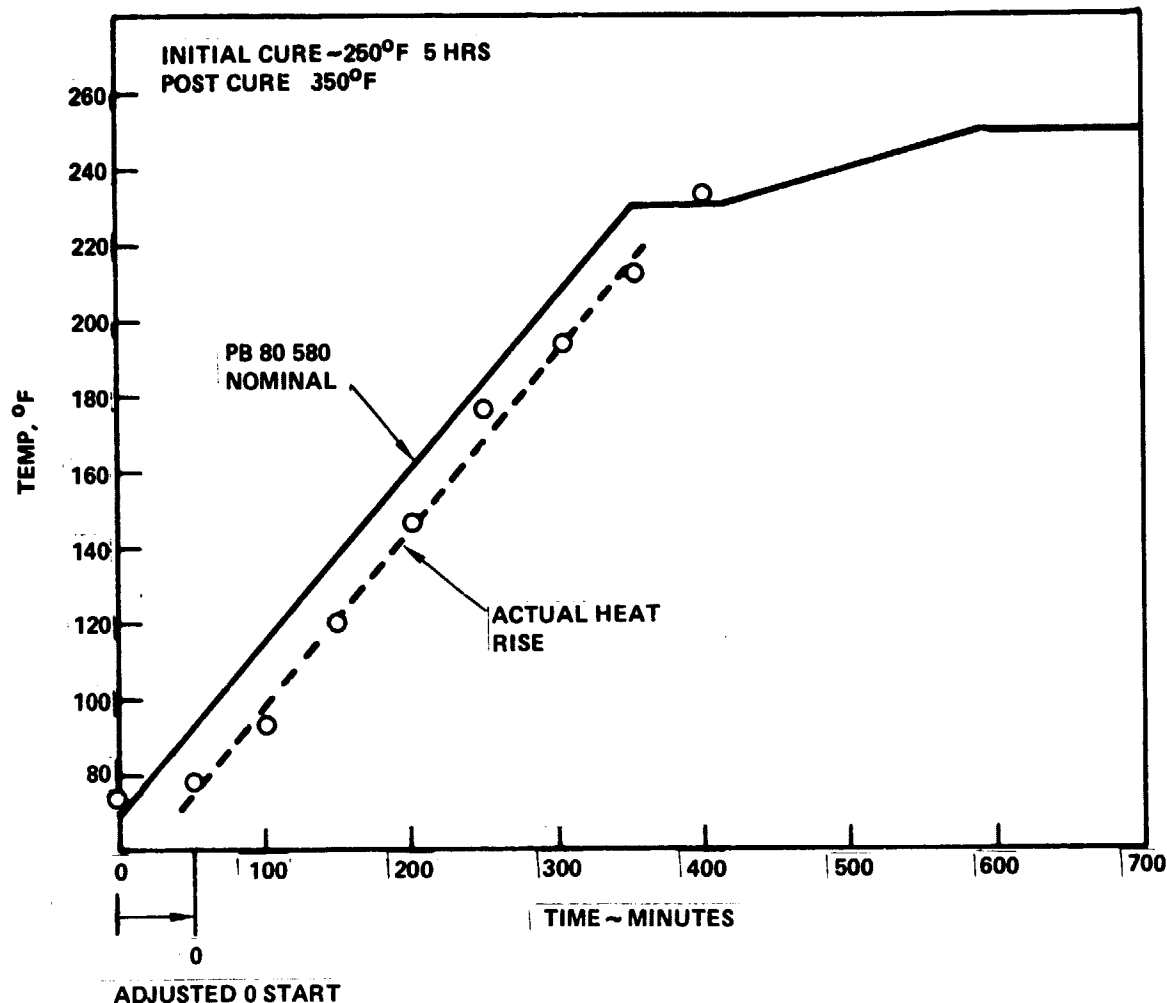


Figure 3-28. Illustration of Time Scale Adjustment Required During Cure Cycle

3.3 CONCEPT VERIFICATION

The concept verification task provides for the substantiation of the structural integrity of selected areas of the ACVF and for the verification of analysis methods.

3.3.1 Spar Test Fixture

All parts for the spar test fixture required for Ancillary Test Items H20 and H23 have been made, and assembly of the fixture has been initiated.

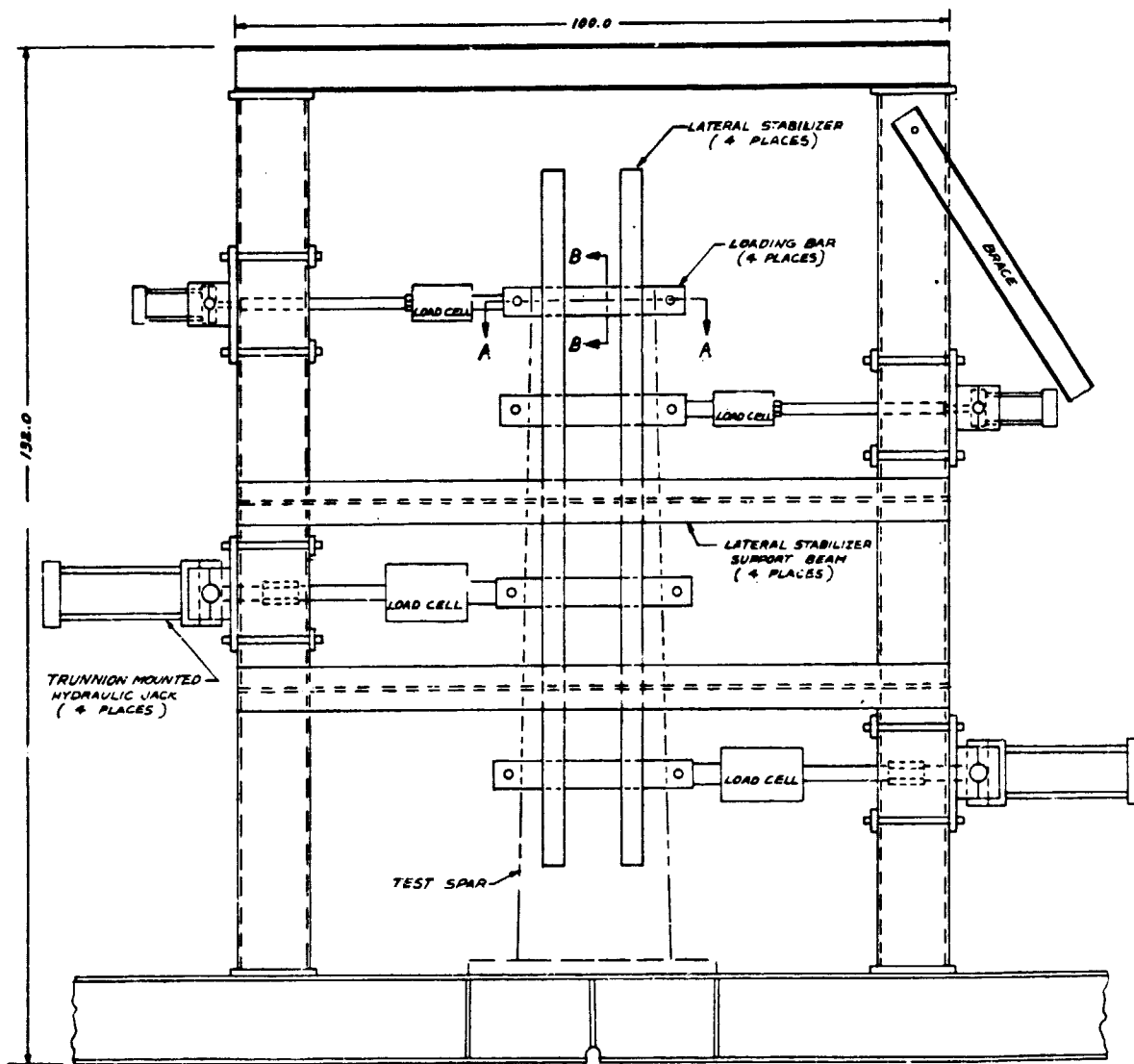
A general drawing of the fixture concept is shown in Figure 3-29. The vertical positions of the loading actuators can be varied along the support beams, making the fixture adaptable to load point requirements for both H20 and H23. Tunnion-mounted actuators having their rod ends attached to the spar loading bars by pin joints are used to minimize loads induced by spar deflection. A hydraulic marginator will control actuator loads which will be verified using load transducers. A load bar-spacer arrangement will be assembled on the spars at each station requiring introduction of load. This assembly will use both mechanical fasteners and adhesive bonding as illustrated by the sections in Figure 3-30. Lateral stabilizers, shown in Figure 3-29, will react against the loading bars to prevent torsion and hold the spar in plane. Teflon will be used at the reaction points to minimize friction.

3.3.2 Rear Spar Test Specimens - Test Item H20

Tool design for the H20, stub rear spar specimen was completed, and tool alteration is currently under way. The tool is expected to be completed during the next reporting period, and fabrication of the first of two test specimens H20 will be also begin during the next reporting period. The lower 100 inches of the full-size rear spar tool are used to fabricate the two H20 specimens.

3.3.2.1 Environmental Chamber

An environmental chamber required for testing one of the H20 specimens at 180°F has been constructed and is currently being evaluated for temperature distribution. A dummy spar instrumented with thermocouples is being used for those evaluations. The dummy spar has overall H20 dimensions and is constructed of aluminum sheet for the web and extruded aluminum "T" caps. The chamber is compatible with the Figure 3-29 fixture, and the general arrangement is illustrated in Figure 3-31. The previously described lateral stabilizers are constructed of square tubing and are being used as hot air manifolds inside the chamber. The upper ends of the stabilizers extend into a plenum where hot air is introduced. The wall in one side of each stabilizer contains a lengthwise series of holes which are used to distribute the air inside the chamber. Positioning of the stabilizers with respect to the wall containing



ORIGINAL PAGE IS
OF POOR QUALITY

Figure 3-29. Test Fixture for H20 and H23 Spar-to-Fuselage Specimens

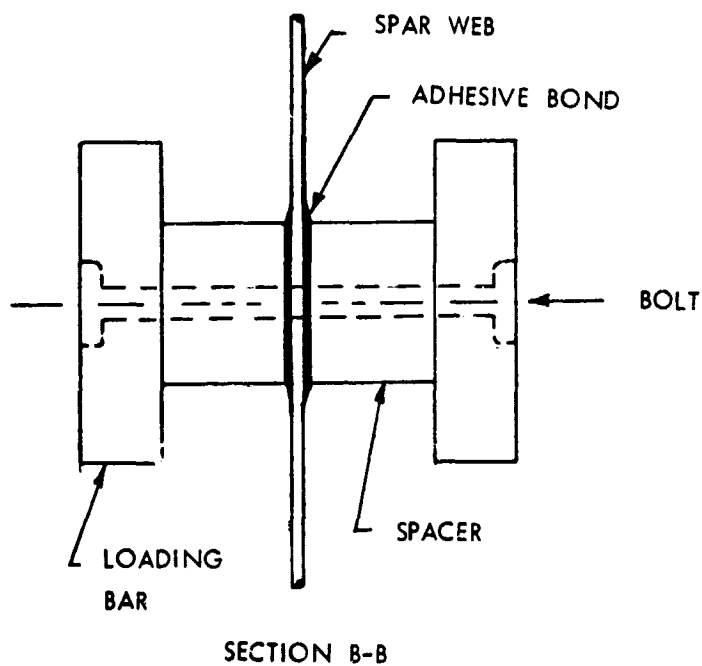
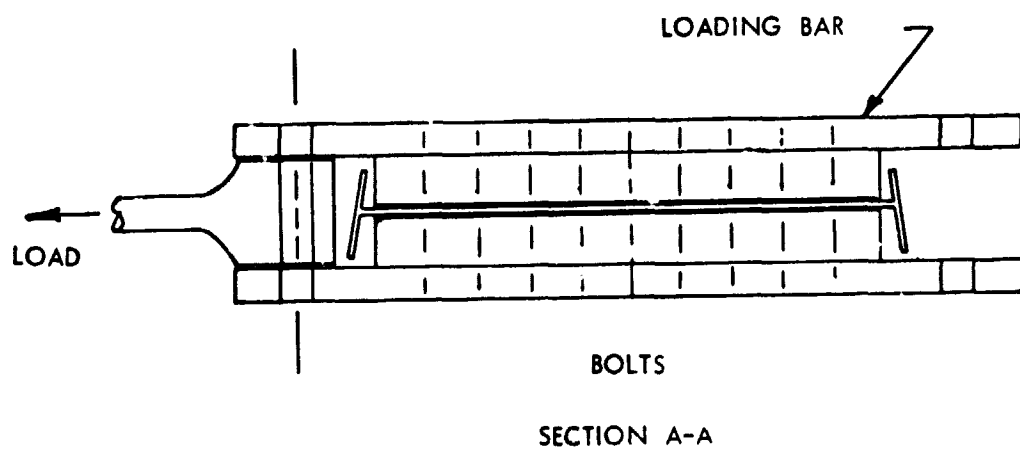


Figure 3-30. Loading Bar for Applying Point Loads to H20 and H23.

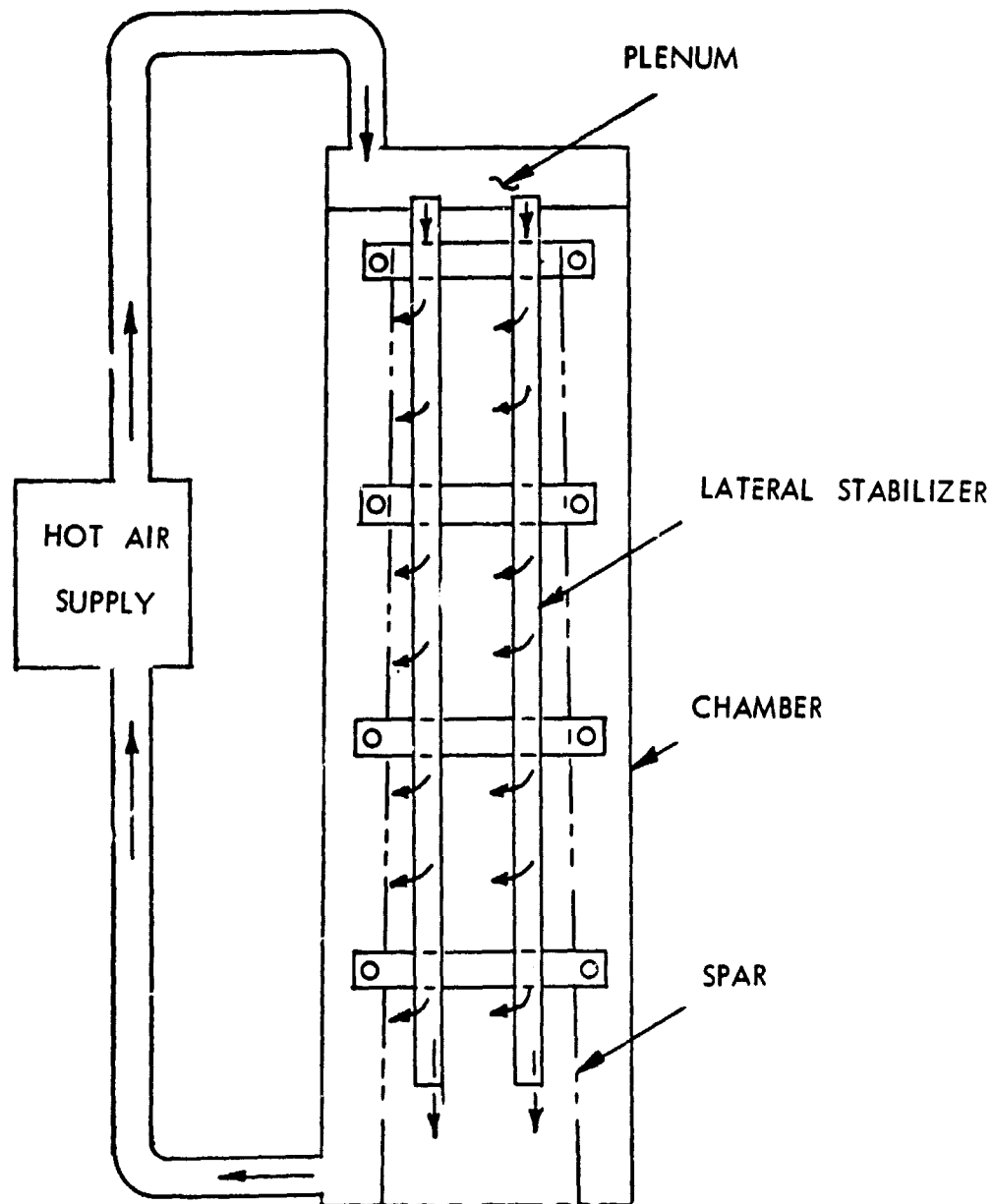


Figure 3-31. Diagram of Environmental Chamber for H₂O.

the holes is such that a circular flow around the spar is achieved. Flow distribution is varied by using aluminum tape over selected holes. The heat source is a temperature controlled, recirculating type manufactured by Missimers.

Current temperature distribution evaluations and flow distribution optimization in progress indicate that the required 180°F test temperature can be maintained to within $\pm 10^\circ\text{F}$ over the entire length and width of the spar.

The specimen will be bagged using either nylon or polyethylene sacs to maintain the moisture content during static test.

One of the H20 rear spar tests requires preconditioning in order to account for moisture effects. This specimen will be conditioned, at 95 percent relative humidity and 160°F, long enough to reach a moisture content of 1 percent at the critical section. This critical location is in the spar web at VSS 124.5, an area that is 0.122 inch thick (24 plies). In other spar areas, thicknesses as low as 0.08 inch and as high as 0.185" occur. In these areas, the moisture content is calculated to be as much as 1.22 percent and as low as 0.75 percent, as illustrated in Figure 3-32. Travelers or monitoring coupons will be exposed along with the test specimen. These will be removed periodically and weighed to verify the moisture accumulation.

3.3.3 Spar Web Test Specimens - Test Item H21

3.3.3.1 Specimen Fabrication

Fabrication of the two H21A picture-frame test panels was completed this reporting period. Both panels had local areas where the maximum thickness exceeded the currently defined maximum tolerance and both had local markoff between the metal and rubber exceeding the maximum permissible in PB80-580. Otherwise, the quality of the laminate was acceptable.

Overall, the two H21A panels weigh 7 pounds 11 ounces and 7 pounds 12 ounces versus a predicted weight of 7.75 pounds. The overall density is within tolerance, and the process control specimens are acceptable. The

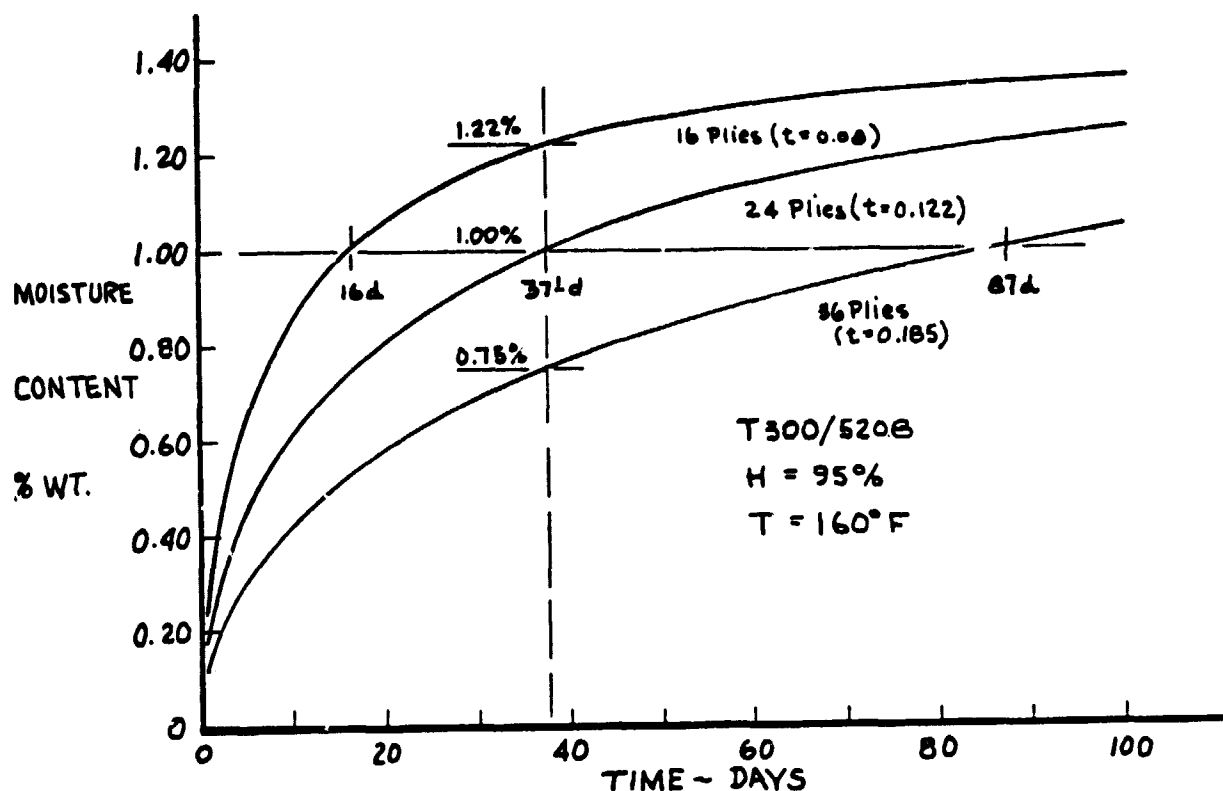


Figure 3-32. Calculated Moisture Pick-up for T300/5208 in Humidity Chamber

average thickness is within the acceptable tolerance. Apparently, the corrective action taken in this aluminum tool, corrects the area where applied but shifts the thicker material to another local area. The ultrasonic inspection identified three small voids in one of the panels, but these were smaller than void sizes allowed in the specification.

Discrepancy reports were written against both panels, stating the over-thickness and web mark-off conditions. Earlier panels made in this tool - specifically, the H21B and H21BX panels - had exhibited similar conditions, yet both had significantly exceeded all requirements in crack growth/static and static tests, respectively. On this basis of previous experience, it was concluded that the arbitrary PB80-580 limits had been made to be too restrictive, and that these conditions were likely to recur with the T300/5208 system. As a result:

- (1) The discrepancies were dispositioned to accept the panels for structural testing.
- (2) A specification variation notice is being prepared to more realistically define the mark-off requirements in PB80-580.

3.3.3.2 Spar Web Tests

The H21A-1, RTD shear panel with two stiffeners and 4-inch diameter, unreinforced access hole was static tested to failure. Figure 3-33 shows the test set-up. This panel represents the highest loaded section of the web in either the front or rear spars. The panel held 170 percent limit load, and the gages were read at this load before failure.

The failure mode shown in Figure 3-34 was almost identical to the failure mode for H21B shown in Figure 3-10 of Quarterly Technical Report No. 8. Both H21A-1 and H21B failed after reading the strains @ 170 percent design limit load; the strains were similar and indicated that web buckling occurred prior to failure. H21X, the first of this series of panels, was rejected because of delaminated stiffeners and over thickness tolerance. H21X was repaired, as shown in Figure 3-1 of Quarterly Report No. 8, tested and failed at 188 percent design limit load.

The H21A2 specimen designated for testing after moisture exposure has been machined to fit the test fixture and instrumented with strain gages. It was subsequently placed in the high humidity chamber at 160°F on 3-8-78. A 40 to 50 day exposure is planned prior to applying thermal cycles and subsequent static testing. A chamber, in which to perform the thermal cycling, has been constructed and is currently being checked for temperature distribution. One of the previously tested H21 specimens has been instrumented with thermocouples and is being used for the temperature distribution evaluations.

The planned thermal cycle is shown in Figure 3-35. This cycle was based on reaching a maximum temperature of 180°F on the ground, dropping to -65°F during flight, and returning to room temperature after the end of one flight. This cycle is similar to the cycle planned for the PRVT specimens as shown

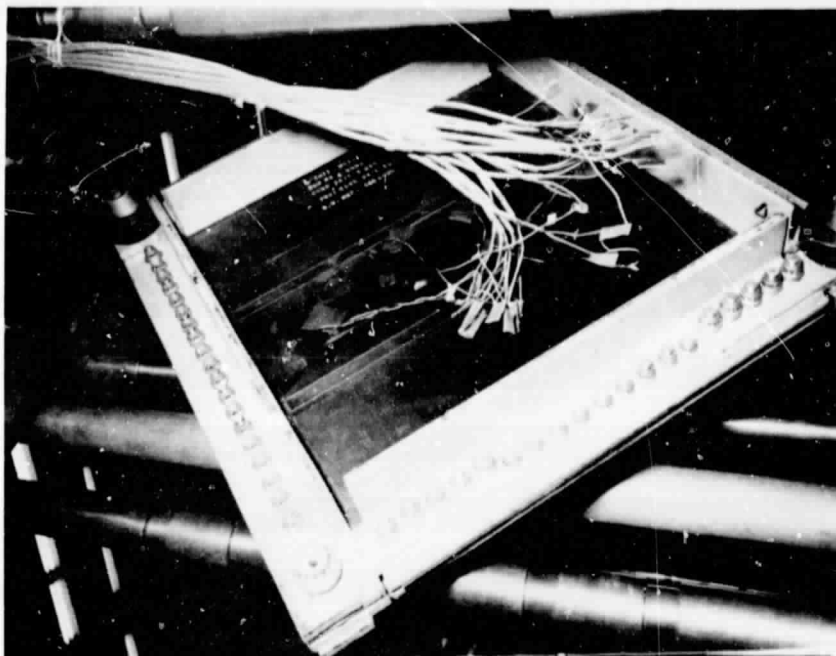
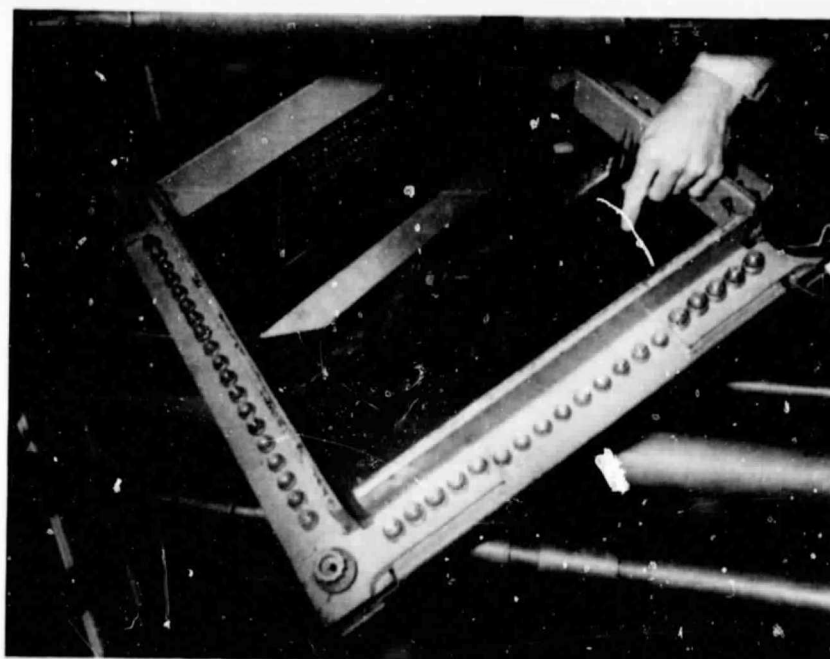
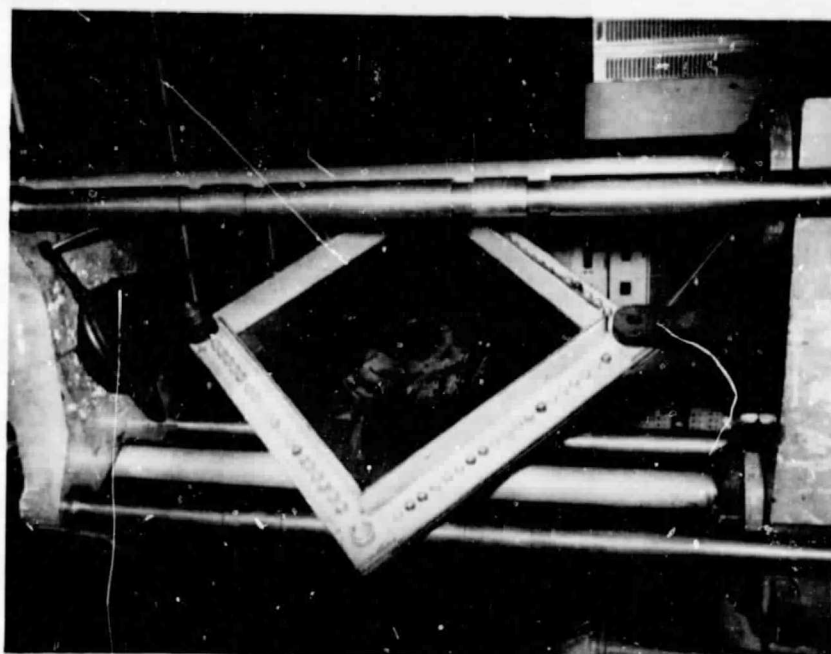


Figure 3-33. Test Set-up for H21A-1 RTD Shear Web Specimen



ORIGINAL PAGE IS
OF POOR QUALITY

Figure 3-34. Failure Mode for H21A-1 RTD Specimen After Sustaining 170 Percent Limit Load.

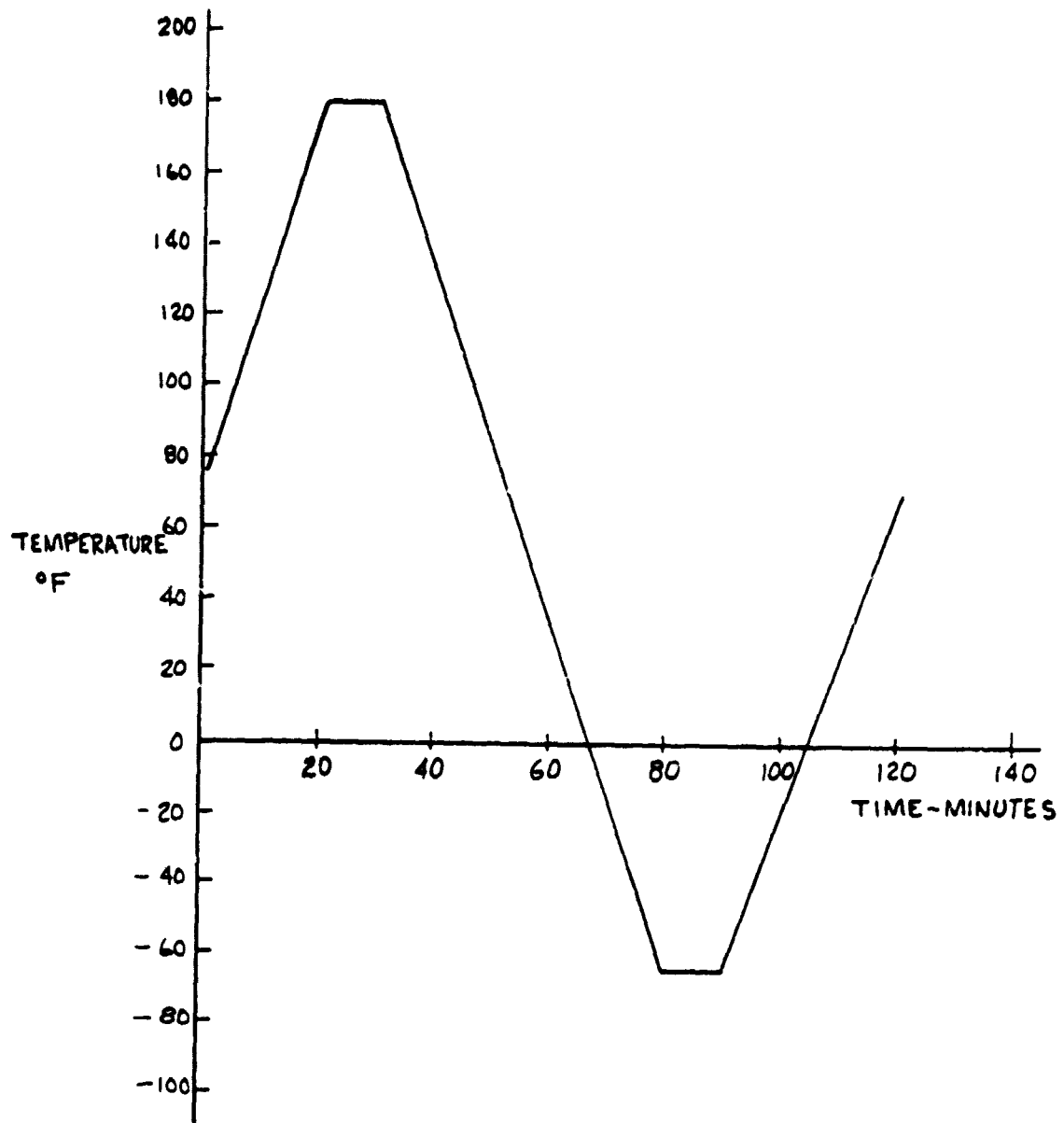


Figure 3-35. Temperature Cycle for H21A-2

in Figure 4-1 of Quarterly Technical Report No. 8. Five cycles are planned prior to static testing the H21A-2 wet specimen.

3.3.4 Front Spar Test Specimen - Test Item H23A

3.3.4.1 Specimen Fabrication

The second composite spar planned for use in the H23A test, has been fabricated in the same tool used to fabricate H14. The over tolerance problem in the forward flange of the lower end of the H14 spar cap was repeated in the H23A spar. Rework of the steel rails provided only a slight improvement in this area. A steel channel with rubber behind it is used to compress the flange at the lower end of the spar cap. It appears that, for some reason, this steel channel is not moving as it should. The thickness of the flange is over tolerance in a manner very similar to that found in H14. There are also similar, but fewer voids and less porosity indicated by NDI in the lower cap flanges of this second spar.

The H23A front spar test specimen will be tested to verify both the spar capability and the structural integrity of the spar-to-fuselage joint. A special set of root-end attachments have been designed and fabricated to realistically simulate the spar-to-fuselage load introduction. An exploded view of these attachments is presented as Figure 3-36. The root of the composite spar specimen will be fastened to the test frame through these fixtures, allowing loading of the spar as a cantilevered beam. A similar setup is planned for the static tests of the PRVT spars.

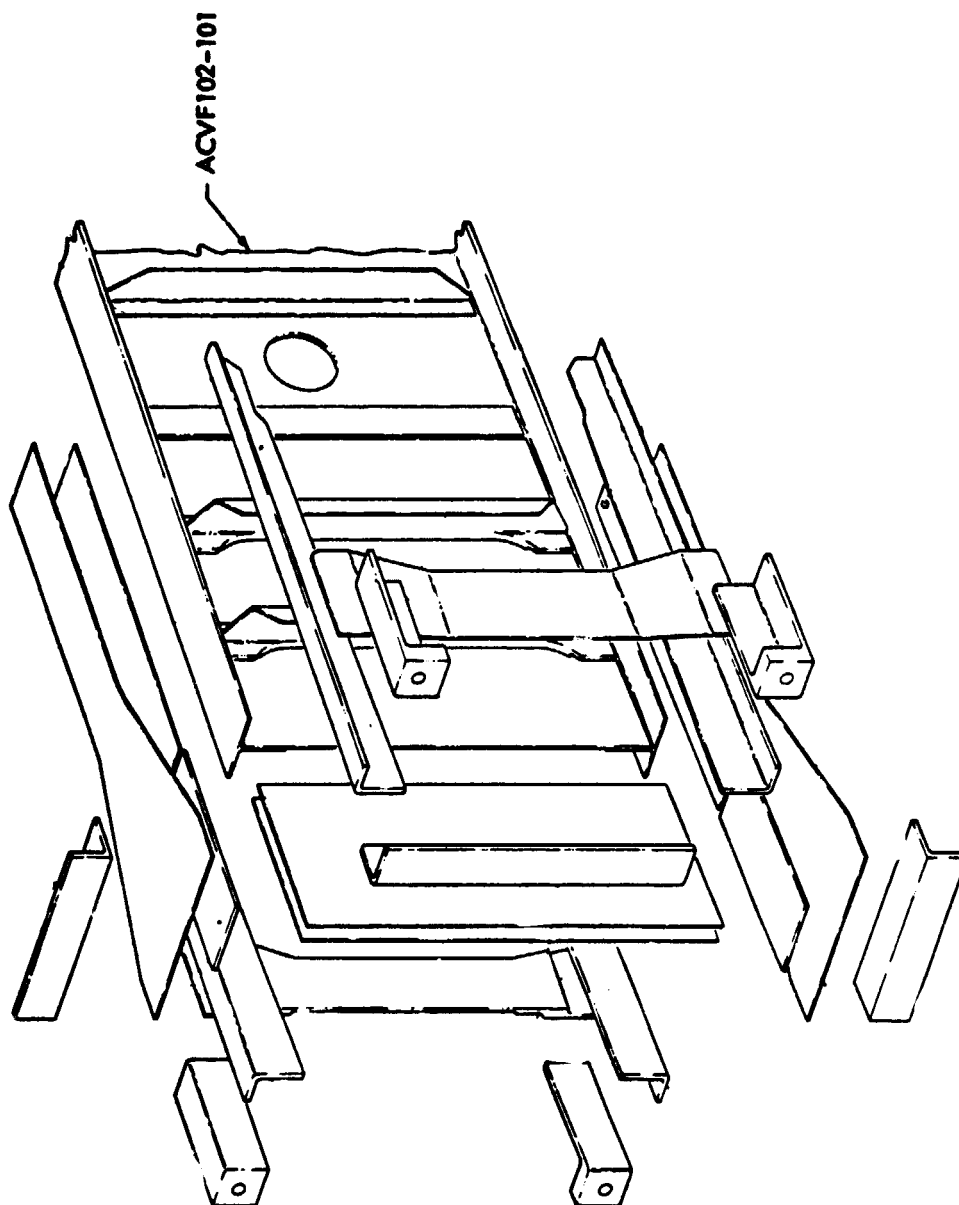
3.4 QUALITY ASSURANCE

Quality Assurance activities in this reporting period include in-process inspections for all fabrication activities, as well as process control testing, and coordination of all activities relating to test specimen conformity.

3.4.1 Laboratory Tests

3.4.1.1 Acceptance Tests

Batch 1015 of T300/5208 graphite/epoxy material was received just prior to the strike and did not have receiving inspection tests performed until



ANCILLARY TEST NO. 23 - FRONT SPAR,
L-1011 ACVF (DWG. NO. ACVF-100)

Figure 3-36. Illustration of H23 Front Spar-To-Fuselage Test Attachments

restart of the program on 3 January 1978. Test data for Batch 1015 are presented in Table 3-2:

TABLE 3-2. RECEIVING INSPECTION TESTS - BATCH 1015
(PER C-22-1379/111)

Test	Requirement	Result
Longitudinal Flexural	210 ksi	249.6 ksi
Short Beam Shear	13 ksi	17.4 ksi
Flow	15 - 29%	20.0%
Gel Time	Report	12 mins.
Fiber Volume	60 - 68%	67.3%
Specific Gravity	1.55 - 1.62	1.57
Resin Content	41 <u>+</u> 3%	39%

3.4.1.2 Process Control Tests

The process control tests on the H14 specimen were completed during this reporting period. The results of these tests are given in Section 3.2.1.

The two H21A spar web shear specimens were also completed this reporting period and thorough Quality Assurance inspections were conducted, including visual, dimensional, and ultrasonic inspections. As discussed in Section 3.3.3.1. in, the specimens both included some thickness and mark-off non-conformances. The process control tests showed excellent mechanical properties, but a slightly high resin content, as shown in Table 3-3. The panels were accepted for test, and the DR's appropriately dispositioned.

3.4.2 Nondestructive Inspection (NDI)

Nondestructive inspection of the H14 process verification specimen and the H23A ancillary test specimen has been completed. Areas of non-conformance to the engineering requirements are shown on Figure 3-37 for the H14 specimen and on Figure 3-38 for the H23A test specimen. Both of these spars have been accepted by Engineering for the planned tests.

TABLE 3-3. RESULTS OF H21A1 & H21A2 PROCESS CONTROL TESTS

Test Req'm'ts	Unit 1	Unit 2
Flex/Report	61.6 ksi	63.5 ksi
Short Beam Shear/8 ksi	10.3 ksi	9.3 ksi
Resin Content/26-32%	34.0-34.9	34.2-34.4
Sp. Gr./1.54-1.60	1.57-1.59	1.55-1.57
Porosity/ <2%	<2%	<2%
Compression/52 ksi	65.7-75.0 ksi	68.9-91.8 ksi

During inspection of the first H21A panel, ultrasonics indicated three small voids. Although these were small and within specification tolerances, the Proficiency Development Laboratory was requested to review the ultrasonic techniques being used and to make any modifications needed to assure that voids are properly identified and sized. This should eliminate one source of potential confusion resulting from interpretation of the ultrasonic inspections.

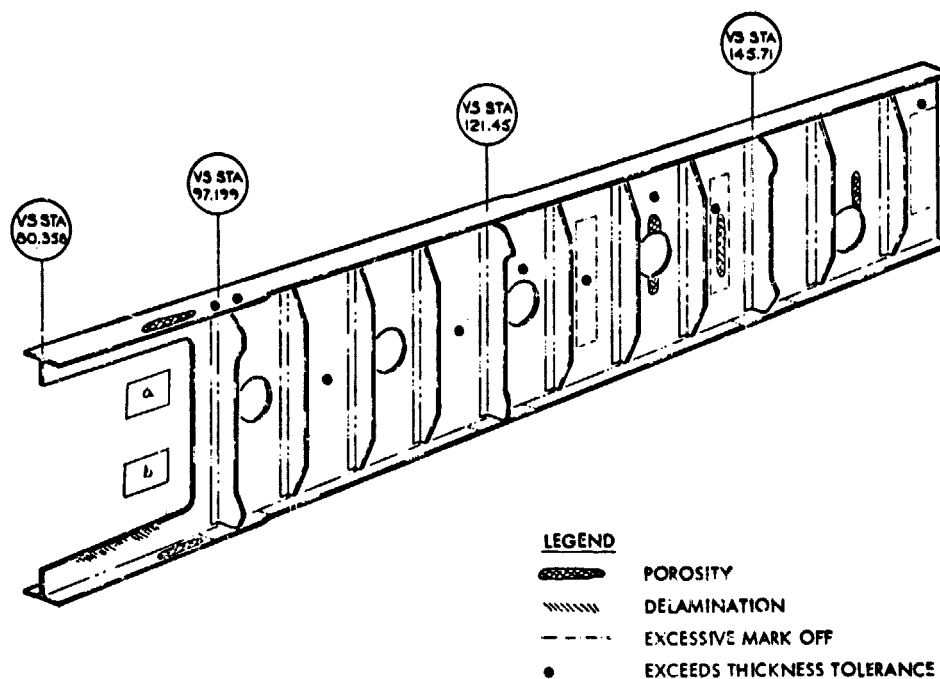


Figure 3-37. Summary of H14 Test Specimen Manufacturing Discrepancies

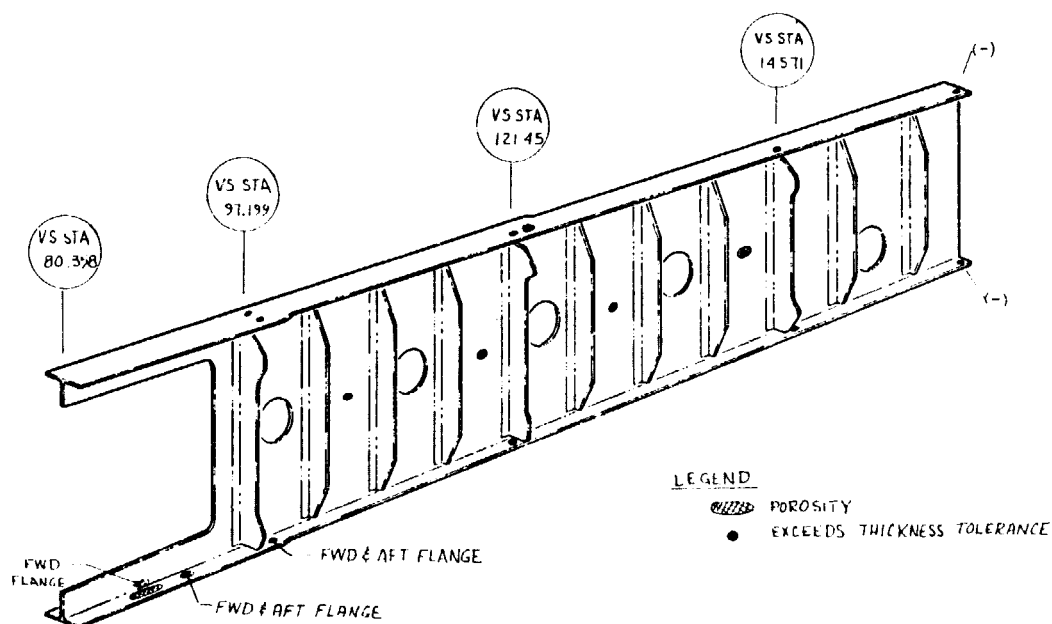


Figure 3-38. Summary of H23A Manufacturing Discrepancies

SECTION 4

PHASE III - PRODUCTION READINESS VERIFICATION TESTS

The ACVF program does not include flight service evaluation but alternately provides for multiple large-scale subcomponents of the structure for evaluation of variability in static strength and for assessment of durability under extended-time laboratory tests involving both load and environment simulation. The production readiness verification program (PRVT) is supplemental to the ancillary test program. These tests are designed to provide information to answer the following questions:

- What is the range of production qualities that can be expected for components manufactured under conditions similar to those expected in production, and how realistic and effective are proposed quality levels and quality control procedures?
- What variability in static strength can be expected for production quality components, and are the margins sufficient to account for this variability?
- Will production quality components survive extended time laboratory fatigue tests involving both load and environment simulation of sufficient duration and severity to provide confidence of in-service durability?

The questions are not primarily directed towards basic material properties. It is believed that the combination of service experience on secondary structures and coupon tests in the ancillary test program provide confidence in durability of the basic material. The questions are directed instead to the realities of production quality as influenced by cost objectives and by scale-up and complexity effects which will cause structural quality to differ from that represented by idealized small coupons.

Ten static-strength tests and ten durability tests will be conducted on each of two key structural elements of the ACVF. One element will represent

the front spar/fuselage attachment area, and the other element will represent the cover/fuselage joint area.

4.1 TEST SUPPORT

4.1.1 Environmental Chamber Design

Based on the results of a thermal analysis it was determined that the 10 durability cover specimens will require two chambers with 90 by 52.5 by 32 inches internal working dimensions, and the 10 durability spar specimens will require two chambers measuring 105 by 120 by 40 inches internally. A schematic of the chambers with specimens in place is shown in Figures 4-1 and 4-2.

The chambers will be constructed of a continuously heliarc welded series 304 stainless steel inner liner and an angle frame reinforced 16 gauge cold rolled steel outer case insulated with Upjohn Company Trymer CPR 9545 modified isocyanate cellular plastic. The cover chamber will have double doors on the front and back sides permitting easy access for inspection of panels. The spar chamber will have one large door on the front exposing the entire working volume. The doors will be designed with both an inner and outer gasket to minimize water buildup in the gasket space and reduce thermal losses through the door breakers. The floor will have drains for condensed moisture.

Air circulation within the workspace will be accomplished by a blower system drawing air from the workspace, blowing it through heating and cooling coils, and returning it to the workspace. Maximum temperature variation will be $\pm 5^{\circ}\text{F}$.

Ducting has been deleted from the design to minimize chamber mass and reduce heating and cooling requirements. The louver system has proved adequate in similar chambers for temperature uniformity throughout the workspace.

One central refrigeration system will be used for all four chambers by staggering the environmental cycle as shown in Figure 4-3.

System temperature will be reduced by a four compressor, two per stage cascade water cooled semihermetic mechanical refrigeration system. The system will include:

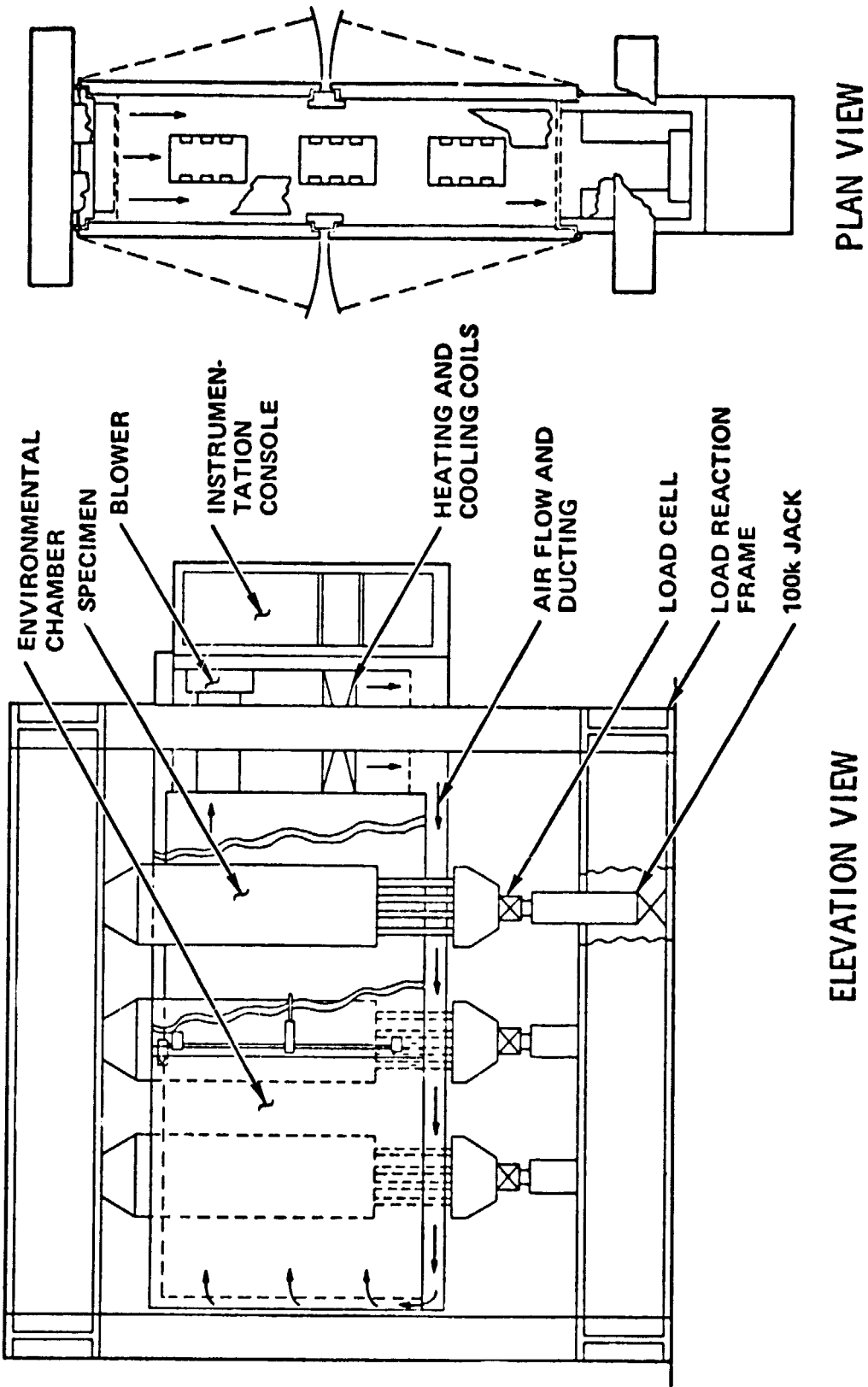


Figure 4-1. Cover Chamber and Loading Frame

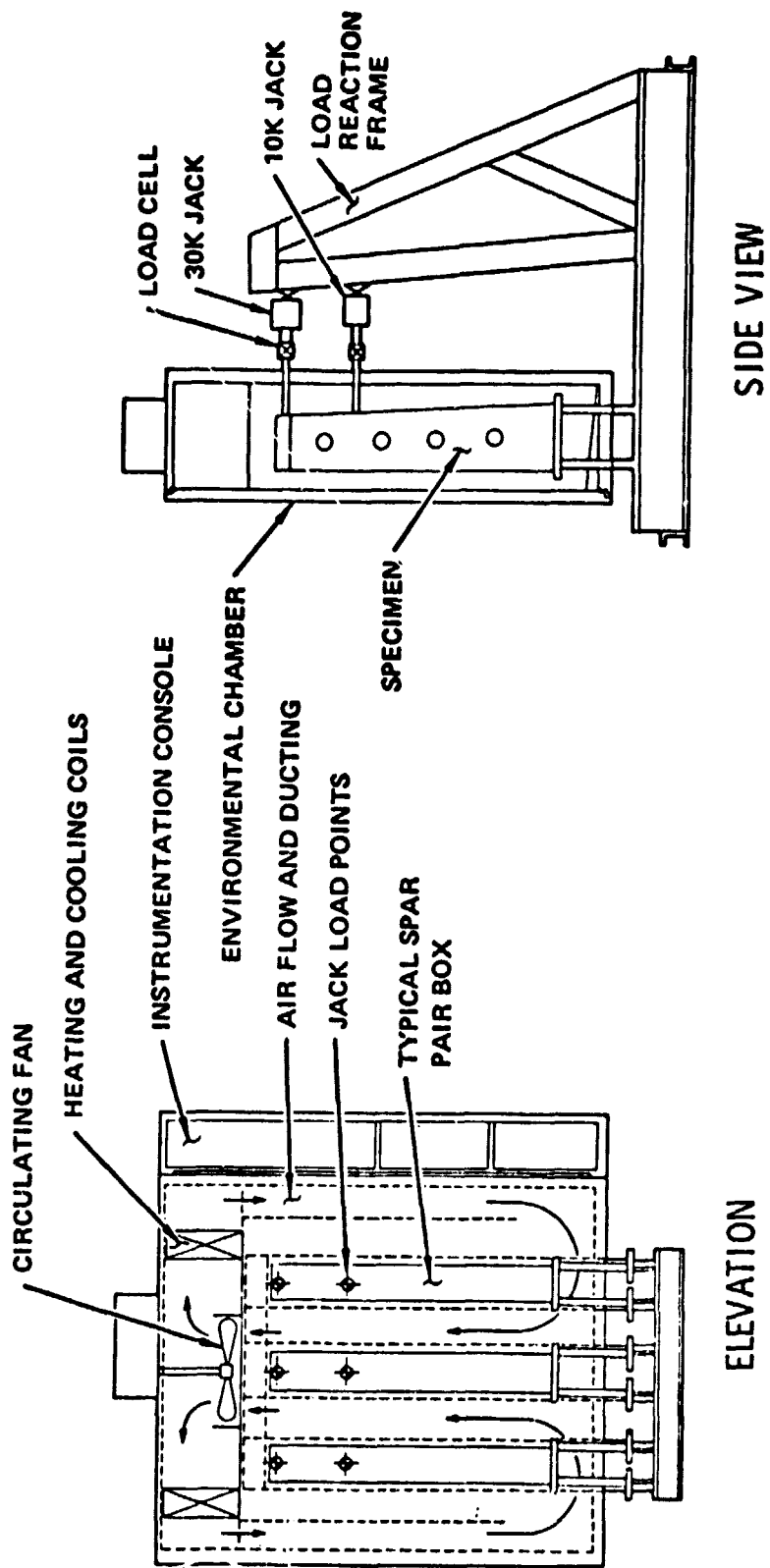


Figure 4-2. Spar Chamber and Loading Frame

A 90 MINUTES
 B 10 MINUTES
 C 72 MINUTES
 D 82.4 MINUTES
 E 15.6 MINUTES
 F 30 MINUTES
 TOTAL: 300 MINUTES

CYCLE 1: BOTH COVER CHAMBERS START 0.00 HRS.
 CYCLE 2: ONE SPAR CHAMBER START 1.67 HRS.
 CYCLE 3: ONE SPAR CHAMBER START 3.33 HRS.

● START CYCLE

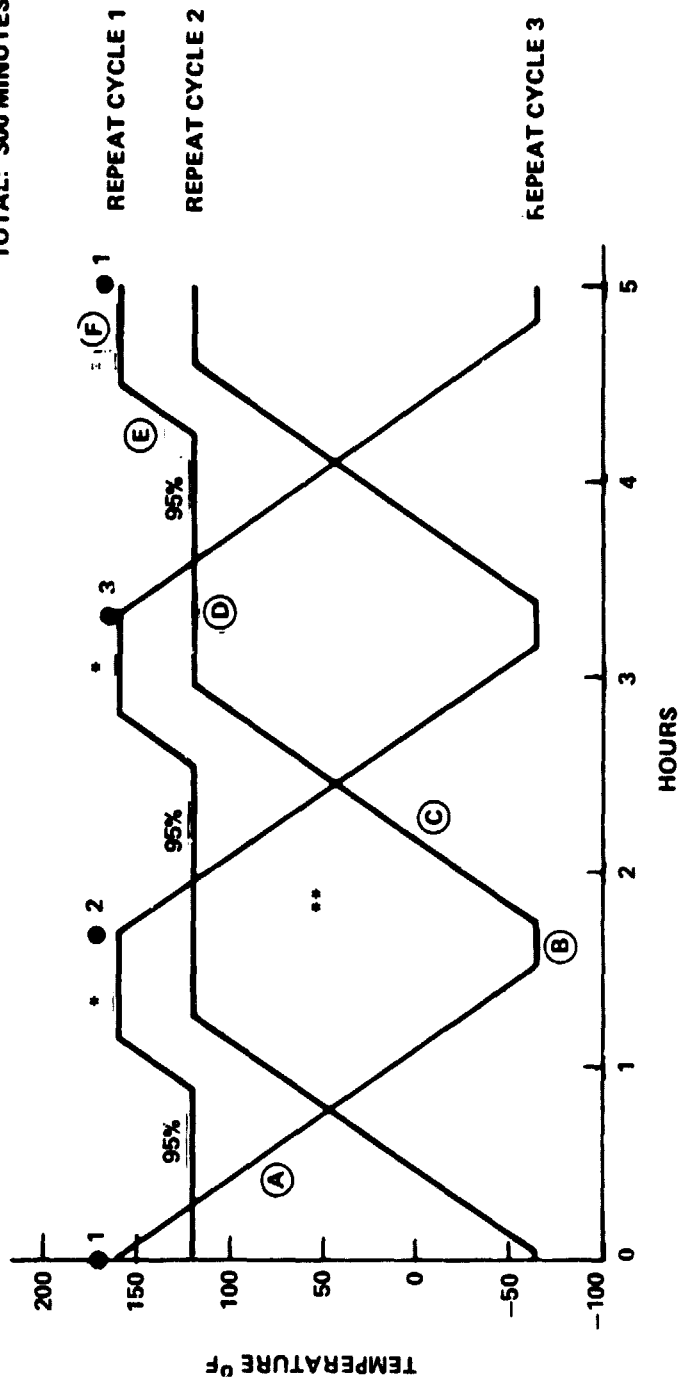


Figure 4-3. Thermal Cycle-PRVT

- Four 20 hp semihermetic mechanical refrigeration compressors.
- Dual pressure refrigerant suction and discharge safety switches.
- An automatic hot gas bypass proportioning valve.
- An automatic suction cooling and suction pressure limiting thermal expansion valve to limit the suction temperature to a safe level for the compressor.
- Thermal expansion valves with automatic suction pressure limiting, adjustable superheat and external pressure compensation to modulate refrigerant flow to the cooling coils in the various chambers.
- Modulating valves to proportion fluid flow of refrigerant versus thermal load controlled by the temperature controller in the various chambers.

A central steam generator will be contained in the refrigeration system machinery console to increase vapor content in the various chambers. The steam generator will include: a sight glass; an automatic low water cut-out; an automatic water level control; and a pressure control and relief valve. Steam will be proportioned by the humidity controllers via a solenoid valve.

Chamber temperature will be increased by using Nichrome element heaters controlled by heavy duty mercury relays integrated with a dry bulb temperature controller. The heaters will be protected by a separate power controller interlocked with a high temperature safety thermostat and a solid state electronic high-low temperature safety control interlocked with the set-up relay and a visual and audible alarm, as well as the central computer monitoring system. Approximately 15 KW of heat will be required for each cover chamber and 24 KW for each spar chamber to maintain the specified heating rate.

Control instrumentation specifically for each chamber will be contained in a rack mount on the right side of each chamber. All central control systems will be mounted in a separate console with the minicomputer and data acquisition system.

As seen in Figure 4-1 the cover specimens will protrude out the top of the chamber. This was done to get the potted ends out of the high humidity and temperature environment since the desirable potting materials would be severely degraded by the environment over the 4 year test time span.

The lower end of the specimen will be gripped by a built-up metal structure and the load will be transmitted through the chamber bottom by four 2 inch diameter hollow stainless tubes per specimens. These tubes were selected to minimize heat transfer through the chamber wall. Similar tubes are used at the base of the spar beams.

Penetration of the spar chamber will be placed on the back side for the hydraulic jack rods which are solid stainless rods insulated for minimum thermal excursion. All penetrations through the chamber will be lined and welded. Rubber boot seals will be attached to the rods and chamber inner liner to prevent leakage yet permit motion transfer.

To simulate the flight conditions of the covers more closely, the back-to-back pairs will be baffled at each side to prevent air flow through the inside over the hats. This will allow moisture build up on the inner surface with ice formation during the cold cycle.

4.1.1.1 Thermal Analysis

Using a simple finite-difference lumped-parameter CPS computer program, the heating and cooling loads for a complete hot and cold cycle were predicted. The spar chamber was chosen as being representative of the maximum chamber loading. Because of the complexity of the actual conditions, a number of simplifying assumptions were made:

- Each thermal mass is all at the same temperature.
- The individual masses are decoupled, i.e., thermally independent. (Not true but description of thermal resistances between items is extremely difficult and not cost effective for this analysis.)
- A single value of external heat transfer film coefficient over the exposed surface areas can be used.
- There is no air exchange between inside and outside of chamber.

The calculated chamber thermal loads are given in Table 4-1. With all temperatures starting at 70°F (for ease of computation) the chamber air temperature is programmed through the cycle shown in Figure 4-4. A schematic depiction of the chamber is also given in Figure 4-4.

TABLE 4-1. CHAMBER LOAD SUMMARY - 6 SPARS

No.	Item Description	Weight lb	Thermal Cap. Btu/°F	Surface Area Ft	Remarks
1	Graphite/epoxy spar + fittings and titanium hydraulics	175	40.5	107.5	Loading jacks with thermal resistance, $R_1 = 4.31^\circ \text{Btu/hr to}$ outside.
2	Caps - aluminum	110	22	11	Jack resistance $R_2 = 3.15$
3	Aluminum Stringers	165	36	30	Assumed floating
4	Aluminum Structure	168	37	48	Assumed floating
5	Steel Base + bolts	518	111	42	Could be insulated if desired. Loading connections $R_5 = 0.12$
6	Conditioning equipment + chamber details, 135 lb al. angle, 20 lb baffle, 100 lb HX equipment	255	59	200	Assumed floating
7	Walls, 0.016 in. aluminum on 3 in. polyurethane foam.	-	-	190	C for 1 ft ² wall 0.11 Btu/°F for 1st inch, 0.04 per inch thereafter.

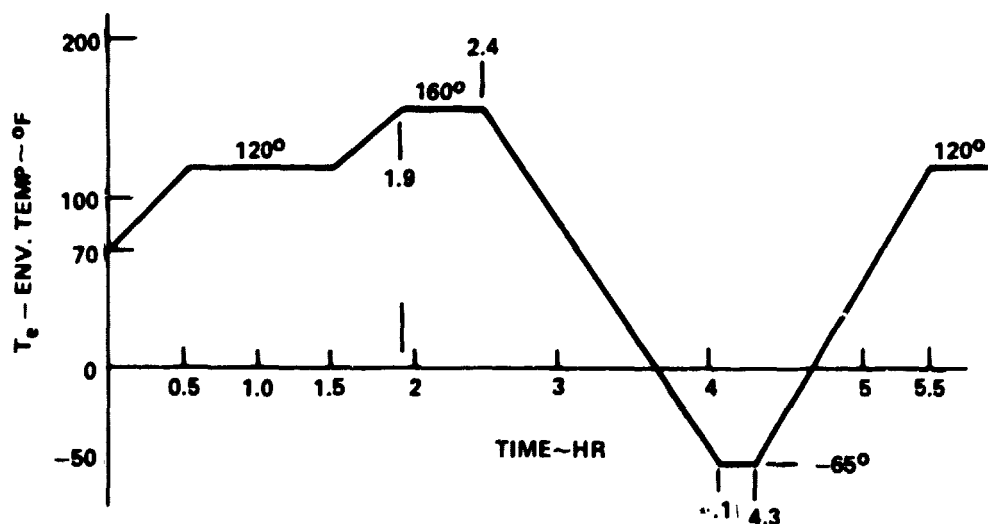
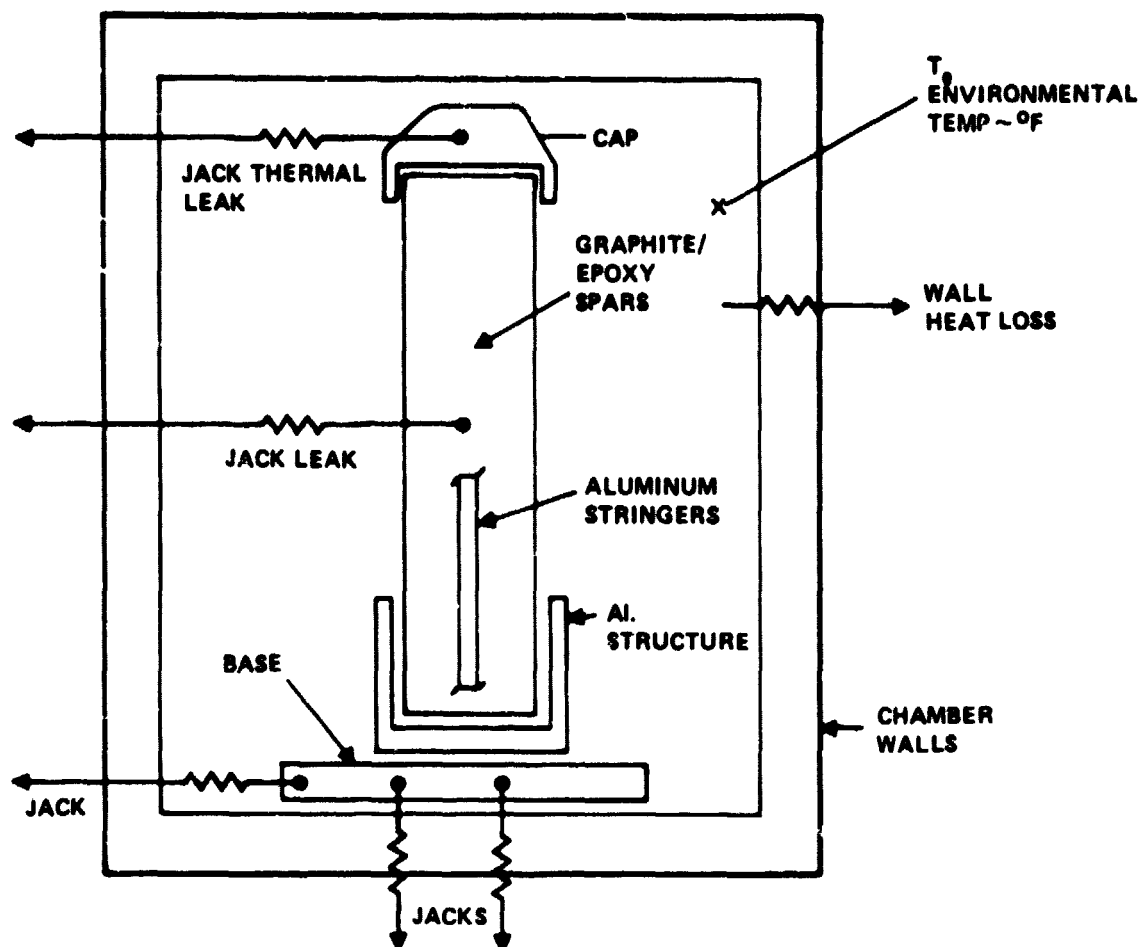


Figure 4-4. Chamber Schematic and Temperature Cycle

Two different conditions were computed. Table 4-2 presents the predicted performance for modest air circulation rates (film coeff. $h = 2.5 \text{ Btu/hr ft}^2\text{-}^\circ\text{F}$) while Table 4-3 represents fairly vigorous air circulation ($h = 5.0$). The predicted spar temperatures (T_1) follow the environment quite closely, while the base temperatures (T_5) stay in the range from 55 to 99 $^\circ\text{F}$. This is because of the mass of the base plus the thermal short circuit represented by the jacks. The maximum refrigeration load under either condition is 3.5 tons, while the maximum heating load is 8.4 kW. The unconservative aspects of the analysis (decoupling the aluminum structure from the base) can be particularly offset by eventual insulation of the base, which was assumed to be uninsulated.

4.1.2 Durability Test Specimens

Specimen configuration for the spar durability test is shown in Figure 4-5. This consists of the first 84 inches of the spar as measured from the fuselage attachment end (VS STA 80.358). To obtain the required cap/web loads a box configuration, with loads applied at two points, has been designed for tying two spars together with additional aluminum stiffeners. This configuration, shown schematically in Figure 4-6, reduces the number of hydraulic jacks and servo loops required if spars were tested individually without added stiffeners, although it does necessitate a substantial number of fasteners. Three of these double spar boxes will be mounted in one environmental chamber, as shown schematically in Figure 4-2, and two boxes in the other chamber.

Specimen configuration for the cover durability test is shown in Figure 4-7. It consists of a 21 inch wide by 62 inch long three-hat stiffened panel. The fuselage attachment end is angled and will be mated with an aluminum "tee" section through a series of aluminums and graphite/epoxy tapered fillers, the opposite end will be potted and attached with a similar aluminum and glass/epoxy doubler arrangement to get more load transfer into the doublers. Each specimen will have two ribs attached transversely to the doublers.

4.1.2.1 Loading Configurations

Spar loading is shown schematically in Figure 4-6. Loads will be applied to each spar box with a 10 kip jack located 42 inches from the fuselage end, and a 30 kip jack located 89.5 inches from the same end.

ORIGINAL PAGE 1
OF POOP QUALITY

LR 28573

TABLE 4-2. ENVIRONMENTAL CHAMBER PERFORMANCE PREDICTION (h = 2.5)

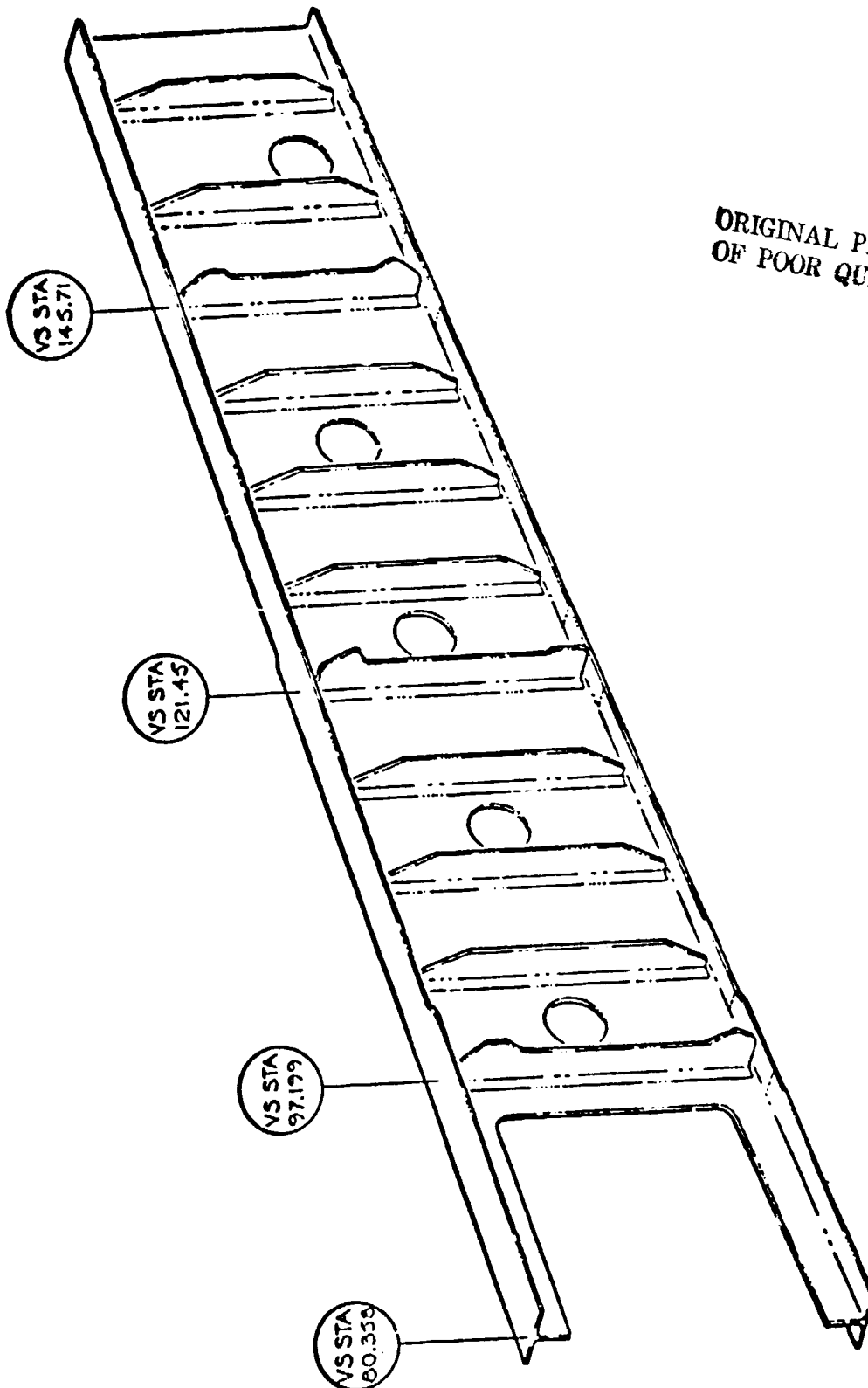
Time hours	T-env F	T1-spar F	T2-cap F	T3-Struc F	T4-Struc F	T5-base F	T6-syst F	0-1000 psi/ton
0.00	70	70	70	70	70	70	70	0.00
0.10	70	74	71	72	72	70	75	2.25
0.20	70	92	73	7	77	71	84	3.46
0.30	100	91	76	84	83	71	93	4.23
0.40	110	100	80	91	90	72	103	4.41
0.50	120	110	84	100	99	73	113	5.78
0.60	120	116	89	106	105	75	115	3.43
0.70	120	118	92	111	109	76	119	2.58
0.80	120	119	96	114	113	77	120	2.13
0.90	120	120	99	116	115	78	120	1.65
1.00	120	120	101	117	116	79	120	1.67
1.10	120	120	103	118	117	80	120	1.54
1.20	120	120	105	119	118	81	120	1.44
1.30	120	120	107	119	119	82	120	1.36
1.40	120	120	109	119	119	83	120	1.30
1.50	120	120	110	120	119	84	120	1.24
1.60	130	124	112	122	122	85	125	3.44
1.70	140	132	115	127	127	86	134	4.61
1.80	150	141	119	134	133	87	143	5.35
1.90	160	150	124	141	140	89	153	5.89
2.00	160	156	128	147	146	91	156	4.06
2.10	160	158	132	151	150	92	159	3.24
2.20	160	159	135	154	153	94	160	2.80
2.30	160	160	135	156	155	96	160	2.52
2.40	160	160	141	157	157	97	160	2.33
2.50	147	154	142	155	155	98	153	-0.22
2.60	134	144	141	149	149	99	142	-0.71
2.70	120	132	139	141	142	99	129	-1.03
2.80	107	120	135	131	132	99	116	-1.27
2.90	94	107	130	120	122	99	103	-1.46
3.00	81	94	125	109	110	99	90	-1.63
3.10	67	81	116	97	98	98	76	-1.78
3.20	54	67	111	84	86	96	63	-1.91
3.30	41	54	103	71	74	95	50	-2.04
3.40	28	41	94	58	61	93	37	-2.16
3.50	14	26	85	45	48	91	23	-2.27
3.60	1	15	75	32	35	88	10	-2.38
3.70	-12	1	65	19	22	86	-3	-2.48
3.80	-25	-12	54	6	9	83	-16	-2.58
3.90	-38	-25	43	-7	-4	80	-29	-2.68
4.00	-52	-38	32	-20	-18	76	-43	-2.77
4.10	-65	-52	21	-33	-31	73	-56	-2.86
4.20	-65	-59	11	-43	-41	69	-62	-2.10
4.30	-65	-62	2	-50	-48	66	-64	-1.73
4.40	-50	-57	-5	-51	-50	63	-56	-0.53
4.50	-34	-46	-9	-47	-46	60	-43	0.49
4.60	-19	-33	-10	-39	-39	58	-29	2.04
4.70	-3	-18	-10	-29	-29	56	-14	3.19
4.80	12	-3	-8	-17	-18	55	2	4.13
4.90	23	12	-4	-4	-6	55	17	4.92
5.00	43	28	2	10	8	54	32	5.63
5.10	58	43	8	24	22	54	48	6.26
5.20	74	58	16	39	36	55	63	6.85
5.30	89	74	24	54	51	56	79	7.40
5.40	105	89	34	69	66	57	94	7.91
5.50	120	105	44	84	81	59	110	8.40
5.60	120	113	53	95	93	60	117	5.39
5.70	120	117	61	103	101	62	119	3.98
5.80	120	119	68	108	107	64	120	3.21
5.90	120	119	74	112	111	65	120	2.74
6.00	120	120	80	115	113	67	120	2.42
6.10	120	120	85	116	115	68	120	2.19
6.20	120	120	89	117	117	69	120	2.02
6.30	120	120	93	118	118	71	120	1.86
6.40	120	120	96	119	118	72	120	1.77
6.50	120	120	99	119	119	73	120	1.68

max
zone

max
zone

TABLE 4-3. ENVIRONMENTAL CHAMBER PERFORMANCE PREDICTION (h = 5.0)

Time Hours	T-env F	T1-spar F	T2-cap F	T3-Struc F	T4-Struc F	T5-Base F	T6-syst F	η-LOAD klu/-ton
0.00	70	70	70	70	70	70	70	0.00
0.10	80	78	72	75	74	70	79	2.14
0.20	70	87	76	82	82	71	99	3.41
0.30	100	97	81	91	91	71	99	4.21
0.40	110	107	87	101	100	72	109	4.89
0.50	120	117	94	111	110	73	119	5.51
0.60	120	120	100	116	115	75	120	3.76
0.70	120	120	105	118	116	76	120	3.25
0.80	120	120	108	119	119	77	120	2.96
0.90	120	120	111	120	120	78	120	2.79
1.00	120	120	113	120	120	79	120	2.66
1.10	120	120	115	120	120	80	120	2.56
1.20	120	120	116	120	120	81	120	2.48
1.30	120	120	117	120	120	82	120	2.40
1.40	120	120	117	120	120	83	120	2.33
1.50	120	120	118	120	120	84	120	2.27
1.60	130	128	120	125	124	85	129	4.55
1.70	140	137	124	132	132	86	139	5.57
1.80	150	147	130	141	141	87	149	6.31
1.90	160	157	136	151	150	89	159	6.95
2.00	160	160	142	156	155	91	160	5.19
2.10	160	160	146	158	158	92	160	4.64
2.20	160	160	149	159	159	94	160	4.35
2.30	160	160	152	160	160	96	160	4.16
2.40	160	160	153	160	160	97	160	4.01
2.50	147	150	152	154	154	98	148	0.79
2.60	134	137	149	144	144	99	135	-0.21
2.70	120	124	143	132	133	99	122	-0.54
2.80	107	110	135	119	120	99	108	-0.82
2.90	94	97	126	106	107	99	95	-1.08
3.00	81	84	116	93	94	99	82	-1.32
3.10	67	71	105	80	81	98	69	-1.55
3.20	54	58	94	67	68	96	55	-1.77
3.30	41	44	82	53	55	95	42	-1.98
3.40	28	31	70	40	41	93	29	-2.19
3.50	14	18	58	27	28	91	16	-2.39
3.60	1	5	45	14	15	88	2	-2.58
3.70	-12	-9	33	0	2	86	-11	-2.77
3.80	-25	-22	20	-13	-11	83	-24	-2.95
3.90	-38	-35	7	-26	-25	80	-37	-3.13
4.00	-52	-48	-6	-39	-38	76	-50	-3.30
4.10	-65	-62	-19	-52	-51	73	-64	-3.47
4.20	-65	-65	-30	-60	-59	69	-65	-2.76
4.30	-65	-65	-38	-63	-62	66	-65	-2.52
4.40	-50	-53	-41	-57	-57	63	-51	-1.35
4.50	-34	-33	-40	-46	-46	60	-36	-0.77
4.60	-19	-23	-36	-32	-33	58	-20	-0.34
4.70	-3	-7	-29	-17	-19	56	-5	0.12
4.80	12	8	-20	-2	-4	55	11	1.30
4.90	28	24	-10	13	12	55	26	2.39
5.00	43	39	2	28	27	54	42	3.43
5.10	58	54	14	44	42	54	57	4.43
5.20	74	70	28	59	58	55	72	5.38
5.30	89	85	41	75	73	56	88	6.30
5.40	105	101	55	90	89	57	103	7.19
5.50	120	116	70	106	104	59	119	8.06
5.60	120	120	81	114	113	60	120	5.29
5.70	120	120	90	117	117	62	120	4.45
5.80	120	120	97	119	118	64	120	4.02
5.90	120	120	103	120	119	65	120	3.74
6.00	120	120	107	120	120	67	120	3.54
6.10	120	120	110	120	120	68	120	3.38
6.20	120	120	112	120	120	69	120	3.25
6.30	120	120	114	120	120	71	120	3.14
6.40	120	120	115	120	120	72	120	3.03
6.50	120	120	116	120	120	73	120	2.94



ORIGINAL PAGE IS
OF POOR QUALITY

Figure 4-5. SPAR PRVT Specimen

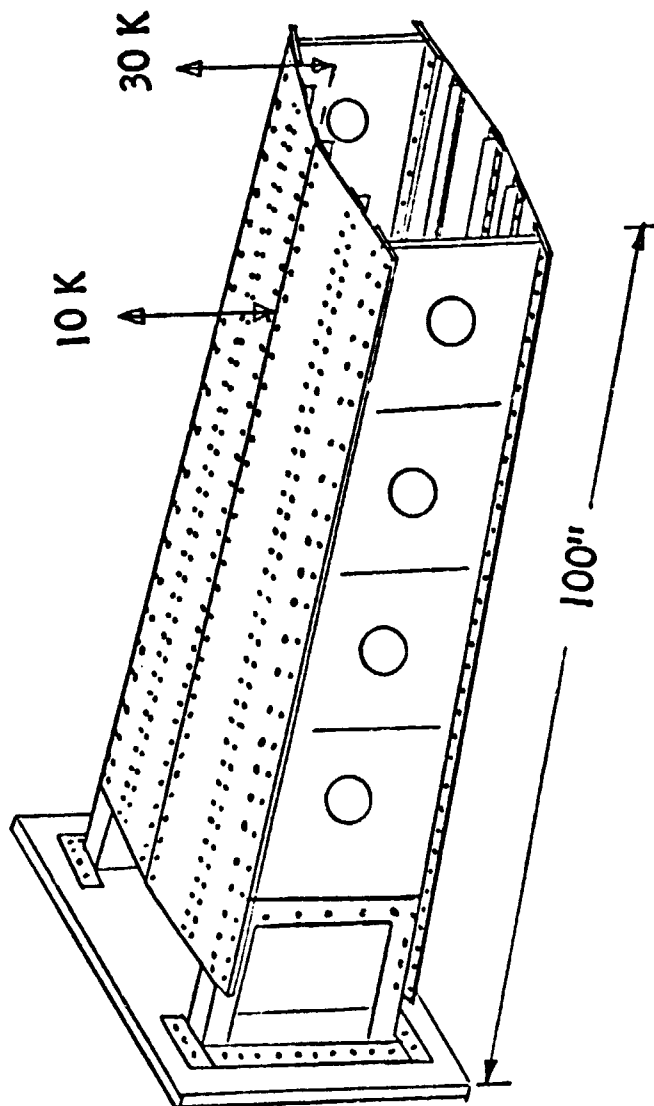


Figure 4-6. Twin Spar Beam

ORIGINAL PAGE IS
OF POOR QUALITY

LR 28573

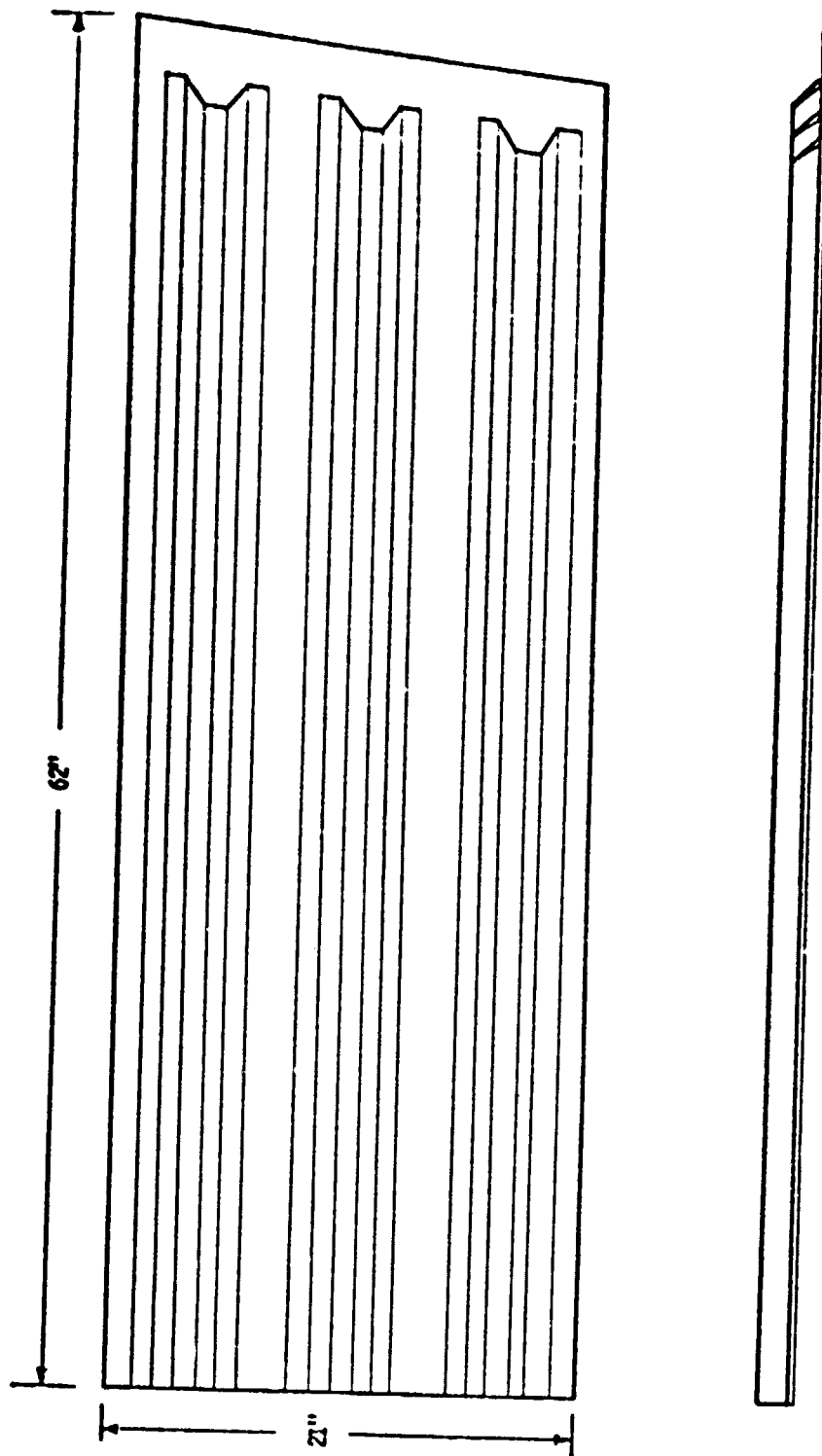


Figure 4-7. Cover Test Specimen

Each jack train will contain a dual bridge transducer load cell for load monitoring even though all jacks of the same capacity in each chamber are plumbed to a common hydraulic source and all jacks of the same capacity (eg 10 kip) will have matched equal areas. Each spar box will also be instrumented with a linear variable displacement transducer (LVDT) to monitor deflection which will yield data on changes in specimen stiffness. Additionally each specimen will be instrumented with strain gages and thermocouples.

All jacks are equipped with mechanical stops to prevent excess deflection in the event of system malfunction or specimen failure.

Each cover specimen will be loaded by individual 100 kip jacks through a dual bridge transducer load cell. Specimens will be mounted back-to-back in pairs as shown in Figure 4-1, with three pairs in one environmental chamber and two pair in another chamber. Buckling restraint will be obtained by connecting the transverse ribs from one specimen to the other and attaching the fuselage attachment end tees together. Although the specimens are tied together all jacks in each chamber operate in phase.

Should one specimen fail, mechanical stops would prevent damage to the other mating cover specimen. As in the spar test system, all 100 kip jacks are of matched equal areas.

There are separate servo valves for each chamber hydraulic system so that shutdown of one chamber does not affect performance or schedule of the other chamber. Each specimen will be monitored for stiffness by a LVDT and will be instrumented with strain gages and thermocouples.